KU Leuven
Biomedical Sciences Group
Faculty of Pharmaceutical Sciences
Department of Pharmaceutical and
Pharmacological sciences

COAXIAL ELECTROSPRAYING TO PRODUCE COATED AMORPHOUS SOLID DISPERSION PARTICLES

FROM POLYMER SOLUTION TO FIXED DOSE COMBINATIONS

Annelies SMEETS

Jury:

Promoter:	Prof. dr. Guy Van den Mooter
Co-promoter:	Prof. dr. Christian Clasen
Chair:	Prof. dr. Jef Rozenski
Jury members:	Prof. dr. Deirdre Cabooter
	Prof. dr. Mathy Froeyen
	Prof. dr. Chris Vervaet
	Prof. dr. Henderik Frijlink

Dissertation presented in partial fulfillment of the requirements for the degree of Doctor in Pharmaceutical Sciences

December 2019

Acknowledgements

Performing research in the Drug Delivery and Disposition lab and eventually writing this PhD thesis would not have been possible with the help and support of a lot of people. I am looking back at four remarkable years, a professional and personal journey, and want to take a minute to express my gratitude.

First of all, I want to thank my supervisor prof Guy Van den Mooter to give me the opportunity to be part of his research group. I admire your passion for research and the enthusiasm for our work. Your door was always open if I needed any advice or to discuss ideas. I am grateful for your mentoring, it was an honour and joy working with you. I am also thankful for the help of my co-supervisor prof Christian Clasen. I appreciate your advice, the time you took to discuss our projects and improve the manuscripts.

I want to thank the jury members, Prof Jef Rozenski, Prof Deirdre Cabooter, Prof Mathy Froeyen, Prof Chris Vervaet and Prof Henderik Frijlink to assess my thesis and provide me with constructive feedback, improving the quality of my work. I also want to thank Prof Mario Smet for the collaboration on the polymer derivatization.

During the past four years, there was not even one day I went to the lab being unhappy, my dear colleagues, you are a bunch of wonderful people. I want to thank Duong to get me started with the project and pass your knowledge on electrospraying. Abhishek, Thao, Aswin and Tu to show me around in the lab and answer all my questions. Manoela, Anna, Giulia and Ida to bring the southern vibes into the lab and make the long days of experiments flying by in no time. Timothy, Bart, Elene, Sien, Melissa and Fan to be enjoyable office mates and Timothy, so many thanks for all your help with our HPLC troubles. Maarten, David, Max and Piyush to be inspiring coworkers. Jenny and Sonia to help with practical issues. Eline to be an awesome master student. And off course, special thanks to Bernard. Bernard, you are always there for us, no matter what, no matter the problem. I cannot tell how grateful I am for all you did, you are such an admirable person.

I also want to thank all my great colleagues from the SMaRT division in Heverlee, where I also spent a lot of time in the lab and whose company during lunchtime was always a refreshing break. Special thanks goes to Robin for our enjoyable collaboration on coaxial electrospraying and to Wouter for the help with the polymer derivatization. Thanks to Anja, Nico and Danny for the practical support.

Lastly, my friends and family, who supported me not only during the past four years, but every second, minute and year before. I want to thank my parents a thousand times, to be always so supportive, enthusiastic, encouraging, … in all I did and raised me to the person I am today. I am also incredibly grateful to you Andy, to have you at my side. Klop klop. Wie is daar? Het is slecht oplosbaar! I want to end thanking Ann-Sofie, you were so enthusiastic about my project, asked every week what was new, what was going on. I hope you could find peace up there, liefste An-So, dit is voor jou.

Abbreviations

ACE	Acetone
ACN	Acetonitrile
API	Active Pharmaceutical Ingredient
ASA	Acetylsalicylic acid
ASD	Amorphous Solid Dispersion
ATE	Atenolol
AUC	Area Under The Curve
BCS	Biopharmaceutics Classification System
CES	Coaxial Electrospraying
DCM	Dichloromethane
DCS	Developability Classification System
DoE	Design of Experiments
DRV	Darunavir
DSC	Differential Scanning Calorimetry
c*	critical overlap concentration
c_e	entanglement concentration
CAP	Cellulose acetate phthalate
EC	Ethyl cellulose
ES	Electrospraying
EtOH	Ethanol
EDX	Energy Dispersive X-ray Spectroscopy
FDC	Fixed Dose Combination
FEN	Fenofibrate
FITC	Fluorescein Isothiocyanate Isomer 1
GI	Gastrointestinal
HPC	Hydroxypropyl cellulose
HPLC	High Pressure Liquid Chromatography
HPMC	Hydroxypropyl methyl cellulose or hypromellose
HPMC AS	Hydroxypropyl methyl cellulose acetate succinate
HPMC P	Hydroxypropyl methyl cellulose phthalate
IPA	Isopropanol
LOV	Lovastatin
LOVh	β-hydroxy acid metabolite of lovastatin
MeOH	Methanol
NMR	Nuclear Magnetic Resonance
PAR	Paracetamol
Pe	Peclet number

Ph. Eur.	European Pharmacopoeia
PLGA	Poly(lactic-co-glycolic acid)
P(MAA/MMA)	Copolymer poly(methacrylic acid-co-methyl methacrylate)
P(MAA/EA)	Copolymer poly(methacrylic acid-co-ethyl acrylate)
PMMA	Poly(methyl methacrylate)
P(MV/MA)	Poly(methyl vinyl ether-alt-maleic anhydride)
PVP	Polyvinylpyrrolidone
PVP-VA	Poly(vinylpyrrolidone-co-vinyl acetate)
SEM	Scanning Electron Microscopy
SD	Spray Drying or Standard Deviation
TGA	Thermogravimetric analysis
TEM	Transmission Electron Microscopy
T_g	Glass transition temperature
T_m	Melting temperature
ToF-SIMS	Time of Flight Secondary Ion Mass Spectrometry
mDSC	modulated Differential Scanning Calorimetry
XPS	X-ray Photoelectron Spectroscopy
XRPD	X-Ray Powder Diffraction

Table of Contents

Chapter 1
General introduction

1.1. ORAL BIOAVAILABILITY

1.1.1. Gastrointestinal absorption

The costs to develop new medicines have been increasing significantly throughout the years and today, launching a new drug is estimated to cost up to 2.6 billion dollar[1]. These high expenses can, amongst others, be attributed to the high attrition rate during drug development, which means that many compounds that seem very promising and potent during early discovery will be discarded in course of the further development process. One of the reasons is that it is not always evident to formulate these potent molecules into a final dosage form. While various administration routes for medicines are nowadays available, oral drug delivery stands undoubtedly out and is generally preferred by both patients and manufacturers[2]. However, to qualify for oral delivery, an active pharmaceutical ingredient (API) needs to fulfil certain physicochemical criteria. For example, once a tablet reaches the stomach, it needs to disintegrate and the API needs to dissolve into the gastrointestinal (GI) fluids. Only the free and molecularly dissolved API fraction can permeate through the intestinal membrane and reach the systemic circulation[3]. Hence, the API has to be sufficiently soluble and have the right properties regarding permeability in order to get absorbed through the intestinal membrane. Furthermore, the API will be metabolised by the enzymes present in the liver and intestinal mucosa[4,5]. This together with efflux transport by transporters like P-gp (P-glycoprotein) and MRP (Multidrug Resistance-associated Protein) will decrease the bioavailability[5]. In conclusion, the interplay between the solubility, permeability, metabolism and efflux will determine the systemic exposure after oral administration.

In 1997, Lipinski *et al*. published the "Rule Of Five" which correlates four basic physicochemical properties of the API to adequate aqueous solubility and intestinal permeability[6]. The rule states that the molecular weight should be less than 500 g/mol, the calculated logP (octanol-water partition coefficient) and the amount of hydrogen-bond donors should be less than five and lastly, there should be no more than ten hydrogen-bond acceptors. If an API is in compliance with the Lipinski Rule of Five, it is likely to display a good oral bioavailability[7]. Overall, a high molecular weight and large number of hydrogen-bond possibilities hampers the intestinal permeability, a high logP is on the other hand associated with a poor aqueous solubility[6].

During the past decades, the amount of new APIs, both under development and on the market, with properties beyond the Rule Of Five and poor systemic exposure after oral administration, has grown remarkably[8]. This increase can be attributed to a drastic change in the generation of new chemical leads in drug discovery during the early nineties[6]. In the past, discovery of new compounds was guided by the knowledge on drugs that already existed, which led to hits with similar physicochemical properties and good oral bioavailability *in se*. However, with the advent of combinatorial chemistry in the nineties, an enormous amount of new molecules with a wide variety of chemical features could automatically be synthesised. Coupled with the fast evolution in high throughput screening and growing knowledge in molecular biology, these new molecules could be screened in a vast amount of *in vitro* tests for biological activity[9]. Furthermore, screening was performed with organic stock

solutions implying concentrations above the aqueous solubility of the compounds and with the shift to target based discovery, hits became more lipophilic as the targets and receptors ask for lipophilic ligands[6,8]. All in all, these new approaches in drug discovery yielded very potent hits, but did not take the physicochemical properties regarding oral administration into account.

1.1.2. Biopharmaceutics Classification System

Due to the increasing impact of the APIs defined by a low oral exposure and the need for harmonization, the Biopharmaceutics Classification System (BCS) was developed[10]. The BCS is based on the application of Fick's First law, which implies that the drug flux through the intestinal membrane is proportional to the permeability for the membrane and drug concentration at the surface of the membrane. Hence, in the BCS, molecules are categorized into four classes based on their aqueous solubility and intestinal permeability as they are the main factors governing drug absorption (Fig 1.1). Class I is characterised by both high solubility and permeability; Class II compounds are poorly soluble; Class III compounds are poorly permeable; Class IV is characterised by both poor solubility and poor permeability. A compound is classified as highly soluble if the highest dosage strength dissolves in ≤ 250 mL of water over the entire pH range of 1.2 till 6.8 and a compound is highly permeable if ≥ 85 % of the administered dose is absorbed, as compared to an intravenous bolus or obtained via mass balance calculations[11].

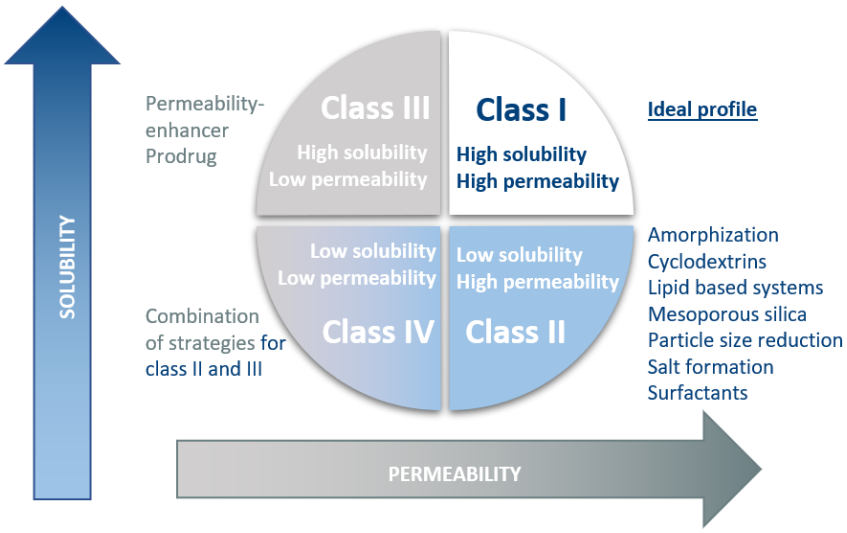

Figure 1.1. Biopharmaceutics Classification System (BCS) and methods to improve the oral bioavailability based on enhancing the permeability and/or solubility. Figure adapted from Singh and Van den Mooter 2016 [19].

In a publication by Takagi *et al*., 200 top drug products from the worldwide market were classified resulting in only 30 % belonging to class I[12]. Overall, more than 40 % was poorly soluble and it is estimated that this amount even rises to 90 % for compounds under development[12,13]. Consequently, the need for technologies to improve oral absorption cannot be overestimated. As depicted in Fig 1.1, absorption can be enhanced at the level of solubility as well as permeability. However, the latter is out of scope for this thesis and focus lies on improving the apparent solubility of class II and IV compounds.

1.1.3. Improving solubility and dissolution rate

Beside the limitation of a low thermodynamic solubility, the absorption can as well be limited by the rate of dissolution. Indeed, the aqueous solubility of an API can be high enough, but dissolution can be extremely slow, exceeding the time-window for absorption in the intestinal region[14]. For this reason, the interplay between the solubility and dissolution rate should be taken into account, which is also incorporated in the Developability Classification System (DCS). The DCS arose from the BCS, but where the BCS was originally designed for regulatory purposes concerning bioequivalence studies, the DCS aims to adapt more accurately to the *in vivo* situation and guide the early stages of drug development[15]. For the DCS, the solubility is measured in fasted-state simulating intestinal fluid (FaSSIF) rather than over the entire GI pH range, because the concentration in the upper small intestine is most relevant regarding the absorption. The permeability is measured via permeation experiments through cells or estimated *in silico*. Additionally, class II of the DCS is subdivided into IIa with compounds being dissolution rate limited and IIb for the compounds which are solubility limited. For compounds in class IIa, the high permeability can outbalance the poor solubility and complete absorption can be achieved by modifying the rate of dissolution via control of the particle size. Smaller particles have in comparison a larger surface area, which is proportional to the dissolution rate as given by the Nernst-Brunner equation (Eq 1.1):

$$\frac{dC}{dt} = \frac{DA(C_s - C)}{hV} \quad \text{(Eq 1.1)}$$

in which C represents the API concentration, dC/dt the dissolution rate, D is the diffusion coefficient, A the surface area, C_s the solubility of the API in the dissolution medium, h the thickness of the diffusion layer and V the volume of the dissolution medium[16].

Contrary, the compounds in class IIb are truly solubility limited and will need an enabling technology to attain proper absorption after oral administration. The classification systems are dynamic and continuously optimised with the scientific advancements. An illustration is the revised Developability Classification System that was published last year[17].

The dissolution process itself is visualised in Fig 1.2 and can be divided in three consecutive steps[8]. First of all, a drug molecule needs to be detached from the crystal by breaking the bonds with the neighbouring molecules, a process that consumes energy. Secondly, the solvent in which the drug is dissolving needs to be rearranged to form a pocket that can accommodate the dissociated molecule. This step requires in turn energy. In the last step, the molecule is incorporated in the solvent and energy is released.

As depicted in Fig 1.2, the dissolution process can be hampered in the first or last step. For molecules with a high melting point (above 200 °C), strong intermolecular interaction will hinder the dissociation process and these molecules are commonly referred to as *brick dust* molecules. The other type of poorly solubles are the *grease balls*, which are highly lipophilic (LogP above 3) and solvation limited. Both limitations can be addressed to improve the dissolution process and different methods which are used in oral drug delivery are listed in Fig 1.1. As amorphization is the method applied in this thesis, it will be discussed in detail in the next section.

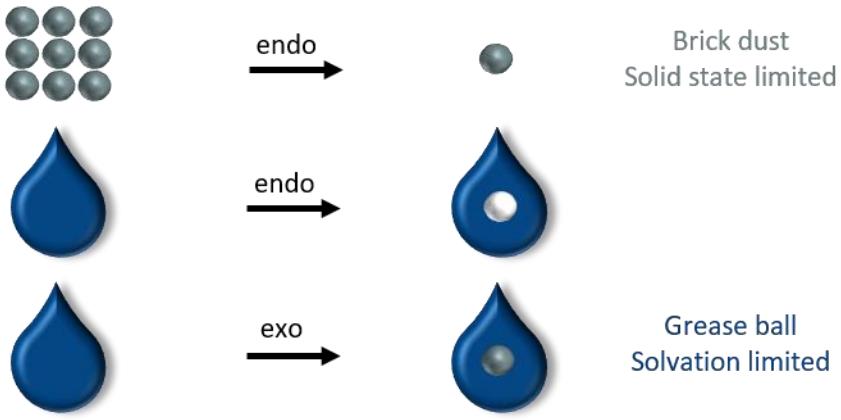

Figure 1.2. The dissolution process can be divided in three steps. Brick dust *compounds have a high melting point, the dissolution is solid state limited. Grease balls are highly lipophilic and the dissolution is limited by the solvation step. Endo = endotherm process; Exo = exotherm process. Figure adapted from Bergstrom* et al. *2016* [8].

1.2. AMORPHOUS SOLID DISPERSIONS

1.2.1. Theoretical aspects

Amorphous materials are solids, but they are isotropic and lack any long range symmetry that characterises crystalline solids. In fact, they can be visualised as frozen liquids with such a high viscosity that they occur as solids[18]. The amorphization process can be explained trough the enthalpy/entropy versus temperature relation, plotted in Fig 1.3[19]. During the heating of a crystalline material, the enthalpy will slightly increase. The crystals will melt at a certain temperature, called the melting point (T_m), and they transform into a liquid, which is coupled with a step change in the enthalpy. If the liquid is now cooled slowly (Fig 1.3A), the material will follow the path in opposite direction and the molecules will be rearranged into a lattice and form crystals. In contrast, if the liquid is cooled at a very high rate (Fig 1.3B), the timeframe for rearrangement is too short. The enthalpy continuously decreases and the liquid will become supercooled. Further decrease of the temperature will cause a drop in mobility and the molecules will not be able to follow the fast cooling rate. They fall out of equilibrium at the glass transition temperature (T_g) and the super cooled liquid is transformed into an amorphous solid or glass.

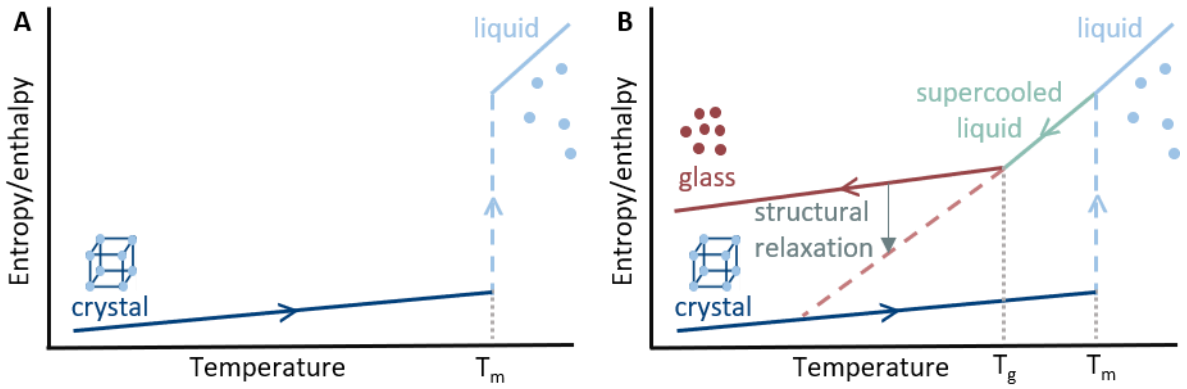

Figure 1.3. Schematic graphs of the enthalpy/entropy of a material in function of the increasing temperature and A: A slow cooling rate versus B: A fast cooling rate. T_m = melting temperature; T_g = glass transition temperature. Figure adapted from Singh and Van den Mooter 2016 [19].

Another fact that is visualised in Fig 1.3, is that amorphous solids are more energetic and not organised in a long range but organised on a length scale of a few molecular dimensions. Hence, the first step in the dissolution process will require less energy compared to crystalline solids for which the crystal lattice energy needs to be overcome. Nonetheless, amorphous solids represent the non-equilibrium state and will spontaneously tend to lower the free energy via structural relaxation in order to reach the enthalpy level of the extrapolated supercooled liquid or even to nucleate and crystallise[20]. Consequently, pure amorphous APIs are very rarely used in a final drug product as such, because the risk of conversion to the crystalline state during storage[21].

One way to improve the stability is the use of inert carriers. Often, amorphous polymers are used in which the API is molecularly dispersed to form an amorphous solid dispersion (ASD) or glass solution[18]. A glass solution is thus a homogeneous system showing one T_g and stabilisation by the carrier is an interplay of multiple phenomena. Interactions between functional groups of the API and carrier like hydrogen bonds or dipolar interactions induce a local decrease in the molecular mobility[22]. The high viscosity and lack of other API molecules in close vicinity, form a physical barrier that prevents clustering of the API and phase separation into a polymer rich and API rich phase[23]. Additionally, the carrier has often a high T_g and acts as an anti-plasticizer which is beneficial as it is generally accepted that the molecular mobility is strongly reduced at 50 K below the T_g[24]. Hence, if the T_g of the system is high, the ASD should be stable at room temperature. However, the 'T_g - 50 K' rule is a prevailing rule of thumb, but during the past years it has been investigated that it is not conclusive. The molecular mobility of an ASD can be subdivided into the global/primary α-relaxation and local/secondary β-relaxation. The α-relaxation is the type of molecular mobility that causes the $T_{g(\alpha)}$ as described above whereas the β-relaxation is defined by a lower activation energy and consequently occurs at temperatures below the $T_{g(\alpha)}$. It has been studied that the T_g of the β-relaxation is a better indicator for the stability and onset of crystallisation[25,26].

The beneficial effect of the carrier in the ASD in not only limited to the stability, but also favourable in terms of dissolution. With the intention of immediate release dosage forms, hydrophilic carriers are used, which also improve the wettability. The hydrophilic carriers dissolve at the moment they come

into contact with the aqueous GI fluids, releasing the drug to form a supersaturated solution[23]. Subsequently, the carrier contributes in maintaining the supersaturation. More precisely, the increased viscosity and drug-polymer interactions prevent precipitation and, moreover, absorption of the polymer on nuclei prevents crystal growth[22]. Lastly, in an ASD, the particle size of the API is strongly reduced as the API is dispersed in the carrier at the molecular level, which increases the dissolution rate as follows from the Nernst-Brunner equation (Eq 1.1). In addition to the fact that the amorphous solubility is higher than the crystalline solubility because of the increased free energy as mentioned above, formulation as an ASD is thus advantageous regarding the dissolution rate.

Throughout the years, several hydrophilic amorphous carriers have reached the market for ASD manufacturing. Most notably are the cellulose derivatives such as hydroxypropyl methyl cellulose (HPMC) and hydroxypropyl cellulose (HPC) and the polyvinyl polymers: polyvinylpyrrolidone (PVP), poly(vinylpyrrolidone-co-vinyl acetate) (PVP-VA) and vinyl caprolactam-polyvinyl acetate-polyethylene glycol graft copolymer (Soluplus®)[22,27]. To date, it is not possible to predict *a priori* which polymer would be most suited for an ASD of a specific API[22]. Moreover, the way of manufacturing will also influence the properties of the ASD[28-30]. Hence, the physicochemical properties of both API and polymer as well as the type of manufacturing process should be taken into account to achieve an ASD with optimal stability and dissolution profile.

1.2.2. Solid state analysis

To investigate the solid state of ASDs, a variety of analytical methods is available. A few examples are the calorimetric methods like differential scanning calorimetry and isothermal microcalorimetry; spectroscopic methods like solid state NMR or infrared spectroscopy; microscopic methods like polarised light and atomic force microscopy; scattering methods like X-ray powder diffraction or X-ray photoelectron scattering[3,31]. In this thesis, modulated differential scanning calorimetry (mDSC) and X-ray powder diffraction (XRPD) are the main methods used. Applying at least two complementary methods to evaluate the amorphicity/crystallinity of an ASD is highly recommended[29,32].

Modulated differential scanning calorimetry (mDSC). DSC is the most widely used thermal analysis technique in the characterization of ASDs[33,34]. During DSC, the ASD sample is subjected to a linear temperature ramp and the difference in heat flow to the sample and a reference is measured. The results are compiled in a thermogram that shows the heat flow in function of the increasing temperature. Melting of crystalline material will be seen as an endothermic peak, while the glass transition will be seen as a step change in the baseline due to the change in heat capacity. Because the events often overlap with the evaporation of moisture or residual solvent in the ASD, and the change in heat capacity at the T_g can be very small, mDSC is commonly used. A sinusoidal temperature modulation is superimposed on the linear heating ramp in such a way that the total heat flow, as measured with DSC, can be deconvoluted in a reversing and non-reversing heat flow. Events that respond to the temperature modulation, like the glass transition, appear in the reversing heat flow. Contrary, the events resolved in the non-reversing heat flow e.g. crystallisation and evaporation of solvents, are kinetically hampered to follow the fast heating changes[35]. Additionally, phase separation

in an ASD can be detected as two separate T_g's, one corresponding to the API-rich and one to the polymer-rich domain.

X-ray powder diffraction (XRPD). In XRPD, the sample is irradiated with monochromatic X-rays and the incident beam is diffracted by the atoms composing the material[31,33]. In case of a crystalline material, positive interference of the scattered waves by the crystal lattice planes only occurs when these waves are in phase, cfr. Braggs law, generating the characteristic Bragg peaks in the diffractogram. Hence the angle between the incident beam and the diffraction planes (ϑ) is continuously increased during the experiment in order to allow positive interference for each plane of the crystal lattice which leads to the characteristic Bragg peaks of crystalline material in the diffractogram (plot of diffraction intensity in function of 2ϑ). Since amorphous materials lack any long range order and lattice structure, a diffuse halo instead of Bragg peaks will be observed.

1.2.3. Manufacturing methods

The most conventional methods to manufacture ASDs can be classified into the solvent or the fusion based methods, with spray drying and hot melt extrusion the most commonly used examples of each category[28,36,37]. The choice of the manufacturing technique will not only depend on the characteristics of both API and polymer, but will greatly affect the properties of the produced ASD like stability, solid state, morphology and pharmaceutical performance.

In case **solvent based methods** are applied, the API and polymer are dissolved in a common organic solvent after which the solvent is evaporated. With spray drying as golden standard, the organic API-polymer solution is pumped through a nozzle into a drying chamber filled with a hot gas[38,39]. The nozzle atomizes, for example via pressurised air, the fluid into fine droplets which allows fast evaporation of the solvent to form microparticles. The particles are transferred with the drying gas to a cyclone where they are isolated to be collected (Fig 1.4A)[39]. The short time scale for evaporation kinetically traps the API in the polymer carrier, yielding no time for organisation into a crystal lattice and thus amorphous material can be obtained. Other methods are fluidised bed coating, in which the solution is atomized

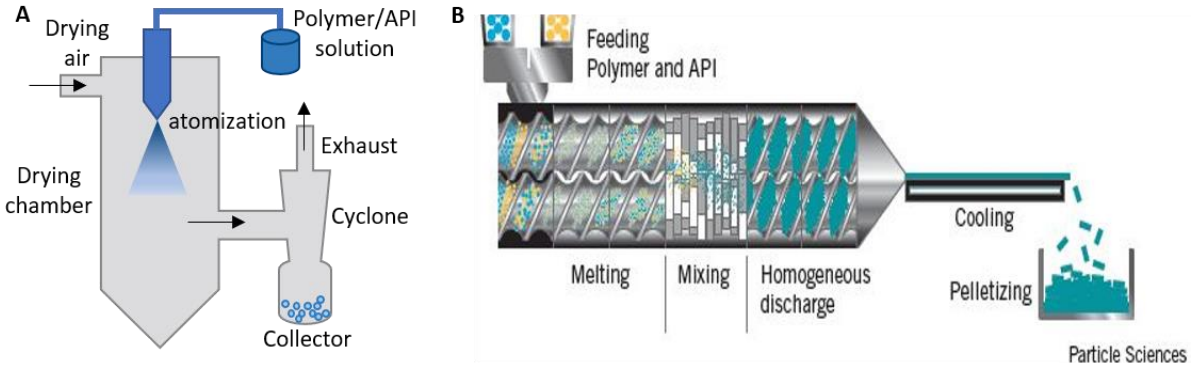

Figure 1.4. Schematic representation of the two most common ASD manufacturing methods. A: Spray drying, adapted from Sosnik and Seremeta 2015 [39]. B: Hot melt extrusion copied from https://www.particlesciences.com/news/technical-briefs/2011/hot-melt-extrusion.html.

onto inert beads, or freeze drying, where the solution is frozen and the solvent removed via sublimation[40,41].

Fusion based methods rely on the principle that was illustrated in Fig 1.3: a polymer-API powder mixture is heated and the melt is cooled rapidly. More specifically in hot melt extrusion, the powder mixture is heated in a barrel above the T_g or T_m and, via rotating screws, intimately mixed to molecularly disperse the API in the polymer (Fig 1.4B)[42]. Subsequently, the mixture is passed through an extrusion die to obtain strands, sheets, granules, etc.[43]. An example of a less conventional method is spray congealing, where the heated mixture is sprayed into a chamber with cold air[44]. Besides, ASDs can be manufactured via mechanochemical activation techniques such as milling or cryogrinding[45,46].

1.2.4. Downstream processing

For administration to patients, ASDs manufactured with the above described methods need to be processed into a final drug product. According to a recently published study, most of the ASD that are on the market are formulated as tablets, with capsules representing the second place[47]. However, spray dried powders often show poor flowability and compressibility, which hinders tablet compression and capsule filling[19]. Hence direct compression is often not possible and a pre-compaction step can be introduced to densify the ASD powder. Still, more noteworthy is the use of a granulation step to improve the powder properties[48,49]. This can either be dry granulation via roller compaction or wet granulation. Regarding hot melt extrusion, the extrudates can be ground to achieve a processable powder or the extruded strands can directly be cut in a tablet shape e.g. calendaring. Important to note is that all these steps can have a detrimental impact on the ASD as they involve mechanical stress or introduce moisture. This can lead to physicochemical changes, crystallisation and therefore, a different bioavailability.

Often, a coating layer is applied on the tablet or capsule. This can be done in order to protect the final drug products against moisture during storage, to mask the taste of the API, for site specific targeting in the GI-tract or for example to attain a sustained release profile. Most commonly, the film forming polymer is dissolved or dispersed in either an organic or aqueous solvent and sprayed onto the tablets that are rotated in a drum[50]. Again caution must be taken regarding the effect of the mechanical stress, elevated temperature and moisture on the stability of the ASD[48,51]. Dry coating or solvent free coating methods are available that can be an alternative to avoid some of these problems[51,52]. Examples of polymers that are used as coating agents are the basic amino methacrylate copolymer (Eudragit® E100), typically used for taste masking as it only dissolves below pH 5, and the following acidic polymers, which are often used for enteric coatings: hydroxypropyl methyl cellulose acetate succinate (HPMC AS), hydroxypropyl methyl cellulose phthalate (HPMC P), cellulose acetate phthalate (CAP) and the copolymer poly(methacrylic acid-co-methyl methacrylate) P(MAA/MMA) in different monomer ratios, commercially available as Eudragit® S100/L100[52-54]. Ethyl cellulose in turn is a water insoluble cellulose derivative used to achieve sustained release[55].

Despite the general predilection for tablets or capsules, it is not evident for many patients to swallow these large solid dosage forms. Crushing and splitting of tablets or opening of capsules with a

functional coating can be very dangerous and even fatal as the specific functionalities of the dosage form will be lost and the release profile will be altered[56,57]. Consequently, there is a need for easy-to-swallow solid dosage formulations where the release of the ASD can still be tuned via a coating layer. A less conventional but auspicious method in this context is coaxial electrospraying whereby ASD particles can be produced that are individually coated. The obtained particles can serve as a powder for reconstitution that can be mixed with food or drinks, offering easy administration for the patient. Moreover, coaxial electrospraying produces the coated particles in one single production step, bypassing the additional downstream processing steps and related risks regarding stability. While proof-of-concept studies can be found in literature that show the ability of coaxial electrospraying to produce core-shell structured particles, the knowledge on adapting the release of ASDs remains limited, and consequently the topic of this project[58,59]. In the following part, the general principles of electrospraying will be explained, succeeded by a more specific introduction on coaxial electrospraying.

1.3. ELECTROSPRAYING

1.3.1. Fundamentals of electrospraying

Electrohydrodynamic atomization or electrospraying is based on the ability of an electric field to atomize a liquid stream into droplets. More precisely, the term electrohydrodynamic relates to the effects of an *electric* stress on the *dynamics* of fluids. The first foundations of electrospraying date from centuries ago, when Lord Rayleigh described in 1882 the maximum a droplet can be charged before it will shatter. The first electrospraying experiments were conducted in the beginning of the 20th century and it was observed that a liquid stream deforms into a triangular cone under influence of an electric field. This cone is now known as the Taylor cone, named after Geoffrey Taylor who described the electrospray phenomenon and cone formation in the sixties[60,61]. Afterwards, the electrospraying process became widely used as ionisation method in mass spectrometry and more recently it gained interest for the production of nano-/microparticles and as an amorphization method in the pharmaceutical field[59,62].

A basic setup to perform electrospraying consists of a pump, nozzle, high voltage generator and collector (Fig 1.5). In case of ASD manufacturing, electrospraying can be classified as a solvent based method, thus the API and polymer are dissolved in a common organic solvent. The solution is pumped through the nozzle at a very low feed flow rate (range of µL-mL/h) and an electric field is applied. If the generated electric stress is high enough to balance the surface tension, the meniscus of the solution will be deformed into a Taylor cone[63]. The surface charges are accelerated with the direction of the electric field towards the apex of the cone resulting in the formation of a thin jet, which will exist over a certain distance and will than split up to form an aerosol of tiny droplets[64]. The solvent will almost instantaneously evaporate from the droplets as they fly towards the collector. Consequently, dry ASD particles can be collected because the API is kinetically trapped and dispersed in the polymer, similarly as explained before for spray drying. However, in this case, the time frame for evaporation is much faster and there is no need for heat to achieve evaporation of the solvent.

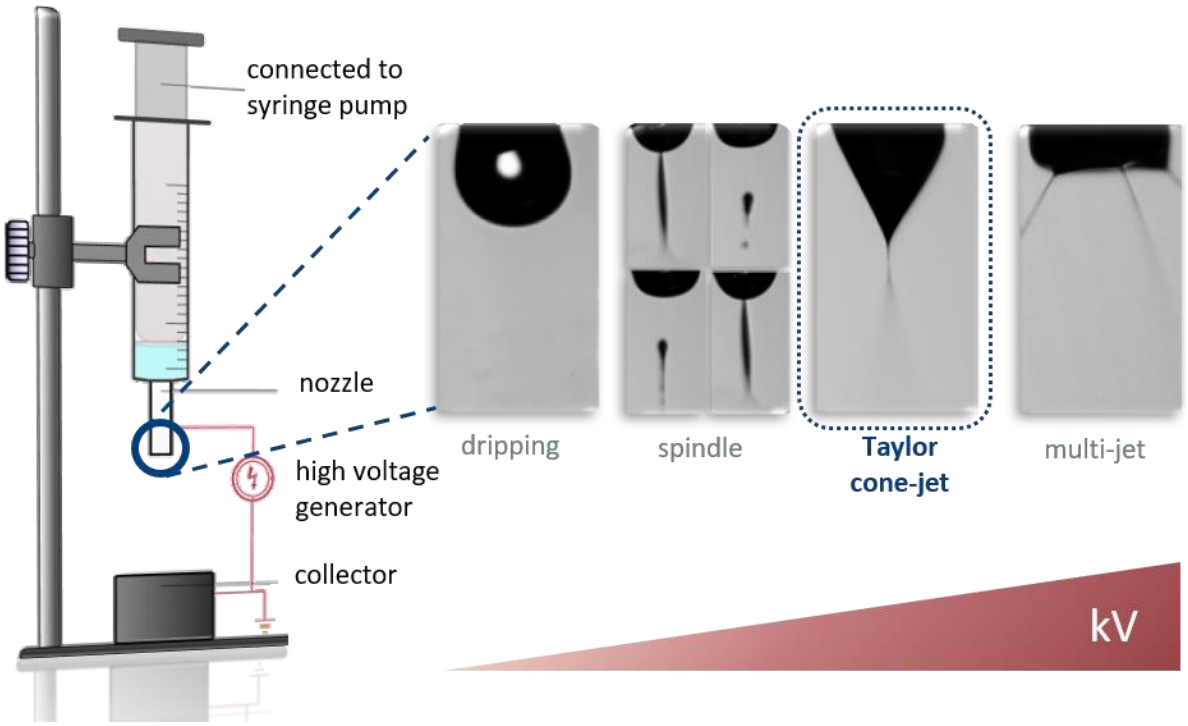

Figure 1.5. Electrospraying setup consisting of a syringe pump, nozzle, high voltage generator and collector. Images from left to right illustrate the different spraying modes obtained when the potential difference is gradually increased. Figure adapted from Smeets et al. *2017* [65].

The formation of the cone-jet is a result of different forces acting on the solution but briefly, if the applied electric field is not strong enough, it will not be able to contend the surface tension resulting in an dripping or spindle mode and collection of wet droplets. If on the other hand the electric field strength is too high, multiple jets will be created (Fig 1.5)[65]. Hence, key point for reproducible production of particles is a stable cone-jet mode.

1.3.2. Electrospraying versus electrospinning

When using higher molecular weight polymers or higher polymer concentrations, the electrospraying process risks to shift towards electrospinning, another but closely related electrohydrodynamic phenomenon. While during electrospraying the tip of the cone-jet splits up and creates an aerosol, the jet is stabilised in electrospinning, which inhibits the jet break-up. Ergo, the jet grows in length and moving toward the collector, the solvent evaporates which will lead to the collection of thin fibres. Whether particles or fibres are formed is mainly governed by the amount of chain entanglements in the polymer solution, which again is a function of the polymer molecular weight, concentration and the solvent quality as this will determine the chain conformation[66].

At low concentrations, below the critical overlap concentration (c*), the separate polymer chains do not interact with each other and this is called the dilute regime (Fig 1.6A)[67]. Once c* is reached, the semi-dilute unentangled regime is entered (Fig 1.6B). Despite the fact that chains start to overlap, there is insufficient entanglement to completely stabilise and inhibit jet break-up. Consequently, a mixture of beads and fibres will be produced. Further increase in concentration will lead to the semi-dilute entangled regime were beaded as well as uniform fibres can be obtained (Fig 1.6C). The entanglement concentration (c_e) is now reached with interlocking of the separate polymer chains. Shenoy *et al*. determined that this shift to electrospinning occurs for low molecular weight polymers, as is the case for most of the ASD carriers, from 2.5 entanglements per chain onwards[68].

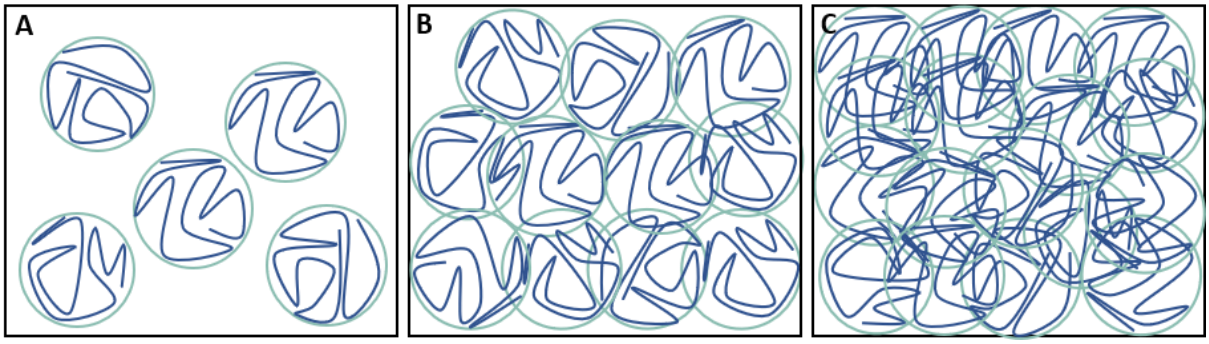

Figure 1.6. Visualisation of the polymer chains in the electrospraying/spinning solutions with increasing polymer concentration. A: Dilute regime, the polymer concentration is below the critical overlap concentration c. B: Semi-dilute unentangled regime, concentration above c* but below the entanglement concentration c_e. C: Semi-dilute entangled regime, concentration above c_e. Figure adapted from Gupta* et al. *2005* [67].

Since the underlying principle of both spinning and spraying is the same, electrospinning can also be used for the production of ASDs[69]. In view of powders for reconstitution with specific release requirements, yet minimising the amount of processing steps, particles are preferred over fibres, because the core-shell fibres will need to be cut in smaller pieces and the blunt ends will not be coated anymore. Consequently, electrospraying is the method of choice in this thesis.

1.3.3. Particle formation

To explain the solidification of the droplets ejected from the cone-jet during electrospraying, the link is made to droplet drying during spray drying. Comparably, a fluid stream is atomized into droplets followed by evaporation of the solvent, diffusion of the solutes and polymer chain entanglement. Since spray drying is the golden method for ASD manufacturing and also extensively used in other industrial fields like the food industry, much more literature is generated to date on the spray drying process. Moreover, in the second experimental project of this thesis (chapter 4), a one on one experimental comparison is made between particles produced with spray drying and electrospraying, hence a parallel description of the solidification process is made in the following paragraphs.

Spray drying. Many models have been developed during the years to describe the solidification process but basically, it can be explained using the Peclet number (Pe) which is a dimensionless number that can simplified be defined via the following equation[70,71]:

$$Pe = \frac{\kappa}{8D} \quad \text{(Eq 1.2)}$$

In this equation, D is the diffusion coefficient of the solute in the droplet and κ represents the droplet evaporation rate which is described as followed, with d being the droplet diameter:

$$d^2(t) = d_0^2 - \kappa t \quad \text{(Eq 1.3)}$$

Once a droplet enters the drying chamber (Fig 1.4A), evaporation of the solvent begins, leading to shrinkage of the droplet (Fig 1.7). As evaporation starts from the outside of the droplet, solutes are concentrated at the surface and the ensuing concentration gradient causes them to migrate to the centre. From this point onwards, two scenarios are possible, defined by the Pe being larger or smaller than 1[71]. If Pe < 1 (right hand side of Fig 1.7) the rate of evaporation will be rather slow compared to the diffusion of the solutes. This means that migration of the solutes can keep pace with the evaporation and shrinkage goes on till the saturation concentration of the solutes is reached. At this point, the solutes will homogeneously solidify yielding a smooth and dense particle.

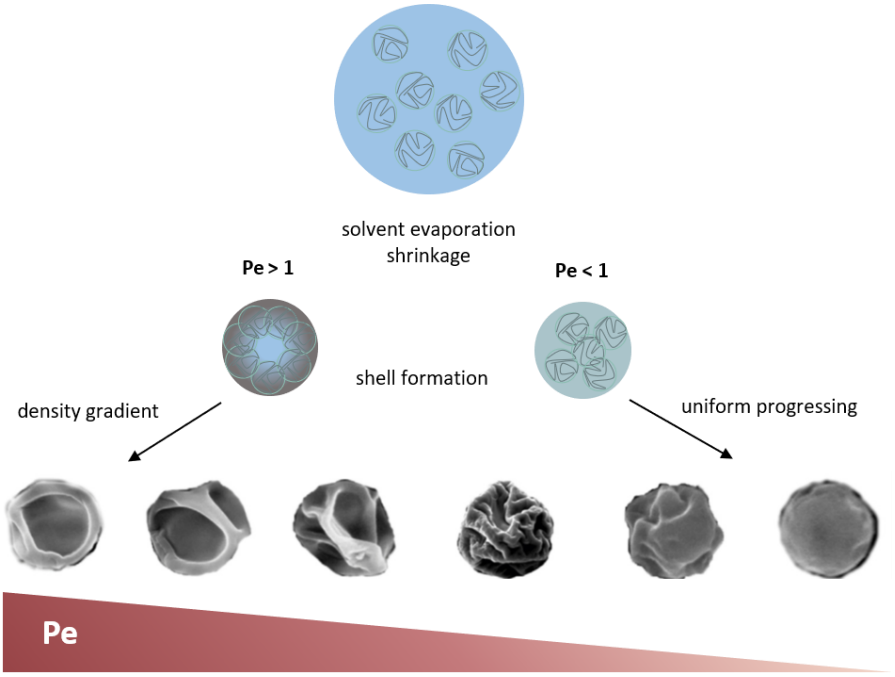

Figure 1.7. Droplet drying and solidification process in spray drying/electrospraying. Solvent evaporation leads to shrinkage of the droplet. If the Peclet number Pe > 1, collapsed or wrinkled particles are obtained. If Pe < 1, smooth and dense particles are obtained. Figure adapted from Nguyen et al. *2016* [64].

However, most polymer-solvent combinations to make ASDs have a Pe > 1 (left hand side of Fig 1.7). The solvent evaporates quickly but the diffusion of solutes (polymer) is slow. Migration of the solutes towards the centre is limited and the saturation concentration at the surface will rapidly be reached creating a shell that covers the surface. The remaining solvent is trapped inside the shell and the pressure build-up will eventually cause cracks or explosion of the particles. This explains the characteristic wrinkled, dimpled morphology of spray dried ASD particles.

Electrospraying. The literature on droplet drying during electrospraying is less extensive but one can partially rely on the evaporation/diffusion phenomenon as described for spray drying. Nonetheless, the process is more complex due to the effects of the electric stress. The droplets emitted from the jet are charged (Fig 1.8)[64]. During the evaporation of the solvent, the total surface charge does not change but as the droplet shrinks, the charge density increases[71]. At a certain point, the charge density will reach the Rayleigh limit, which is defined as the maximum surface charge a droplet can carry. Above this limit, the surface tension can no longer withstand the electrostatic repulsion and the droplet will split up into smaller offspring droplets, a phenomenon which is better known as Coulomb fission. The evaporation process and shrinkage will continue and the competition between evaporation and diffusion can also be described with the Pe.

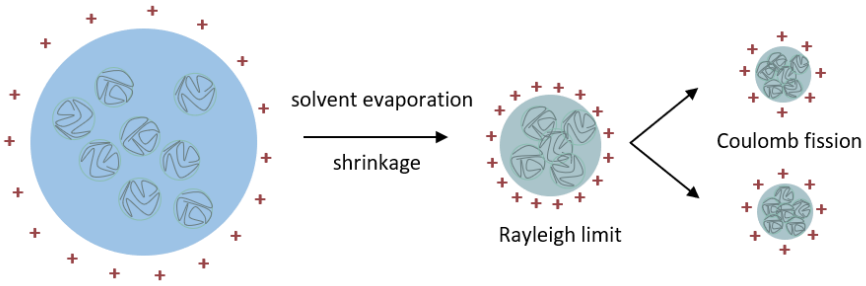

Figure 1.8. The primary droplet emitted from the cone-jet during electrospraying is charged. Due to solvent evaporation and shrinkage of the droplet, the charge density will reach the Rayleigh limit and Coulomb fission will occur, resulting in smaller offspring droplets. Figure adapted from Nguyen et al. *2016* [64].

Furthermore, the amount of chain entanglements that are already present at the moment Coulomb fission occurs will also affect the solidification process and final morphology of the particles. An interesting study in this context is the one performed by Almería *et al*. who controlled the morphology of poly(lactic-co-glycolic acid) (PLGA) particles[72]. They concluded that spherical particles are collected if enough polymer chain entanglement is reached before Coulomb fission takes place because the fission energy cannot break up the polymer network. Contrary, if Coulomb fission precedes formation of entanglements, the droplet will shatter into smaller droplets. Still, when already a certain degree of entanglement is created the moment the droplets stretch to split, the droplets will freeze in this elongated shape or form particles with irregular (tail-like) shapes.

1.3.4. Influence of process and formulation parameters

The different parameters that can be varied during the electrospraying process do not only affect the properties of the produced particles but will also affect the working window. The latter is defined as the limits for the parameters that still lead to the formation of a stable cone-jet mode and thus production of solid particles. Only for a limited amount of setting combinations, electrospraying in the cone-jet mode will be achieved. Today, the working window is often determined via trial and error. Hence, in the first experimental part of this thesis (chapter 3), it is investigated how both process and formulation parameters impact and change the working window in electrospraying polymers applied in ASDs, allowing the development of a more rational approach in choosing the appropriate settings.

The influence of the parameters on the morphology and size of the particles is described below. It must be noted that these are general trends and not specifically obtained for ASDs.

Process parameters. Referring to the electrospraying setup in Fig 1.5, the parameters to be varied are the feed flow rate, the applied potential difference and the distance between the tip of the nozzle and the collector. Increasing the feed flow rate will lead to the collection of larger particles. Indeed, the particle size is related to the size of the generated droplets and scaling laws are developed which state that the size of the droplets is proportional to the feed flow rate[59]. This also implies that only low flow rates (µL-mL/h) can be used if particles with size in nano/micro range want to be collected. Moreover, if the flow rate is too high, the droplet drying will not be completed when the droplets reach the collector. Finally, higher flow rates will promote the formation of satellite droplets, leading to polydispersity[73].

Regarding the effect of the potential difference, a decrease in particle size has been reported with increasing voltage and thus electric field strength[74]. Besides, particles become more elongated as a result of the increased electric stress. Lastly, a higher tip-to-collector distance will generate larger particles as the strength of the electric field decreases, but a short distance can lead to the collection of wet or collapsed particles as they reach the collector before the evaporation process is completed[73]. Additionally, the diameter of the nozzle can be altered. However, there is limited evidence that the nozzle diameter affects the properties of the particles, it is stated that smaller needle sizes are more suitable[73,74].

Formulation parameters. As explained in the section on electrospinning, changing the type of polymer for the ASD, the polymer concentration and the solvent quality will affect the amount of chain entanglement and thus the morphology of the particles (or fibres). The influence of increasing the polymer concentration together with effects of the feed flow rate and potential difference is summarised in Fig 1.9[74]. With respect to the solvent, the influence of its volatility is incorporated in the Pe number. Thus, solvents with high volatility will give rise to rather dimpled and porous particles while a low volatility is related to smaller and dense particles. Care must be taken that the volatility is not too low so proper drying is ensured before the particles hit the collector[73].

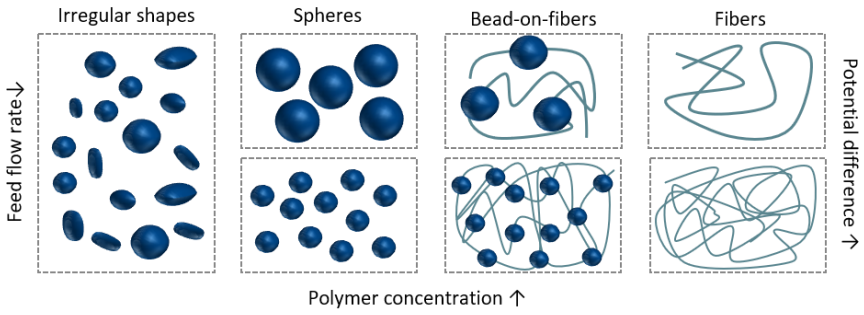

Figure 1.9. Influence of the feed flow rate, potential difference and solids concentration on the properties of the electrosprayed particles. Adapted from Alehosseini et al. 2018 [74].

The interplay between the formulation parameters also implies changes in characteristics like the conductivity, surface tension and viscosity of the solution, which will all affect the electrospraying process. Most notably is the effect of the conductivity on the size of the particles. A higher conductivity will lead to smaller particles and increased polydispersity because the droplets emitted by the jet will be smaller and Coulomb fission is incited[64]. Important to note is that the temperature and relative humidity greatly affect the viscosity, conductivity, surface tension, evaporation rate, etc. Working in a climate controlled environment is thus advisable.

1.3.5. Advantages and limitations

Electrospraying offers several advantages which are listed and briefly commented below:

- The particle sizes that can be produced cover a broad range. For example, in a review by Bock *et al.*, an overview was made of different studies on API loaded polymer particles, reporting particle sizes ranging from 100 nm till 22 µm[73]. This is an interesting feature as the particle size can affect the dissolution rate and can consequently be used to tune the release rate.

- Electrospraying has the ability to produce particles with a narrow size distribution, however this is not self-evident. In the same review of Bock *et al.*, the polydispersity of the different sized particles were reported, revealing that for particles in the same size range, very narrow but also broad particle size distributions were obtained, depending on the settings of both operation and formulation parameters[73]. In general, a narrow distribution is achieved at lower conductivity, flow rate and potential difference (less electric stress prevents uncontrolled Coulomb fission, which is the cause of the polydispersity) and higher polymer concentrations (more resistance against Coulomb fission). Furthermore, a neutralizer, often a stainless steel ring connected to a second high voltage generator, can be used to discharge the droplets and thereupon can prevent Coulomb fission[64].

- Since the droplets all carry the same charge, they repel one another, creating a self-dispersing aerosol which is a favourable aspect that other atomization methods do not display[64,73]. It inhibits the coagulation of the droplets during the solidification process, and in this way aggregation, a factor that decreases the reproducibility.

- High encapsulation efficiencies can be achieved, rendering a minimal loss of the often valuable API[75,76].

- Electrospraying consists of an easy to assemble setup, with a minimum requirement of resources (pump, nozzle, high voltage generator and collector).

- The process can run at ambient conditions, which is a major advantage for thermolabile APIs, but it also allows processing of challenging biological compounds like proteins, enzymes, DNA, living cells and even whole organisms[64].

- Electrospraying offers versatility towards the collection method. The particles can be collected on a flat surface like a petri-dish or aluminium foil, but they can also be collected on a rotating

drum or directly into a fluid bath to form a suspension[77,78]. Moreover, setups are designed that offer a more continuous collection, as for example in the publication by Grafahrend *et al*[79], where via a flow of air, the electrosprayed particles are transported through a tubing to a cyclone-type collector.

Despite these numerous advantages, electrospraying is not pervaded yet in the ASD manufacturing industry, in contrast to spray drying and hot melt extrusion. Examples of ASDs on the market are Crestor by AstraZeneca, a spray dried ASD of rosuvastatin and HPMC or Norvir, a hot melt extruded ritonavir-PVP ASD produced by Abbott. Besides this, also fluidized bed coating is commercially used for the production of Sporanox, which is an ASD of itraconazole and HPMC, manufactured by Janssen[47].

The two major disadvantages, which most likely cause the underrepresentation of electrospraying, are the limited knowhow and low production capacity of the process. Compared to spray drying, whose research and commercial use, not only regarding pharmaceutical applications but also in other fields like the food industry, goes back for many years, electrospraying is still in its infancy. As an illustration, a quick search in the online library of the university gives more than 120 000 hits for the term 'spray drying', but only 6 500 for 'electrospraying'. Since spray drying is widely spread and commercially established, it is used in the second experimental part (chapter 4) of this thesis as a benchmark to compare to the electrosprayed ASDs.

Regarding the production rate, the throughput of a laboratory single nozzle setup as depicted in Fig 1.5 is extremely low, in the range of a few milligrams to maximum grams per production hour. This off course is a major limitation with the aim of commercialization. Due to the nature of the process, just using a larger nozzle and higher flow rates are not an option. As the size of the droplets and consequently the particles is directly proportional to the feed flow rate, nano/micro particles can only be guaranteed for low flow rates. Therefore, different approaches have been addressed regarding the scale-up of the system, ranging from a linear arrangement of multiple nozzles in parallel to more

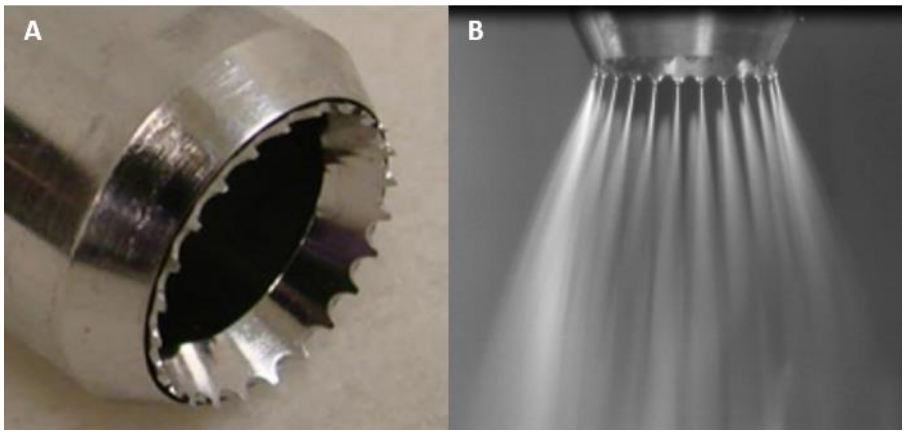

Figure 1.10 A and B: D24 nozzle that generates 24 cone-jets at the time from Nanocopoeia, Inc. copied from http://nanocopoeia.com/wp-content/uploads/2017/01/CRS-2016_07_07-ENS-Poster-Final-crs.pdf.

complex systems. As an illustration, Bocanegra *et al.* designed a nozzle by drilling holes in a plate instead of using needles/capillaries as nozzle[80]. By doing so, a multi-emitter could be created consisting of no less than 115 emitters per square centimetre, which on top is easier and cheaper to manufacture compared to a multi-nozzle consisting of needles.

The biggest challenge regarding multi-emitters is the fact that the different cone-jets disturb each other's electric field and an equal flow to each emitter must be guaranteed. Though, lot of progress has been made and today multi nozzle systems are commercially available. Example is the high throughput ElectroNanospray™ engineered by Nanocopoeia (Minnesota, USA), a company that offers electrospraying following good manufacturing practices (GMP) of commercial materials[81]. By combining 8 nozzles, that each consists of 24 emitters, the system can generate 192 cone-jets at the time (Fig 1.10A/B)[82]. Nevertheless, it must be noted that for specific applications, a low throughput can just be beneficial. As to date, it is hardly possible to predict which polymer carrier, drug loading or solvent will be optimal to manufacture the ASD for a specific API. Consequently, an extensive screening is often necessary in the early stage, with often only a few nano- or micrograms of the API available. Electrospraying can in this context be superior as small amounts and low concentration are sufficient and the product can for example be directly collected into small vials, leading to a very high yield compared to spray drying.

A major advantage not yet touched upon is the flexibility of electrospraying regarding the type of nozzle that can be used, namely a single nozzle, a nozzle with two concentrically aligned channels (coaxial nozzle) or even nozzles with three channels. This way, particles consisting of multiple layers can be produced. The following part elaborates on coaxial electrospraying as production method for coated ASD particles.

1.4. COAXIAL ELECTROSPRAYING

1.4.1. Concept of coaxial electrospraying

The fundamental principle of coaxial electrospraying is exactly the same as in standard electrospraying, the only difference is the nozzle type. A coaxial nozzle exists of an inner and outer part, through which a solution for the core and another solution for the shell layer, are pumped by the use of two syringe pumps (Fig 1.11A). As a result, a two layered cone-jet is formed at the tip of the nozzle that breaks up in droplets, wherein the outer solution completely engulfs the inner one. Therefore, core-shell structured particles are created in just one step, which offers a major advantage over the conventional ASD manufacturing methods. Due to the presence of the second solution, the choice for the appropriate process and formulation parameters, both for obtaining a stable cone-jet as well as to tune the properties of the produced core-shell particles, becomes even more challenging.

The fact that coaxial electrospraying can produce core-shell structured nano- and microparticles is confirmed by a considerable number of papers dealing with the encapsulation of a great variety of materials, ranging from small organic APIs to biological materials like bovine serum albumin and even living cells[58,59,83]. Regarding the fabrication of coated ASDs, only a handful of studies has been

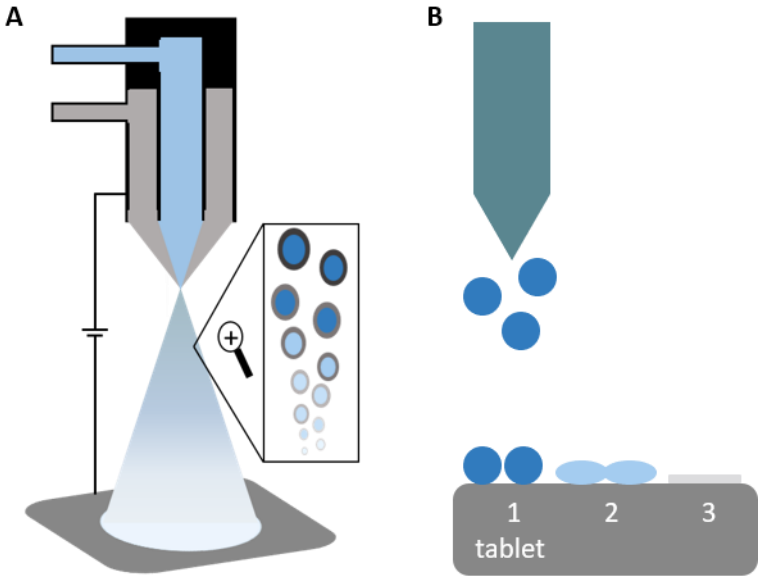

Figure 1.11. A: Schematic representation of a coaxial electrospraying setup. B: Tablet coating process. Droplets are sprayed onto surface, due to solvent evaporation, the droplets coalesce and a polymeric film is formed. Figure adapted from Felton and Porter 2013 [50].

published and challenges like proper amorphization and tailoring of the API release remain[78,84]. As further understanding of these challenges/limitations and optimisation are topic of this thesis, they will be expounded in-depth in the different experimental chapters.

The way the coating layer is formed during the coaxial electrospraying process is thus completely different from the coating formation during a traditional coating process of a tablet (Fig 1.11B). During the latter, the polymer solution is sprayed as an aerosol and the droplets will settle at the tablet surface, where they will start to spread out. As solvent evaporation progresses, a polymeric film will be formed that covers the tablet surface[85]. Contrary, during electrospraying the coating is immediately formed around the core during the solidification process of the entire particle. Consequently, the properties of the coating will depend on the set process and formulation parameters. Furthermore, also the analysis of the coating layer becomes more challenging. Due to the small dimensions of the particles and thickness of the coating layer, the applicability of conventional analysis methods to evaluate coatings on tablets, like analysing a cross-section via scanning electron microscopy, Raman spectroscopy, terahertz pulsed imaging or tomography, is limited[86,87].

1.4.2. Powders for reconstitution

Powders for reconstitution are alluring dosage forms for patients having trouble to swallow tablets or capsules. It is often overlooked that this population not only consists of paediatric patients, but also includes a continuously expanding group of elderly with dysphagia and patients with nausea or physiological issues like the fear of choking[88,89]. It is even estimated that up to 20 % of the total patient population encounters problems with swallowing tablets[89]. In many cases, powders are preferred above liquid formulations due to their stability and compactness regarding transportation/storage and

ease of dosing for the individual patient. Another alternative is the formulation of orodispersible tablets or films, but their applicability regarding modified release is rather limited. In turn, the strength of tablets is the fact that they can easily be coated in order to obtain a modified release profile. Still, as mentioned before, the downstream processing of the ASD and applying the coating can affect the stability of ASDs. This is why coaxial electrospraying can be such an asset, because coated nano- or microparticles are produced in one step avoiding any downstream processing but still leaving the option to tune the release of the API.

Tailoring the release of ASDs via a coating can be attractive for multiple purpose. Normally, when an ASD comes into contact with the aqueous GI medium, the hydrophilic polymer dissolves and the API is ideally released instantaneously to reach supersaturation. Nonetheless, the fast increase in API concentration and generation of supersaturation levels can induce precipitation of the API. One of the strategies is the use of a sustained-release formulation that generates supersaturation more slowly and consequently, reduces the tendency for precipitation[90,91]. A second case were a coating can be interesting is for site specific targeting in the gastrointestinal tract. Examples are colon targeted drug delivery and gastro-resistant formulations that only start to dissolve when transferred to the intestine, both useful for acid-labile APIs and APIs that harm the stomach[92]. Moreover, a core-shell structure can be interesting as a compartmentalised system for fixed dose combinations if the different APIs are incompatible. Powders for reconstitution are indeed extremely interesting for fixed dose combinations, as one powder that is easy to swallow, can replace a whole range of tablets and capsules.

The use of powders for reconstitution is broadly applicable and not limited to a specific therapeutic area. In the second and third experimental part of this thesis (chapter 4 and 5), the API darunavir is used as model compound. Darunavir is a protease inhibitor used in the treatment of HIV and is poorly water soluble. The choice for darunavir is merely governed by a previous PhD project on electrospraying that was conducted in our research group, which revolved around paediatric formulations of HIV medicines.

Chapter 2
Objectives

The general aim of this PhD project is to gain knowledge in the coaxial electrospraying process as manufacturing method for coated ASD microparticles, in order to support the shift from today's trial-and-error based approach to a more rational design. As a consequence, it will become possible to predict the release of the API upfront and meet the specific release requirements from the individually coated microparticles via meticulous tuning of the different process and formulation parameters. In the end, this will allow to use electrosprayed core-shell particles as a flexible platform for particles for reconstitution, regarding a variety of applications.

Despite the simplicity of the fundamental concept of electrospraying, coaxial electrospraying is a complex process, influenced by an intricate interplay of process and formulation parameters and this from no less than two different solutions (core and shell). The parameters do not only influence the working window, i.e. the formation of the cone-jet mode, but will also shape the characteristics of the produced particles. To be able to handle the complexity, a bottom-up and step-by-step approach was developed including four different parts which start with electrospraying of only the polymeric carrier and ends with coaxial electrospraying of a fixed dose combination combining multiple APIs (Fig 2.1). The objectives of each part are defined below.

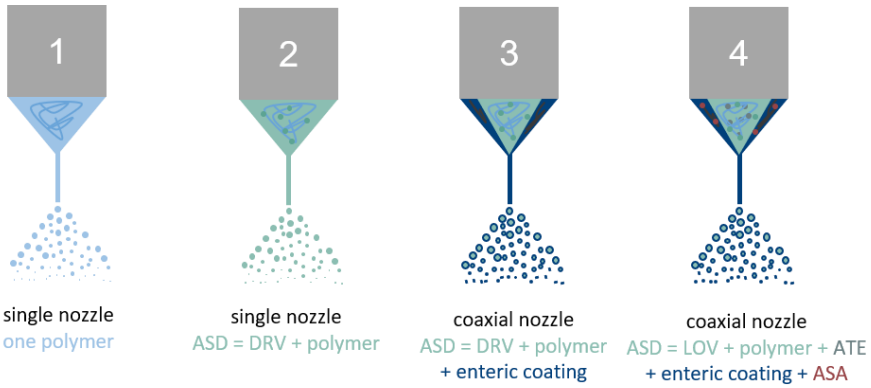

Figure 2.1. Overview of the four experimental parts. DRV = darunavir; LOV = lovastatin; ATE = atenolol; ASA = acetylsalicylic acid.

1. In the first part, **single nozzle electrospraying** is performed of solutions containing only **one polymer**, which can either be used as carrier for an ASD or can be used as coating. The aim is to investigate how these polymers react to the electric field and to identify how the process and formulation parameters influence the working window. This will allow a reasoned selection of the optimal parameters when electrospraying with a specific polymer during the rest of the project, immediately knowing the limits for the working window.

2. The goal of the second project is to evaluate whether electrospraying is an appropriate method to manufacture ASDs of the model API darunavir (which represents the ASD core of the future core-shell particles). With this in mind, **ASDs of darunavir with PVP, HPMC or HPMC AS** were electrosprayed in a **single nozzle** setup and the characteristics of the manufactured ASD particles were compared with the ones obtained by spray drying, as this is a golden standard for ASD manufacturing. Furthermore, the influence of two formulation and two

process parameters of electrospraying on the final properties of the ASD particles containing darunavir and PVP was studied.

3. In the third part, it was aimed to produce**, enteric coated ASDs of darunavir and HPMC** via **coaxial electrospraying**. In a previous study of our research group, a powder for reconstitution of the fixed dose combination containing ritonavir and darunavir was investigated. However, when combining these two APIs, it was observed that they lowered each other's solubility[93]. Therefore, the production of enteric coated particles of darunavir was investigated. This would prevent the release of darunavir in the stomach and when administered with ritonavir (without release modifications), they would be delivered in different parts of the GI tract and the mutual negative effect on their solubility would be countered. Enteric coated particles with an ASD darunavir core could be manufactured with coaxial electrospraying, but a significant burst release of darunavir in acidic medium could not be avoided despite adapting some of the settings[78]. Thereupon, the research plans for this thesis project were set in order to understand and optimise the process to be able to manufacture enteric coated particles which are in compliance with the European Pharmacopoeia (Ph. Eur.) and thus release less than 10 % of the API in acidic medium. For this purpose, different enteric polymers were screened as coating agents and additionally, it was investigated why the different enteric polymers gave rise to a different extent of burst release of darunavir in acidic medium and which underlying phenomena are causing this burst release.

4. During the last project, it was investigated whether **coaxial electrospraying** can be applied to **produce enteric coated ASD particles containing multiple APIs.** These particles will serve as powder for reconstitution of a fixed dose combination for cardiovascular therapy containing lovastatin, atenolol and acetylsalicylic acid, which are three APIs with different physicochemical properties, release requirements and stability.

Chapter 3
Electrospraying of polymer solutions: study of formulation and process parameters

Results of this chapter are based on:

Smeets A, Clasen C, Van den Mooter G. Electrospraying of polymer solutions: Study of formulation and process parameters. Eur J Pharm Biopharm. 2017;119:114-124.

3.1. ABSTRACT

Over the past decade, electrospraying has proven to be a promising method for the preparation of amorphous solid dispersions, an established formulation strategy to improve the oral bioavailability of poorly soluble drug compounds. Due to the lack of fundamental knowledge concerning adequate single nozzle electrospraying conditions, a trial-and-error approach is currently the only option. The objective of this paper is to study/investigate the influence of the different formulation and process parameters, as well as their interplay, on the formation of a stable cone-jet mode as a prerequisite for a reproducible production of monodisperse micro- and nanoparticles. To this purpose, different polymers commonly used in the formulation of solid dispersions were electrosprayed to map out the workable parameter ranges of the process. The experiments evaluate the importance of the experimental parameters as flow rate, electric potential difference and the distance between the tip of the nozzle and collector. Based on this, the type of solvent and the concentration of the polymer solutions, along with their viscosity and conductivity, were identified as determinative formulation parameters. This information is of utmost importance to rationally design further electrospraying methods for the preparation of amorphous solid dispersions.

3.2. INTRODUCTION

A significant number of new active pharmaceutical ingredients (API) suffer from poor aqueous solubility, resulting in low and variable (oral) bioavailability. These poorly soluble compounds are categorized in class II and IV of the Biopharmaceutics Classification System (BCS) and count for up to 70-90 % of all molecules in the pharmaceutical pipelines[94] (Fig 1.1). A vast amount of formulation techniques to overcome the solubility problems were developed during the past years, including amorphous solid dispersion as a popular and successful strategy[18,95]. Solid dispersions are manufactured by methods based on solvent evaporation (e.g. spray drying or film casting), heat based methods (e.g. spray congealing or hot melt extrusion), and methods relying on grinding[21,23,96,97]. However, in this paper, we will focus on a non-conventional solvent-based method, electrohydrodynamic atomization, also referred to as electrospraying. The electrospraying process was already discovered more than a century ago but it only gained in popularity after Fenn's Nobel prize in 2002[98]. He introduced the concept of electrospraying as a soft ionization method for mass spectrometry of large biomolecules[99]. Currently electrospraying is applied in a variety of fields like paint, polymers, ceramics, cosmetics and food industry and is emerging in drug delivery[64].

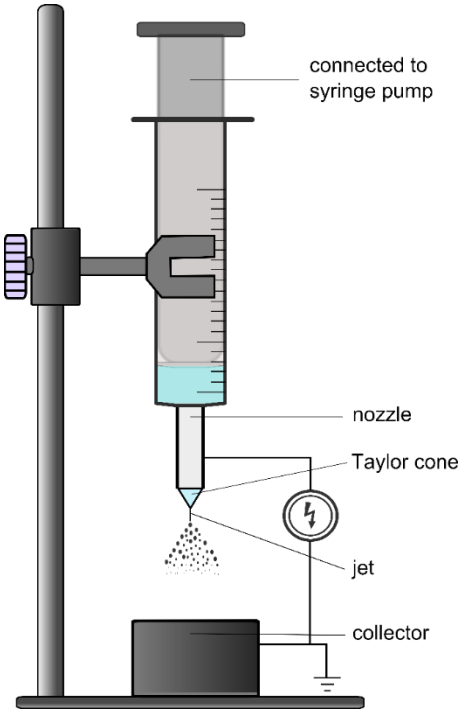

Figure 3.1. Schematic representation of the electrospraying process.

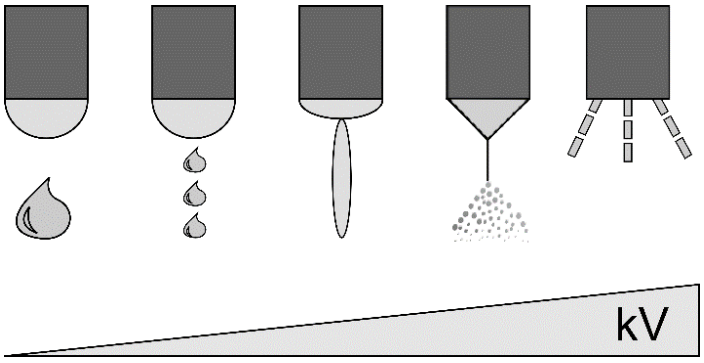

Figure 3.2. Schematic representation of the successive spraying modes when the potential difference is increased: dripping, micro dripping, spindle, cone-jet, multi-jet.

To manufacture solid dispersions via electrospraying, a solution of API and inert polymer is slowly pumped through a nozzle. By applying a high voltage to the nozzle (Fig 3.1), the liquid stream becomes highly charged, causing electrostatic stress inside the fluid leaving the nozzle. When the electric potential between nozzle and collector is sufficiently high, the electric forces will counteract the

surface tension of the liquid. The meniscus of the liquid drop forming at the nozzle tip will deform into a conical shape, called a Taylor cone. The free surface charges are accelerated towards and concentrated at the tip of the cone, leading to the formation of a jet, which further accelerates downwards and subsequently breaks up into droplets. During the flight of the emitted droplets towards the oppositely charged collector, the solvent will quickly and completely evaporate due to the small dimensions (10^{-6}-10^{-9} m) of the droplets. Dry solid dispersion particles of micro- or even nanosize are thus obtained, which can be used for further downstream processing[59,100].

Besides electrospraying in this so-called cone-jet mode, multiple other operating modes exist. Throughout the years, various systems for classification of the modes were developed[63]. In general, the following sequence can be observed when the applied voltage is increased: dripping, micro dripping, spindle, cone-jet and multi-jet mode (Fig 3.2)[98,101]. The mode that is eventually obtained depends on the balance between the surface tension and the electric stress. Hence, both the electric field strength and flow rate, as well as the physical properties of the solution (electric conductivity, viscosity and surface tension) are important and a complex interplay of these different factors determines the operating mode[73,102].

Despite the existence of the different modes, only the stable cone-jet mode is able to produce solid nanoparticles of high monodispersity in a reproducible way[63,73]. Knowledge of how the parameters influence the workspace wherein a Taylor cone can be generated is thus of utmost importance for successful electrospraying. In particular since the system can be very sensitive to even small changes, causing a shift from one mode to another[64,102].

One of the main advantages of electrospraying for the preparation of solid dispersions compared to the conventional methods is the broad range of particle sizes that can be obtained even below the micrometre range, while maintaining a narrow particle size distribution[64,102,103]. Therefore, solubility and dissolution rate problems are tackled by amorphization as well as by particle size reduction. The droplets generated during the spraying process have a high charge density on their surface. This generates Coulomb repulsion, leading to self-dispersing properties and inhibition of agglomeration and coagulation of the droplets during the drying process. The system can run at room temperature, hence it is ideal for thermolabile compounds. In addition, shear stress during droplet formation is lower as compared to spray drying, making it attractive to formulate biomolecules[104]. The short time frame for solvent evaporation is not only beneficial for formation of amorphous materials, but also decreases the risk of protein denaturation[73]. The main drawback of the process is the low yield from a single nozzle, since the production of nanoparticles only allows very low flow rates (order of µL-mL/h)[98]. This hampered the introduction of the technique in drug delivery, although more recently a lot of progress is made in upscaling of the process. Systems with multiple nozzles in parallel have been designed and are already established in other industrial fields[59,105].

Keeping the aforementioned advantages and challenges of electrospraying in mind, multiple research groups already tried to improve the bioavailability of different BCS class II and IV compounds via electrospraying. Examples are listed in Table 3.1 and prove that electrospraying is a promising

technique[78,106-123]. On the other hand, literature also shows that in some cases only partial amorphization could be realized. The methodology of all of the listed studies in Table 3.1 was based on trial-and-error. Reason is the lack of fundamental knowledge concerning adequate single nozzle electrospraying conditions for a given combination of API and polymer. In addition, the process becomes even more complicated when coaxial electrospraying is applied to generate core-shell particles (Table 3.1). In this mode of electrospraying, an inner and outer nozzle are coaxially aligned and fed with a core and shell solution, respectively. Because two distinct fluids are separately pumped through the coaxial nozzle, parameter selection and optimization becomes more difficult.

*Table 3.1. Examples of studies were electrospraying was used to formulate poorly soluble API as solid dispersions. API in the left column were amorphous, whereas for the API in the right column only partial amorphization could be reached. In six studies, marked with *, a coaxial nozzle was used to obtain core-shell structured particles.*

API amorphous	References	API partial amorphous	References
Acyclovir*	106	Carbamazepine	117
Celecoxib	107,108	Clarithromycin	118
Fenofibrate	109	Coenzyme Q10	119
Griseofulvin	110	Darunavir*	78
Indomethacin	111	Fenofibrate*	120
Ketoprofen	112	Griseofulvin*	121
Quercetin*	113	Indomethacin	122,123
Resveratrol	114		
Ritonavir*	115		
Simvastatin	116		

Therefore, the objective of this paper is to study the influence of the different fluid and process parameters, as well as their interplay, on the formation of a stable cone-jet as the only mode to produce spherical monodisperse nanoparticles that can be collected reproducibly. Unlike most other studies, our approach goes back to the basic concepts and focuses on investigating the desired electrospraying mode, rather than optimizing particle formation for one specific API. Briefly, we will determine the workspace for polymers and solvents commonly used in solid dispersion manufacturing. The generated information can be used as guidelines to rationally design future procedures (both single nozzle and coaxial setups), instead of the trial-and-error approach of today.

3.3. MATERIALS AND METHODS

3.3.1. Materials

Hydroxypropyl methylcellulose 2910 5 mPa·s (HPMC) was obtained from Colorcon (Dartford, UK), hydroxypropyl methylcellulose phthalate grade 50 (HPMC P) and hydroxypropyl methylcellulose acetate succinate grade HF 3 mPa·s (HPMC AS) from Acros Organic (Geel, Belgium). Hydroxypropylcellulose 180 mPa·s (HPC) was purchased from Federa (Brussel, Belgium), ethyl cellulose (EC) from Sigma-Aldrich Chemie GmbH (Steinheim, Germany) and polyvinylpyrrolidone (PVP K-12 and PVP K-30) from BASF® ChemTrade GmbH (Ludwigshafen, Germany). Eudragit® L100 and Eudragit® E100 were provided by Degussa Rohm GmbH (Darmstadt, Germany). Absolute ethanol (EtOH) and isopropanol (IPA) were purchased from VWR (Leuven, Belgium). Methanol (MeOH) and acetone (ACE) were obtained from Arcos Organic (Geel, Belgium), acetonitrile (ACN) and dichloromethane (DCM) from Fisher Chemical (Loughborough, UK). All organic solvents were of HPLC-grade and de-ionized water (Maxima Ultra Pure Water, Elga Ltd., Wycombe, England) was used.

3.3.2. Electrospraying setup and assessment of the spraying mode

Experiments were conducted at 25 °C and 50 % relative humidity in an electrospinning chamber with climate-control (Electrospinning Apparatus EC-CLI, IME Technologies, Geldrop, The Netherlands). A nozzle with inner diameter of 25 gauge was used and solutions were supplied by a syringe pump (PHD 4400, Harvard Apparatus, Massachusetts, USA). The copper collector plate was covered with aluminium foil to collect the produced particles. Fig 3.1 shows a schematic representation of the electrospraying setup.

To optimize the assessment of the spraying mode, experiments were performed whereby solutions of different polymers (Eudragit® L100, HPMC and PVP K-12) were electrosprayed. The cone was visualised by using a high speed camera (Fastcam SA2, Photron USA Inc., California, USA), equipped with a long distance microscope system (K2 DistaMax™ Long-Distance Microscope System and CF-4 objective, Infinity Photo-Optical Company, Colorado, USA). To ensure reproducibility and stability of the environmental factors, solutions of PVP K-12 in water, methanol and dichloromethane were electrosprayed at three distinct days.

3.3.3. Polymer solutions: formulation parameters

In order to investigate the influence of the formulation factors on obtaining a cone-jet mode, different polymer solutions were prepared and electrosprayed with the same setup as described above. Both polymers that are frequently used for the preparation of amorphous solid dispersions (HPMC, HPMC P, HPMC AS, HPC, PVP K-12 and PVP K-30) and coatings (HPMC P, HPMC AS, Eudragit® L100 and E100) were included. The chemical structures of the polymers can be consulted in Annex 1. The concentration of the polymer solutions was gradually increased until clogging of the nozzle during electrospraying was observed. Table 3.2 gives an overview of the tested solutions. Viscosity and conductivity of the solutions were varied via the selected solvents and measured by an Ubbelohde capillary viscometer (iVisc capillary viscometer, Lauda, Lauda-Königshofen, Germany) and a conductivity meter with a steel 2-electrode conductivity cell (Orion 150Aplus, Thermo Fisher Scientific,

Massachusetts, USA). All measurements were performed at 25 °C using a water bath with thermostat (Lauda eco silver, Lauda, Lauda-Königshofen, Germany). To investigate possible aggregate formation in the higher concentrated solutions, dynamic light scattering experiments were performed at a fixed angle of 90° (CGS-3 spectrometer, equipped with a uniphase 22 mV He–Ne laser, an avalanche photodiode detector and an ALV-5000/EPP multiangle tau correlator, Malvern Instruments, Worcestershire, UK).

*Table 3.2. Overview of all electrosprayed polymer solutions and their concentrations expressed in % w/V. Concentration of the polymer solutions were gradually increased until clogging of the electrospray nozzle was observed. No stable cone-jet could be obtained for solutions in italics. * Ratio of solvent mixtures: 1/1.*

% w/V	HPMC	HPMC P	HPMC AS	HPC	EC	PVP K-12	PVP K-30	Eudragit® L100	Eudragit® E100
Water	*1; 2.5; 5; 7.5*			*0.25; 0.5; 1*		*1,5,10,20,30*	*1,5,10,20*		
Ethanol				*0.25; 0.5; 1*	1; 2.5; *5*	1,5,10,20,30	1,5,10,*20*	1; 5; *7.5*	1; 5; 10
Methanol				0.25; 0.5; *1*	1; 2.5; 5; *7.5*	1,5,10,20,30	1,5,10,*20*	1; *5; 7.5*	1; 5; 10
Isopropanol					1; *2.5*	1,5,*10,20,30*	1,5,10,*20*	1; *2.5*	1; 5; 10
Acetone					*1*	1,5,10,20,*30*			1; 2.5; *5*
Acetonitrile						1,5,10,20,*30*	1,5,*10,20*		
Dichloromethane						1; *2.5; 5*	*1; 2.5*		*1*
EtOH/DCM*	1; *2.5*	1; *2.5*	1; 2.5; *5*		1; 2.5; *5*				
MeOH/DCM*		1; *2.5*							
EtOH/ACE*		1; *2.5*							

3.3.4. Process parameters

To study the influence of the process parameters, the tip-to-collector distance, the flow rate and the potential difference between nozzle and collector were varied for the polymer solutions listed in Table 3.2. The tip-to-collector distance was varied between 3 cm and 15 cm with steps of 3 cm. The flow rate was initially set at 0.2 mL/h and stepwise increased with 0.2 mL/h until 1 mL/h. For each combination of distance and flow rate, the voltage applied to the nozzle was gradually increased from 0 to 25 kV and the range where a stable cone-jet could be maintained, was recorded.

3.3.5. Data representation and statistical analysis

The SAS software package (version 9.4 of the SAS System for Windows) was used to perform the statistical analysis of all collected data. In general, the data was processed using the logistic regression model. Every solution (listed in Table 3.2) was electrosprayed at every tip-to-collector distance (3, 6, 9, 12 and 15 cm), flow rate (0.2; 0.4; 0.6; 0.8; 1 mL/h) and potential difference (0-25 kV). The observed spraying mode was either scored as “successful” if a cone-jet mode was obtained or “unsuccessful” if another mode was observed. Consequently, the success rate or the percentage of the successful experiments out of all experiments for a single fixed parameter could be calculated and was expressed as “the percentage of obtaining a stable cone-jet”.

3.4. RESULTS

3.4.1. Assessment of the spraying mode

Fig 3.3 visualises an example of the experiments conducted to optimize the evaluation of the spraying mode. For these pictures, the flow rate was fixed at 0.4 mL/h and the tip-to-nozzle distance measured 9 cm. Panels A, B and C show the tip of the nozzle when a solution of 1 % Eudragit® L100 in methanol was electrosprayed using a potential difference of 12-15 kV, 15-20 kV and 20-25 kV respectively. With increasing voltage, the spraying mode changed from a dripping mode to a spindle mode and finally to a stable cone-jet. The lower part of the figure illustrates the pattern the polymer particles formed on the collector. In the dripping mode only wet droplets were collected, whereas in the cone-jet mode, completely dry particles were obtained in a homogenous, circular pattern. The spindle mode yielded a combination of droplets and dry particles. At a higher polymer concentration of 5 % (panel D), clogging at the nozzle occurred. Panel E shows an example of a multi-jet which was observed when a 1 % solution of PVP K-12 in ethanol was tested at a potential difference of 20-25 kV. The formation of the different jets could be visually observed and the particles were collected in a specific pattern. Similar spraying and collection patterns were obtained for all other polymer solutions during the explorative experiments. Consequently, the assessment for the following solutions was based on both visual observation and the collection pattern.

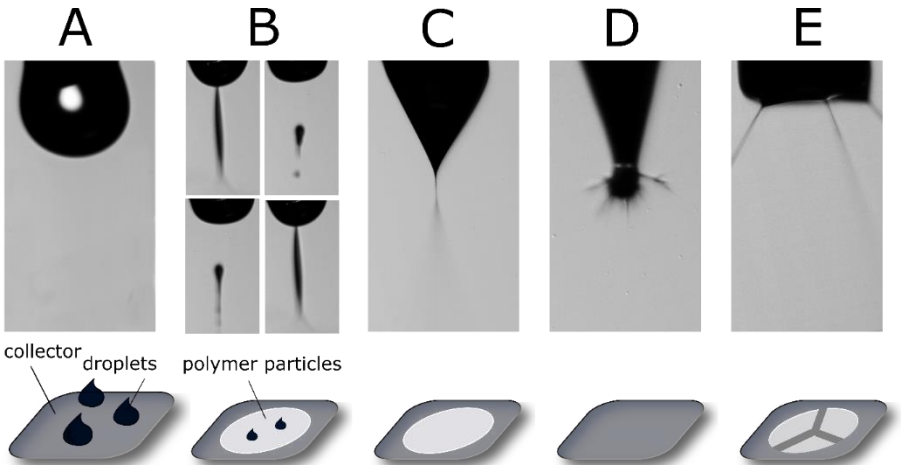

Figure 3.3. Panels A, B and C show a solution of 1 % Eudragit® L100 in methanol, electrosprayed at 12-15 kV (dripping), 15-20 kV (spindle) and 20-25 kV respectively (cone-jet). D: 5 % Eudragit® L100 in ethanol (clogging). E: 1 % solution of PVP K-12 in ethanol at 20-25 kV (multi-jet). In panel B, four consecutive high speed camera pictures illustrate the instability of this spindle mode. The lower part of the figure shows the pattern the polymer particles formed on the aluminium foil.

3.4.2. Formulation parameters

Fig 3.4A and 3.4B present the overall percentage of obtaining a stable cone-jet for all possible parameter variations when looking at specific fixed values of viscosity (Fig 3.4A) and conductivity (Fig 3.4B). Every solution, a unique combination of a polymer, concentration and solvent, has a specific value of viscosity and conductivity and represents a dot in the graph. Each percentage value is a quantification of all possible settings (flow rates, tip-to-collector distances and voltages) leading to a cone-jet for one specific, constant value of viscosity or conductivity. The higher the percentage, the broader the range for all other settings wherein a stable cone-jet is still possible. The solutions with 0 % stable cone-jet (i.e. no cone-jet was observed at any flow rate, tip-to-collector distance or voltage) are marked in italic in Table 3.2.

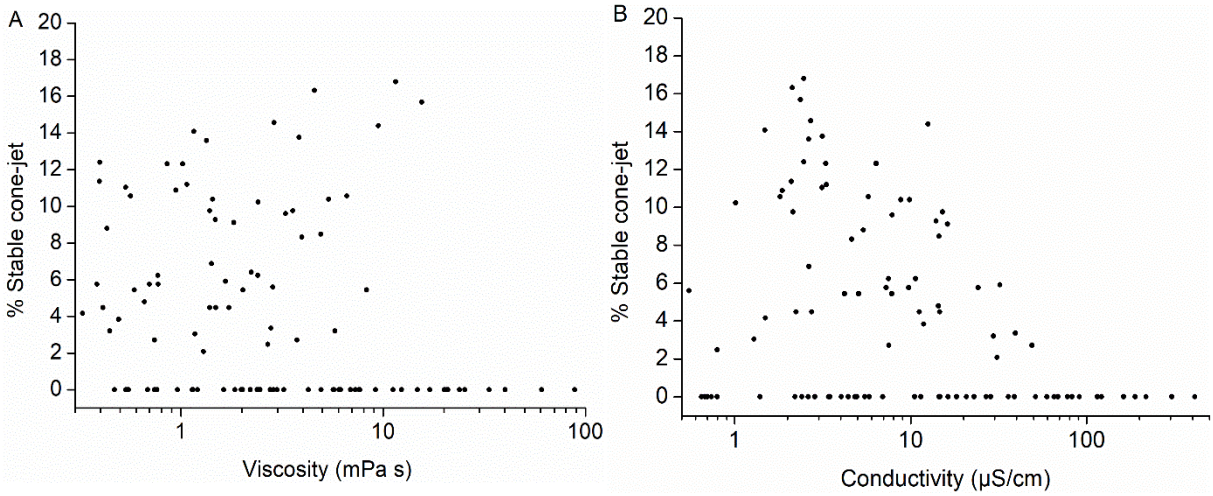

Figure 3.4. Overall percentage of obtaining a stable cone-jet when varying the viscosity (A) and conductivity (B) of the solutions.

As expected, viscosity increased with increasing concentration for each polymer-solvent system. Therefore, solutions with increasing polymer concentration were tested until clogging of the nozzle occurred. In principle increasing viscosity does not clog the nozzle; it is rather the strong further viscosity increase due to evaporation that leads locally to solidification. An exception was made for PVP K-12 in ethanol and methanol and Eudragit® E100 in ethanol, methanol and isopropanol: concentrations higher than 30 % (PVP K-12) and 10 % (Eudragit® E100) were not further tested due to the lack of relevance in the preparation of solid dispersions. So the line of dots in the graph at 0 % mainly represents the highest concentration of each polymer-solvent combination. However, some solutions at a concentration below the one where clogging occurred, did not exhibit a cone-jet mode (Table 3.2). For 1 % PVP K-30 in dichloromethane and 10 % PVP K-30 in acetonitrile, neither a stable cone-jet could be reached, nor was clogging observed, although fibres did appear which connected the nozzle with the collector. Further findings show that the higher the boiling point of the used solvent, the higher the viscosity and therefore the concentration that was still possible to be electrosprayed without any clogging (data not shown). For every polymer except PVP K-12, the conductivity of the solutions increased with increasing concentration. The conductivity of the PVP K-

12 solutions increased until a concentration of 20 % and declined again for the 30 % one, independent of the solvent used. PVP solutions with concentrations of 1 to 40 % in water and ethanol were tested with dynamic light scattering, but no aggregate formation could be assessed.

One general conclusion that can be drawn from Fig 3.4 is that the percentage of cone-jet equals zero for all solutions with a viscosity above 20 mPa·s or conductivity exceeding 50 µS/cm. The solutions with viscosity values above 20 mPa·s exhibited clogging, but, concerning the conductivity, also some non-clogging solutions (HPMC 1-5 % in water, PVP K-12 1-30 % in water, PVP K-30 1-20 % in water and Eudragit® L100 5 % in methanol) could exceed 50 µS/cm. Besides that, for the case of viscosity in Fig 3.4A, below values of 20 mPa·s no clear trend in the percentage could be observed and viscosity appears to be indifferent with respect to a variation of all other parameters. On the other hand, for conductivity as the reference parameter in Fig 3.4B, there is a clear maximum in the percentage observed for values within a range of 2-10 µS/cm.

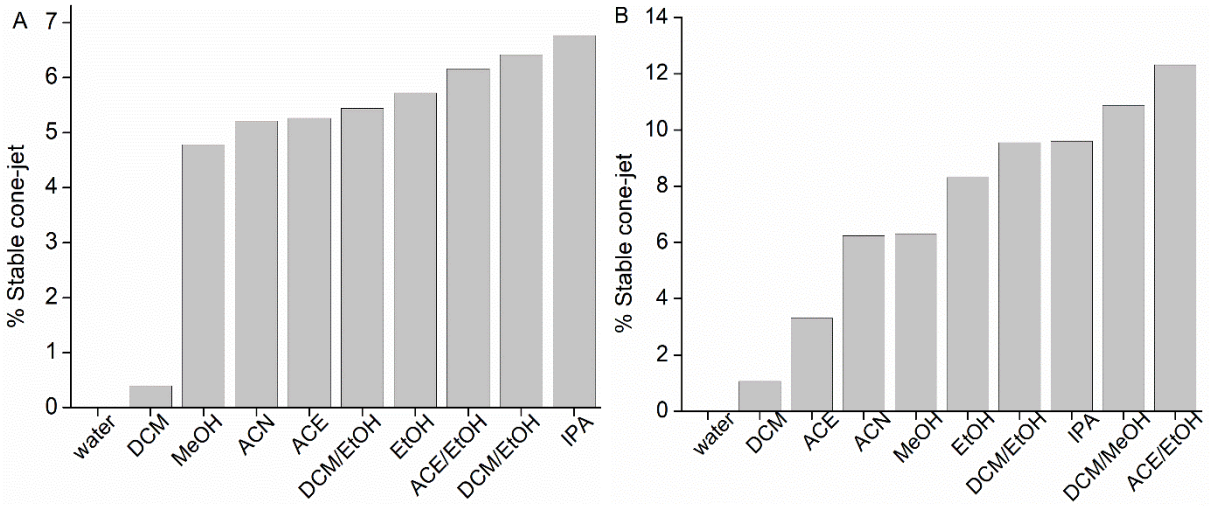

Figure 3.5. Overall percentage of obtaining a stable cone-jet for each solvent or solvent mixture over all tested solutions of Table 3.2 (A) or when only the 1 % concentration of every polymer-solvent system was included (B).

Another parameter against which the success percentage can be evaluated is the type of solvent. To determine whether there were significant differences between the used solvents, the success rate of obtaining a stable cone-jet was calculated for each solvent and solvent mixture. Fig 3.5A shows this percentage for all tested solutions of Table 3.2, including every polymer and concentration reported. For water no cone-jet could be maintained under any condition, and also dichloromethane had a very low success rate. All other solvents had a similar percentage of cone-jet, with the highest one for isopropanol. Since not all polymers could be dissolved and tested in all solvents and a different amount of concentrations was tested for each polymer-solvent combination, the overall solvent success rate could be misinterpreted. For this reason, in a second representation (Fig 3.5B) only the 1 % concentration of every polymer-solvent system was used (as this was accessible for all polymer-solvent systems considered here) to calculate the percentage of stable cone-jet. Here, the differences between the distinct solvents became more clear while maintaining the overall trend. Based on Fig

3.4B an optimal conductivity range could be suggested however, there is no correlation between the conductivity values of the solvents and their ranking by percentage of stable cone-jet.

3.4.3. Process parameters

The polymer solutions listed in Table 3.2 were electrosprayed using different flow rates and tip-to-collector distances. The voltage ranges leading to a stable cone-jet were recorded. As mentioned above, the polymer particles formed a circular pattern on the aluminium foil. However, the circle became larger and more elliptically shaped when the tip-to-collector distance was increased. Fig 3.6 summarizes the influence of the process factors: the percentage of cone-jet mode is plotted as a function of voltage and this at five different levels of flow (represented by solid and dotted lines) and distances (different colours). The percentage in this graph is thus a quantification of the number of settings (polymer x solvent x concentration) leading to a cone-jet at each of these specifications.

Several conclusions can be drawn from this: firstly, the lower the flow rate the higher the success percentage and secondly, increasing the tip-to-collector distances increases the percentage. Thirdly, each combination of flow rate and tip-to-collector distance has a maximum success percentage at certain potential difference. This maximum shifts to higher voltages with increasing tip-to-collector distance or increasing flow rate. Potential difference values lower than 7 kV never led to a stable cone-jet. The highest success percentage was thus observed for the lowest investigated flow rates, largest tip-to-collector distance and consequently, a potential difference at the upper end of the accessible scale. It must be noted that de lines in de graph do not represent a continuous function, they only connect the discrete points (at every integer number of kV) to guide the eye.

3.4.4. Interplay of formulation & process parameters

Fig 3.7 shows how formulation and process parameters influence each other. A dot in Fig 3.7A indicates that this specific combination of viscosity – flow – distance – voltage was successful. In Fig 3.7B the relation between the conductivity and the three variable process factors is visualised. Since the same amount of solutions was tested at every flow rate, it can be noticed that at higher flow rates, only solutions with lower conductivity were successful.

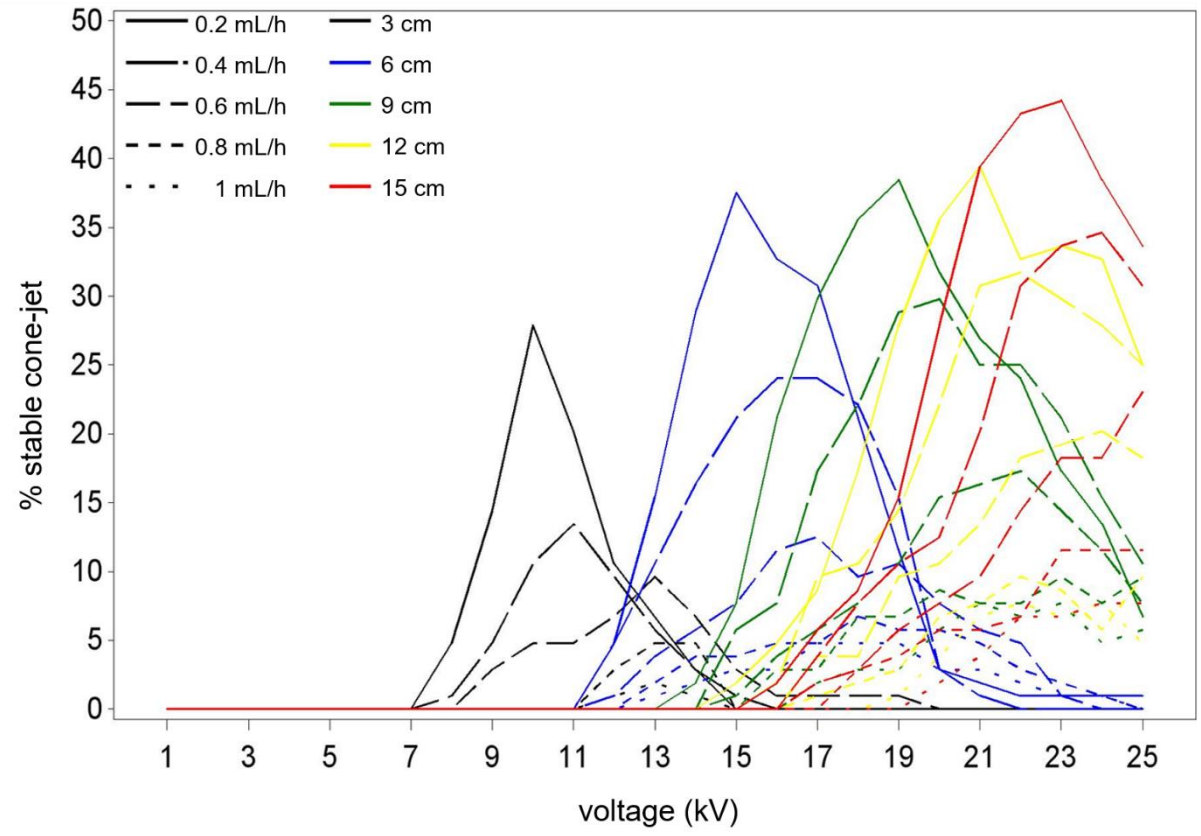

Figure 3.6. Overall percentage of obtaining a stable cone-jet when varying the flow rate, tip-to-collector distance and voltage. The lines in de graph do not represent a continuous function, but they only connect the discrete points (at every integer number of kV) to guide the eye.

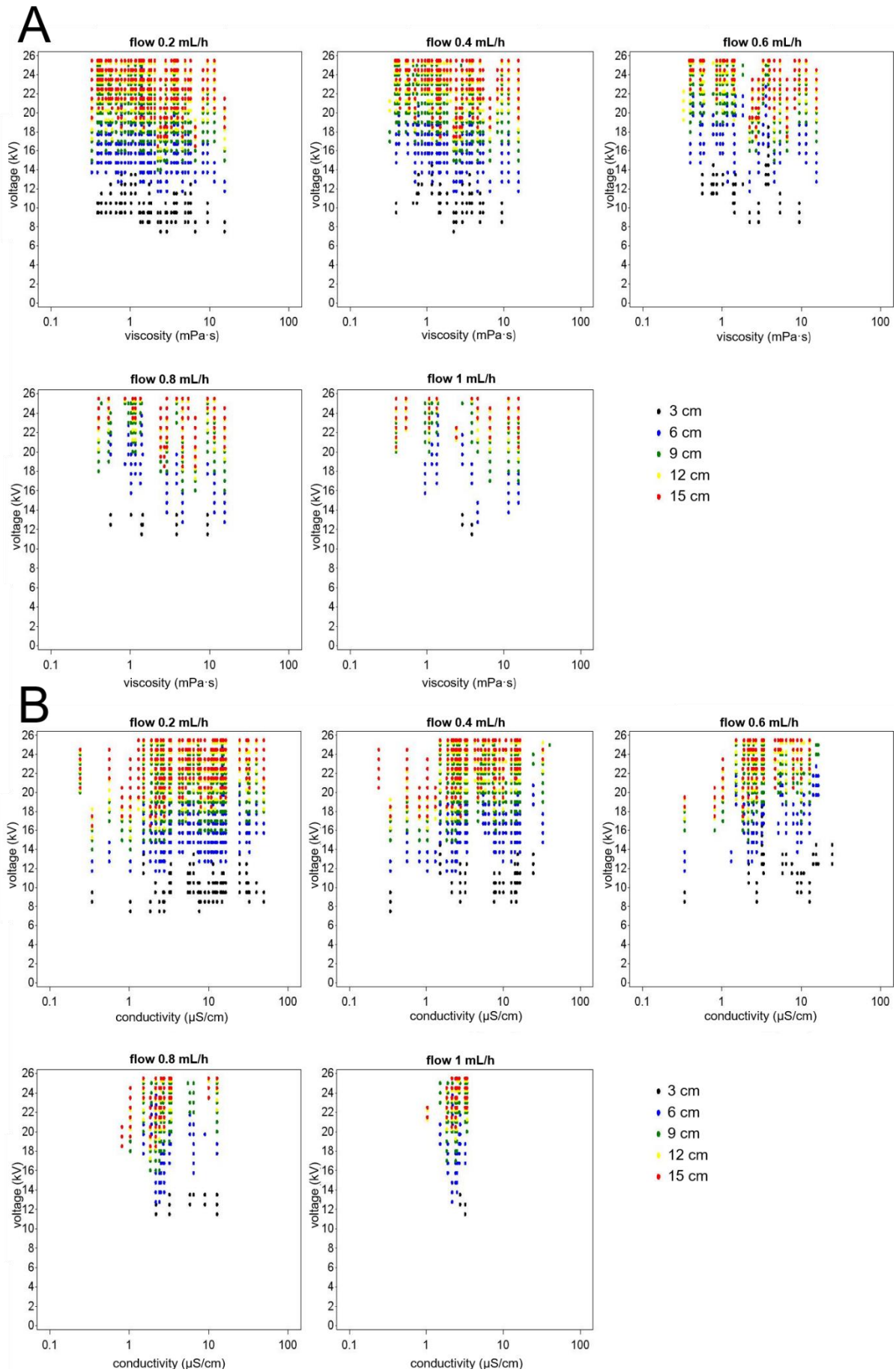

Figure 3.7. A: Interplay of viscosity and the three variable process parameters and B: Interplay of the conductivity and the three process parameters. Dots indicate the specific combinations of settings leading to a stable cone-jet.

3.5. DISCUSSION

3.5.1. Assessment of the spraying mode

In order to shift from a trial-and-error based preparation of solid dispersions via electrospraying towards a more rationally based methodology, we aimed to delimit the range of formulation and process parameters leading to conditions that generate cone-jet mode processes. The importance of this mode cannot be overestimated because it is the most stable and reproducible one. The jet breaks up into uniform droplets, resulting in a nearly homogenous aerosol and subsequently, monodisperse nanoparticles are collected[102-104,124,125]. Other operating modes are often not stable (Fig 3.3B shows three consecutive high speed camera pictures) and jet break-up is unpredictable.

The morphology, size and size distribution of the generated particles can be manipulated when the operating parameters are further varied. Over the years, general scaling laws were developed to predict both the size of the droplets emitted by the cone-jet and the size of the collected particles[126-128]. The particle diameter for example is proportional to the liquid flow rate and inversely proportional to the conductivity of the electrosprayed solution. As one could expect, it is only meaningful to apply these scaling laws in the cone-jet regime. Once the limits of the latter are set, the final conditions can be chosen to meet the desired particle properties. Currently none or almost no coherent information is available about these limits for solid dispersion manufacturing. To report the results of our experiments, the concept of "the percentage of obtaining a stable cone-jet" for selected parameters was used. The higher this value, the broader the window of all other parameters for the cone-jet regime, hence more space for optimization of the particle properties by changing the formulation and process parameters. It is important to stress again that this percentage can easily be misinterpreted: if a specific parameter for example has 25 % of stable cone-jet, it does not mean that a cone-jet is only obtained in one out of four attempts for a specific setting of all parameters. The percentage rather indicates that of all experiments conducted, only a certain percentage of the used parameter settings delivered a stable cone-jet. Once those parameter settings are identified, stable spraying is always possible with those parameters. Plotting the percentage as function of the selected variable yields in principle two types of information: a maximum in the percentage at a certain value of the variable would indicate that this variable has an influence on the successful spraying and a minimum or zero percentage over a range of values would indicate that the selected parameter is indeed the limiting one. On the other hand, no change in percentage over the range of values of the selected parameter would indicate that the spraying process is indifferent to changing this parameter when exploring the whole parameter space.

Since the focus of this paper was on the spraying regime rather than the characteristics of the produced particles, there was a need for a reliable method to determine if the selected parameters led to a cone-jet or not. Ciach suggested to assess the cone by installing a light source behind the nozzle[129]. In this setup, a stable Taylor cone will be observed as a complete black cone because all the light is scattered. In case of instabilities, light will be able to pass and the cone will become partially translucent. The cone-jet regime is also associated with a stable electric current and fluctuations

represent cone instabilities, hence assessment can be based on measuring this spray current[129,130]. Both are indirect methods, so we opted to visualise the cone with a high speed camera, a direct and undisputed way for assessment. To optimize the evaluation method, a series of three polymer solutions in different solvents were electrosprayed. For all solutions, which were repeatedly tested at multiple settings, a specific relation could be observed between the spraying mode and the collection pattern (Fig 3.3). In accordance to what one could theoretically expect, only the stable cone-jet regime led to the collection of dry polymer particles. In the other regimes, the lack of a jet (dripping mode) or instabilities which disturbed the jet break-up (multi-jet and spindle mode), impeded the formation of a homogenous aerosol and led to variable, incomplete evaporation. Consequently, droplets instead of dried particles reached the collector. Based on these experiments, a stable cone-jet was assimilated to collecting a circle of only dry particles.

3.5.2. Formulation parameters

With regard to the formulation parameters, this study mainly focused on the conductivity and viscosity of the polymer solutions, as they play an important role during cone formation. These two solution properties were varied by using different solvents and polymer concentrations. The polymer choice was based on the in house experience with amorphous solid dispersions and on literature (Table 3.1). The solvents were selected to cover a broad range of physicochemical properties and the concentration of the polymer solutions was stepwise increased until viscosity was too high, causing clogging at the tip of the nozzle.

Concerning the influence of the solution's viscosity, looking at the graph in Fig 3.4A, it seems there is no clear correlation between the chance to obtain a cone-jet and the viscosity. As mentioned in the "Results" section, the higher the boiling point of the used solvent, the higher the viscosity and therefore the concentration that was still possible to be electrosprayed without any clogging (data not shown). Acetonitrile was the only solvent which deviated from this trend: even though it has a relative high boiling point of 81 °C, the highest viscosity that could be sprayed was only 1 mPa·s. For isopropanol, which has a similar boiling point, solutions up to 20 mPa·s could be covered. One could conclude to use solvents which are less volatile. In literature it is mentioned that volatility should not be too low, so that during the flight of the droplets towards the collector complete evaporation of the solvent is still possible[64,76]. When testing the solutions of 1 % PVP K 30 in dichloromethane and 10 % PVP K 30 in acetonitrile, fibres were formed at the tip of the nozzle, likely due to their high molecular weight[131]. Despite their relatively low viscosity of 1 and 1.6 mPa·s, the jet did not break up into droplets and the process shifted from electrospraying to electrospinning.

Looking at the relation between viscosity and potential difference, it is intuitively expected that more concentrated polymer solutions, which have a higher viscosity, demand a higher voltage. A stronger electric field is necessary to overcome the elevated viscoelastic forces when forming a cone. However Fig 3.7A (especially the plots with lower flow rates) illustrates that the potential difference required for a cone-jet was the same for low and high viscosities. When for example the solutions of PVP K-12 in ethanol were tested at a flow rate of 0.2 mL/h and 12 cm distance, the cone-jet onset voltage for

the five concentrations (1, 5, 10, 20 and 30 %) ranged between 18 and 19 kV (data not shown). More viscous solutions always had a higher conductivity, except for PVP, and this may have counteracted the need for an elevated potential difference. Our findings correlate with literature stating that onset voltage is independent from fluid viscosity as expressed in the following equation:

$$V_0 = A_l \sqrt{\frac{2\gamma r_c \cos\theta_0}{\varepsilon_0}} ln\left(\frac{4h}{r_c}\right) \quad \text{(Eq 3.1)}$$

where V_0 is the onset potential, A_l a constant, γ the surface tension, r_c is the nozzle radius, θ_0 the cone half-angle, ε_0 the permittivity of free space and h is the tip-to-collector distance[132].

To maintain a stable cone-jet, conductivity should be high enough to allow a sufficient flow of charges, but too high conductivity will lead to instabilities. Throughout the years, multiple conductivity limits were proposed but according to Smith, there is no upper conductivity limit at all[132-134]. In this study, solutions with values above 50 µS/cm could not successfully be sprayed. Fig 3.7B shows a shift towards lower conductivity values with increasing flow rate, i.e. at 1 mL/h, only solutions with conductivity below 5 µS/cm were successful. The same observation was made in a study of electrosprayed polycaprolactone and beta-estradiol particles[135]. Although a clear explanation cannot be given, it can be hypothesized that liquids with high conductivity carry more charges and give more unstable electrospraying. Since increasing the flow rate creates more current, electric stress becomes larger and introduces instabilities.

Interestingly, it was observed that the conductivity of the 30 % PVP K-12 solutions was lower than those of the less concentrated solutions. Extra conductivity measurements were conducted on a series of PVP K-12 and K-30 solutions ranging from 1 to 40 %, and values began to decrease from 15 and 25 % respectively. Possibly aggregates could have been formed in the highly concentrated solution which hampered charge mobility. For this purpose, aggregate formation was investigated with dynamic light scattering, but all results were negative. Also other polymer solutions may exhibit this phenomenon, but their solubility is limited or the high concentrated solutions are too viscous to perform conductivity measurements.

When interpreting Fig 3.4, one must keep in mind that most of the dots of 0 % cone-jet belong to solutions where clogging of the nozzle occurred. Nevertheless, also some lower concentrated solutions showed a 0 % cone-jet. In Table 3.2 all unsuccessful solutions can be found marked in italic with water being an unsuitable solvent for every polymer, whatever the process parameters might be. Water has the highest boiling point and conductivity but the reason lies more likely in the surface tension (78 mN/m, while values for organic solvents range between 22 and 28 mN/m). Due to this high surface tension, corona discharges are initiated before the onset voltage for a cone-jet is reached, which can only be avoided by using an inert sheathing gas[59,133]. It is assumed that the surface tension of the solutions is only determined by the solvent and is not affected by adding polymers or API. Even though they might be surface active, the electrospraying process is a fast and dynamic phenomenon, which leaves less time for the molecules to move to the newly created liquid-air interface[133,136]. In Fig

3.5, solvents were ranked based on the percentage of stable cone-jet formation, revealing that besides water, also dichloromethane was a less suitable solvent. As a result of its high volatility, the cone dried and the nozzle was blocked before any jet break-up could take place. Based on Fig 3.5A, it seems that there is no significant difference between all other solvents. However in this graph all tested solutions were used to calculate the percentage of stable cone-jet, meaning that for some solvents more and other concentrations were covered, as can be seen in Table 3.2. To avoid misinterpretation, a second ranking was made wherein only the 1 % solution of each polymer-solvent system was included (Fig 3.5B) and here we might conclude that the solvent mixtures were more favourable than the pure solvents. One must be aware of that fact that the DCM/MeOH and ACE/EtOH mixtures were only used for HPMC AS because its solubility in pure solvents is very low. It must be further investigated if the success is attributed to the use of mixtures or to other properties of these solutions. In case of pure solvents, isopropanol was the most successful one.

3.5.3. Process parameters

The overall percentage of obtaining a stable cone-jet when varying the three process parameters is shown in Fig 3.6. It is important to mention that the lines in the graph do not represent a continuous function, but they only connect the discrete points (at every integer number of kV) to guide the eye. The tested distances are represented by different colours, ranging from 3 cm in black to 15 cm in red. The success of stable cone-jet rises when using larger tip-to-collector distances. Naturally also a higher potential difference was needed to generate an adequate electric field. Distances lower than 3 cm could not be used due to electric discharge and the upper distance limit was 15 cm. Since a potential difference of maximum 25 kV could be generated, the electric field strength became too weak above 15 cm. However the difference in the voltage corresponding with the top of the peaks, which represent the maximum percentage, between 3, 6 and 9 cm was larger than between 9, 12 and 15 cm. The same can be concluded from Fig 3.7: the difference in voltage between the 3, 6 and 9 cm is larger than the voltage difference between the 9, 12 and 15 cm. This reminds of a logarithmic relation, which was confirmed when the cone-jet onset voltage was plotted in function of the distance (data not shown) and a similar relation was described by Marginean *et al.* and Smith[130,132]. Possible explanation can be found when looking at the electric field lines, which are more curved around the nozzle and become straight and parallel towards the collector plate[137,138]. Thus, when for example the distance is increased from 3 to 4 cm, the related increase in potential difference will be larger compared to an increase between 10 and 11 cm. An additional argument for this hypothesis is the fact that the fibres observed when spraying the two mentioned PVP K-30 solutions, followed the shape of these field lines. An arc-like pattern was formed around the nozzle where after the fibres ran perpendicular to the collector. To conclude, when the distance was increased, the circular area covered by the collected particles became larger and more elliptical. Larger distances need higher potential differences which generate more electric stress. This leads presumably to a whipping motion of the jet and an elliptically shaped collection pattern[128].

Fig 3.6 also shows that more success was obtained at smaller flow rates (solid lines), no matter the value for the tip-to-collector distance. Defining the flow rate is always a compromise between the

yield and the particle size. When nanoparticles are desired, flow must be low (cfr. the scaling laws) and on top of that, too high rates can inhibit solvent evaporation. The solid lines in Fig 3.6, showing the low flow values, display a sharp peak, meaning that there was a specific potential difference for which the success rate was very high. In contrast, there are no clear peaks at higher flow rates, hence the success rate remained the same over a broad voltage range. The fact that the system was less sensitive to changes in the potential difference at higher flow (dotted lines), is most likely caused by the larger volume to which the effect of the increasing electric stress can be divided. However, the maximum percentage of stable cone-jet, represented by the top of the peaks, shifted to higher voltages with increasing flow, concluding that higher flow rates demand a stronger electrical field. Similar in Fig 3.7A, at 1 mL/h, the lower distances and voltage were not successful anymore in comparison to the low flow rates (disappearance of black dots). This increasing potential difference with increasing flow can also be seen in Fig 3.7B: at 0.2 mL/h the voltage lies between 7 and 12 kV but at 1 mL/h only values above 12 kV are successful. Except for the PVP K-30 10 % solution in isopropanol, solutions could not be sprayed at a flow rate above 1 mL/h. Rutledge and Fridrikh visualised the effect of an increasing flow rate on the geometry of the cone[139]. Possibly this geometrical change in combination with the increasing current through the jet, hindered the use of higher flow rates.

3.6. CONCLUSION

The limits of the cone-jet regime for multiple polymer solutions were determined in a single nozzle electrospray setup. The experiments map the importance of the flow rate, electric potential difference and tip-to-collector distance. In general, a higher success rate was obtained at lower flow rates and larger distances between the tip of the nozzle and the collector. Regarding the formulation parameters, the type of solvent and the concentration of the polymer solutions, along with their viscosity and conductivity, were identified as determinative factors. Water and dichloromethane were inappropriate solvents, while isopropanol was proven to be the most successful. The conductivity limited in particular the flow rate, but no specific conductivity boundaries could be set. The concentration and viscosity were especially related to clogging of the nozzle. The collected information is of utmost importance for the first step in the rational design of electrospraying methods.

Acknowledgements

Het Fonds voor Wetenschappelijk Onderzoek-Vlaanderen (FWO, project G0A3916N) is acknowledged for financial support and the authors want to thank Annouschka Laenen for the statistical analysis.

Chapter 4
Amorphous solid dispersions of darunavir: Comparison between spray drying and electrospraying

Results of this chapter are based on:

Smeets A, Koekoekx R, Clasen C, Van den Mooter G. Amorphous solid dispersions of darunavir: Comparison between spray drying and electrospraying. Eur J Pharm Biopharm. 2018;130:96-107.

4.1. ABSTRACT

The interest in using electrospraying as a manufacturing method for amorphous solid dispersions has grown remarkably. However, the impact of formulation and process parameters needs further clarification. In this study, amorphous solid dispersions of darunavir and hydroxypropyl methylcellulose (HPMC), hydroxypropyl methylcellulose acetate succinate (HPMC AS) and polyvinylpyrrolidone K-30 (PVP) were prepared with electrospraying and spray drying, in order to compare both solvent based manufacturing techniques. Our results revealed that electrospraying was as successful as spray drying. The formulations prepared with the two methods were amorphous and had similar characteristics concerning the residual solvent and drug release. Although differences in the morphology and the particle size distributions were observed, this was not reflected in the pharmaceutical performance of the formulations. Electrosprayed amorphous solid dispersions made up of darunavir and PVP were studied in more detail by means of a full factorial experimental design. The impact of two process and two formulation parameters on the properties of the amorphous solid dispersions was determined. The feed flow rate had a significant effect on the diameter and morphology of the particles whereas the tip-to-collector distance had no significant impact within the tested range. The drug loading influenced the homogeneity and the residual solvent, and the total solids concentration had an impact on the homogeneity and the morphology.

4.2. INTRODUCTION

Driven by the high amount of new drug compounds belonging to class II and IV of the Biopharmaceutics Classifications System, a great deal of effort has gone into to the development of amorphous solid dispersions (ASD) as an enabling formulation strategy (Fig 1.1). An ASD formulation can increase the solubility and dissolution rate and hence improve the bioavailability of poorly water soluble compounds[18]. The first solid dispersions were eutectic systems made up of the active pharmaceutical ingredient (API) and a low molecular weight organic carrier such as urea or lactose. Nowadays amorphous polymeric carriers are almost exclusively used in a striving to prepare an ASD in which the API is molecularly mixed with the amorphous carrier to form a glass solution[22].

Likewise, a lot of progress has been made in the manufacturing of ASDs. An established industrial method is spray drying[28]. During spray drying, a solution of an API and polymer is transformed to an aerosol of fine droplets, which will dry upon contact with a heated stream of gas in the drying chamber to form particles. An alternative solvent based manufacturing method which has increasingly been reported in literature is electrospraying[64]. The electrospraying method is also based on the transformation of a liquid stream into droplets, however, droplet formation originates from a different mechanism. As shown in Fig 4.1, a high electric potential difference is applied between a nozzle and a collector. Due to the electric stress, the meniscus of the fluid leaving the nozzle will deform into a Taylor cone-jet. The jet will exist over a certain distance downstream of the nozzle and will then break up into small droplets. The emitted droplets are attracted to the oppositely charged collector and the solvent will quickly evaporate. In contrast to spray drying, there is no need for a drying chamber and thus the process can run at ambient conditions.

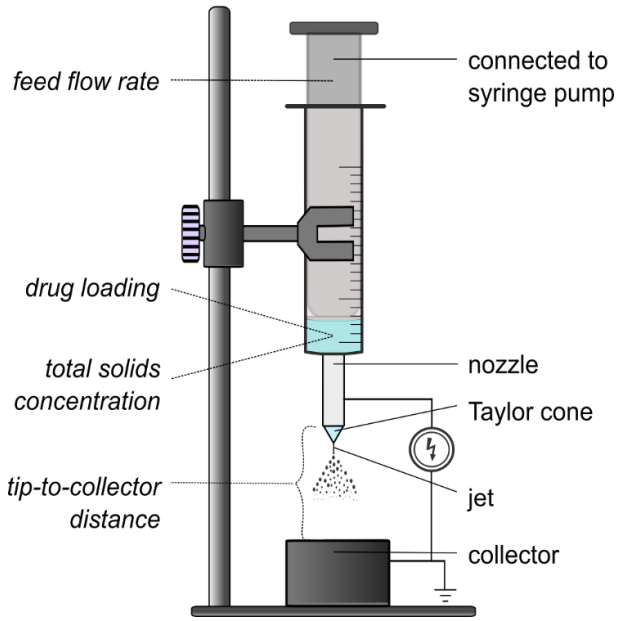

Figure 4.1. Schematic representation of the electrospray setup (adapted from Smeets et al.[65]). At the left-hand site, the parameters studied in the DoE are displayed in italics.

Electrospraying is an attractive method as it offers several advantages. In particular, it can be used to produce core-shell structured particles in one single step by using a dual capillary or coaxial nozzle[59]. We previously reported on the coating of ASD particles of darunavir, an anti-HIV drug, with an enteric polymer to delay its release[78]. In this study, a very high encapsulation efficiency was obtained but contradictory, a high burst release was observed. In addition to this, problems with the amorphization of darunavir were encountered. Despite the number of publications where electrospraying was successfully used for ASD manufacturing, multiple other examples can be found in literature were the API did not become completely amorphous or the formulations did not perform as expected[62,64]. One may also argue that the throughput of electrospraying is remarkably lower due to the limited feed flow rate (order of µL-mL/h) as compared to other manufacturing methods like spray drying[64,73]. To address this problem, large-scale equipment has been developed using multiple nozzles and thus Taylor cone-jets in parallel. Moreover, this large-scale equipment is already established in other industrial fields and nozzles for the production of core-shell particles on a larger scale are under development[59,140]. Due to the latter, it is worthwhile exploring electrospraying into more depth since the possibility of producing core-shell particles in one single step is a substantial benefit over the other manufacturing methods.

Before optimizing the darunavir core-shell particles, we take in this study a step back to tackle first the challenges related to the ASD core. Different factors are influencing the formation of the Taylor cone-jet, which is not thoroughly understood yet. One needs to consider both the process parameters (e.g. feed flow rate, tip-to-collector distance, potential difference and nozzle type) as well as the solution properties as surface tension, conductivity, viscosity, solids content and formulation parameters like drug to polymer ratio[73]. To date a trial and error approach is often the only, yet time consuming, option in selecting the best solution properties and operational settings.

The first objective of the present study was to compare two solvent based manufacturing techniques, electrospraying and spray drying, for the manufacturing of ASDs of darunavir with hydroxypropyl methylcellulose (HPMC), hydroxypropyl methylcellulose acetate succinate (HPMC AS) and polyvinylpyrrolidone K-30 (PVP), three commonly used polymeric carriers. We also verified the capability of the carriers to maintain darunavir's supersaturation state in aqueous environment. The ASD formulations were characterised in terms of solid state properties, particle size distribution, residual solvent and drug release. The second objective was to study in more detail the influence of two process parameters (feed flow rate and tip-to-collector distance) and two formulation parameters (total solids concentration and drug loading) on the properties of darunavir-PVP ASD particles. For this purpose, a screening design of experiments (DoE) approach was used.

4.3. MATERIALS AND METHODS

4.3.1. Materials

Hydroxypropyl methylcellulose 2910 5 mPa·s (HPMC) was purchased from Colorcon (Dartford, UK), hydroxypropyl methylcellulose acetate succinate grade HF 3 mPa·s (HPMC AS) from Acros Organic (Geel, Belgium), polyvinylpyrrolidone K-30 (PVP) from BASF® ChemTrade GmbH (Ludwigshafen, Germany) and ethyl cellulose (EC) from Sigma-Aldrich (Overijse, Belgium) . Darunavir ethanolate (DRV) was a kind gift from Cilag AG (Schaffhausen, Switzerland). Absolute ethanol was acquired from VWR (Leuven, Belgium); acetonitrile, dimethylformamide, formic acid and hydrochlorid acid (HCl) from Fisher Chemical (Loughborough, UK).

4.3.2. Screening of the supersaturation potential of the polymeric carriers

Determination of equilibrium solubility

The equilibrium solubility of darunavir in aqueous medium at pH 1 and pH 7.5 was measured by dissolving an excess amount of darunavir in 0.1 M HCl or phosphate buffer (all experiments were conducted in triplicate, *n* = 3). The oversaturated solutions were placed in a rotary mixer L26 (Labinco BV, Breda, The Netherlands) for 66 hours, where after they were filtered through a polytetrafluoroethylene Whatman syringe filter, pore size 0.1 µm (GE Healthcare, Buckinghamshire, UK). Absence of darunavir adsorption to the filter membrane was confirmed upfront. The concentration of darunavir in the solution was quantified by HPLC-UV (Hitachi LaChrom system, Merck, Darmstadt, Germany) equipped with a L-7420 UV-VIS detector with and an ODS Hypersil C18 column, 4.6 x 250 mm, d_p = 5 µm (Thermo Scientific, Massachusetts, USA). Analyses were run at room temperature and a mobile phase consisted of 50/50 (V/V) acetonitrile/10 mM formic acid in water, adjusted to pH 3.2. The flow rate of the mobile phase was 1 mL/min, the injection volume 20 µL and the detection wavelength was 278 nm. The details of the method validation is given in Annex 2.

Additionally, the solubility of darunavir was determined in the pH 1 and 7.5 media already containing 0.15 or 0.6 % HPMC, HPMC AS or PVP. The chemical structures of the polymers can be consulted in Annex 1. For the samples with HPMC AS at pH 7.5, the ultrapure water in the mobile phase was replaced with phosphate buffer pH 6.8. The solubility of darunavir in the media with and without polymer was compared using a t-test with a 95 % confidence interval.

Determination of the supersaturation level

To evaluate whether the polymers can enhance the solubility of darunavir and maintain the elevated darunavir concentrations, supersaturation experiments were conducted based on the solvent-shift method. HPMC, HPMC AS and PVP were added to 0.1 M HCl (pH 1) or phosphate buffer (pH 7.5) to obtain a final polymer concentration of 0.15 % and 0.60 %. A small amount (200 µL) of a highly concentrated solution of darunavir in dimethylformamide was mixed with 20 mL of the different media and after 15, 30, 60 and 120 minutes samples were taken, filtered and quantified by HPLC (*n* = 3). As a reference, the same experiments were performed without addition of the polymers to the aqueous media. The area under the curve between the first time point at 15 min and the last

at 120 min ($AUC_{15\text{-}120min}$) was obtained by integrating the concentration-time profiles and subsequently, the supersaturation factors could be calculated. This factor is defined as the ratio between the AUC of the supersaturated curve and the theoretical AUC for the constant equilibrium concentration in the same solution or in plain medium. To compare the supersaturation factor of the reference with the supersaturation factors obtained for the media with the different polymers, a t-test with 95 % confidence interval was used.

Adsorption of darunavir to the polymers

Since it was observed that the solubility of darunavir decreased when polymers were added, dialysis experiments were carried out to evaluate whether darunavir would adsorb to the polymers. For this reason, dialysis tubing with a pore size of 3500 MWCO, which is permeable for the darunavir molecules but not for the polymer, was selected (Cellu Sep T1 regenerated cellulose, Membrane Filtration Products Inc, Texas, USA). In a beaker, darunavir was dissolved in 0.1 M HCl and HPMC, HPMC AS or PVP was added. The dialysis bag was filled with 20 mL of 0.1 M HCl and immersed in the beaker with the darunavir-polymer mixture. After an equilibration time of 72 hours, the darunavir concentration inside the dialysis bag was determined with HPLC. Likewise a reference experiment was performed in which no polymer was added to the darunavir solution in the beaker.

4.3.3. Preparation of the amorphous solid dispersions

HPMC and HPMC AS were dissolved (1.5 %) in an ethanol/dichloromethane mixture (1/1, v/v) and PVP was dissolved in ethanol (10 %). Darunavir was added to the polymer solutions to achieve both a low drug loading of 10 % (relative to the polymer weight) and a higher one of 30 % (relative to the polymer weight). The six solutions were electrosprayed in a climate controlled electrospinning apparatus (EC-CLI, IME Technologies, Geldrop, The Netherlands) at 25 °C and 50 % relative humidity. The feed flow rate was set at 0.4 mL/h, the tip-to-collector distance at 6 cm and the voltage at 22-24 kV. The same six solutions were spray dried in a Buchi mini spray-dryer B190 (Buchi, Flawil, Switzerland). The inlet temperature was 60 °C, the feed flow rate 5 mL/min, the atomizing air flow rate 15 L/min and drying air flow rate 28 L/min. A post-drying step was applied to all 12 ASD batches by storage in a vacuum oven at 25 °C for 3 days.

4.3.4. Characterization of the amorphous solid dispersions

Solid state properties

To investigate the solid state properties of the formulations, a Q2000 modulated DSC (TA Instruments, Leatherhead, UK) equipped with a refrigerated system (RCS90) was used. The samples were loaded into standard aluminium pans (TA Instruments, Brussels, Belgium) and heated at 2.5 °C/min with an amplitude of 1 °C and a period of 60 s, while the cell was continuously purged with dry nitrogen (50 mL/min). The glass transition temperature (T_g) was calculated based on the inflection point of the reversing heat flow curve. A reference measurement was run with the pure polymer and with both unprocessed, crystalline darunavir and amorphous darunavir, which was *in situ* prepared by quench cooling in the DSC apparatus. Complementary, the formulations were analysed with X-ray diffraction (automated X'pert PRO diffractometer, PANalytical, Almelo, The Netherlands) in reflection mode using

a Cu X-ray radiation source (Kα 1.5418 Å) at 45 kV and 40 mA. The samples were continuously scanned with a step size of 0.0167° between 4° and 40° (2ϑ) with a counting time of 400 s per step.

Residual solvent

Electrospraying and spray drying are solvent-based methods. Although a post-drying step is applied, traces of organic solvent will remain present in the final formulation. Thus thermogravimetric analyses (TGA) were carried out using a STD Q600 (TA instruments, Leatherhead, UK). Samples were heated to 120 °C at a rate of 5 °C/min and the corresponding mass loss owing to the evaporation of the residual solvent was calculated.

Morphology and particle size distribution

Since the size of the prepared ASD particles ranges in the nano/submicron scale, scanning electron microscopy (SEM) images were acquired to examine the morphology and the size of the particles. Sample preparation was performed by electrospraying the formulations directly onto aluminium foil. For the spray dried formulations, the collected powder was adhered to the SEM stubs using double-sided carbon tape. All samples were platinum coated with a *SCD-030* Balzers Union sputter-coater (Oerlikon Balzers, Balzers, Liechtenstein) and a Phillips XL30 SEM-FEG (Philips, Eindhoven, The Netherlands) equipped with a Schottky field emission electron gun and a conventional Everhart-Thornley secondary electron detector was used to record the images. The acceleration voltage was set at 20 kV and the spot size at 3. For each batch, multiple pictures from different spots throughout the sample were collected and the images were processed with ImageJ version 1.51j (National Institutes of Health, Bethesda, Maryland, USA) to determine the particle size of 300 particles and subsequently calculate the particle size distributions, Dv_{50} and span values. The span value is defined as $(Dv_{90} – Dv_{10})/ Dv_{50}$.

Drug release

To test the pharmaceutical performance of the prepared formulations, dissolution experiments were conducted in acidic medium (0.1 M HCl). To this end, an accurate amount of the formulation was weighted to obtain an equivalent of 0.66 mg darunavir per mL medium. The experiments were carried out in triplicate in test tubes rotating at 40 rpm using a rotary mixer L26 (Labinco BV, Breda, The Netherlands). After 5, 15, 30, 60 and 120 minutes samples were taken, filtered and quantified by HPLC. The percentage of darunavir (DRV) released was calculated by comparing the measured amount of darunavir to the originally weighted amount which was corrected for the residual solvent.

4.3.5. Design of experiments

Parameters

In order to evaluate the influence of the process and formulation parameters on the properties of electrosprayed ASD formulations, the PVP-DRV system was chosen and a two-level full factorial screening DoE (2^4) was applied. As shown in Fig 4.1 the studied parameters were the feed flow rate, tip-to-collector distance, total solids concentration (expressed as PVP concentration) and the drug loading. Preliminary experiments were carried out upfront to determine the lower (-) and upper (+) parameter levels. Subsequently, sixteen batches were produced to cover every combination of upper

and lower parameter level and three batches at centre point level were run to verify the reproducibility. When changing the feed flow rate and the tip-to-collector distance, the voltage necessary to obtain a cone-jet mode will change as well, thus the voltage was adapted correspondingly.

Responses

The influence of the parameters on different characteristics of the ASD formulations, also referred to as responses, was tested and these responses are listed in Table 4.4. The measurements of the crystallinity, residual solvent, Dv_{50}, span, % DRV released after 5 min and the AUC after 120 min were carried out following the same procedure as explained above in section 4.3.4. "*Characterization of the amorphous solid dispersions*". The width of the T_g, a measure of the homogeneity of the formulations, was determined with mDSC[141]. In mDSC, a glass transition can be seen as a jump step of the base line in the reversing heat flow due to the change in heat capacity. The width of the T_g can be inferred from the width of the peak in the temperature derivative of the reversing heat flow after Savitsky−Golay smoothing of the signal (region width 5 min). As a final response the morphology was studied. Based on the SEM images the particles were classified as either "spherical" or "tailed" if the particles were elongated or had a fibrous protuberance. Subsequently, the percentage of tailed particles in a batch could be calculated. To ascertain the effects of the parameters, the collected data of the DoE were analysed with multiple regression analysis using the software package MODDE pro version 12 (Sartorius Stedim Biotech, Umeå, Sweden).

4.4. RESULTS AND DISCUSSION

4.4.1. Comparison between electrospraying and spray drying in the manufacturing of ASDs

In the first part of the study, the ability of electrospraying to manufacture amorphous solid dispersions of darunavir was evaluated. Although electrospraying is a noticeably promising technique, various questions and problems remain to date unresolved. PVP was previously used during electrospraying in other studies but the literature on electrospraying of HPMC and HPMC AS is limited[78,106,109,112,113,120].

In a first set of experiments, the equilibrium solubility of darunavir in the pure media (pH 1 and pH 7.5) and the solubility in the media with polymers was measured (Fig 4.2A). Darunavir's solubility was seven times higher in the acidic than in the neutral medium through protonation of the amino group at low pH values. This protonation can be inferred from the graph in Fig 4.2B, which clearly shows that the charge of a darunavir molecule is dependent on the pH. The choice to use a polymer concentration of 0.15 % and 0.6 % was based on the final polymer concentration that would be reached during dissolution tests of an ASD formulation with a drug loading of 10 or 30 % darunavir.

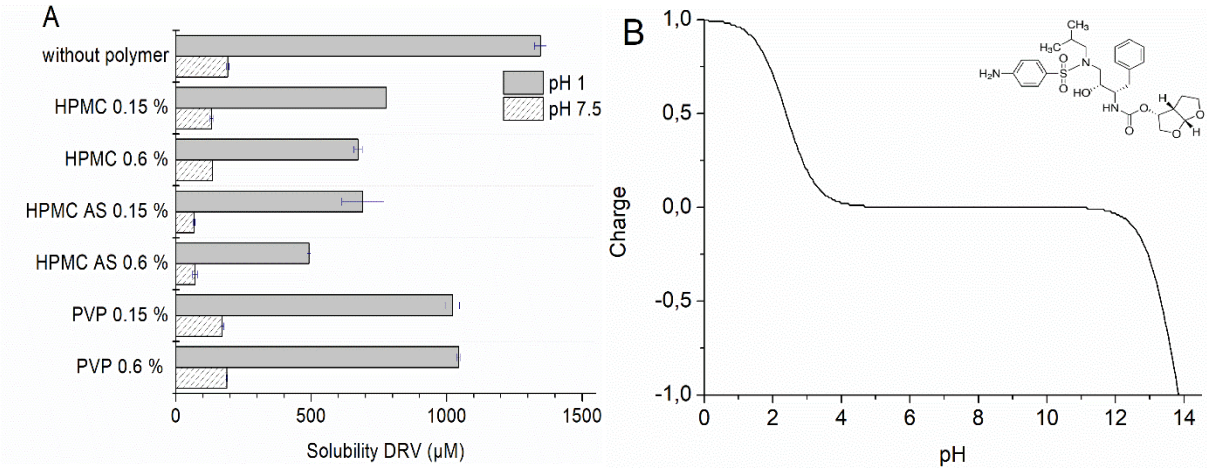

Figure 4.2. A: Solubility of darunavir in plain medium as well as medium with 0.15 % and 0.6 % polymer. The grey bars represent the solubility in 0.1 M HCl pH 1 and the shaded bars in phosphate buffer pH 7.5. (n = 3). In the presence of the polymers, the solubility of darunavir dropped significantly ($p<0.05$) except for PVP 0.6 % in pH 7.5. B: Charge of a darunavir molecule in function of the pH, as predicted by the MarvinSketch Software package (ChemAxon). At low pH values, the amino group can be protonated causing an increase in the solubility.

Furthermore, except for PVP 0.6 % in pH 7.5, the concentration of darunavir decreased significantly when the polymers were present and this solubility drop was larger when adding a higher polymer concentration (0.6 %). A possible explanation is adsorption of darunavir to the polymers, which leads to a lower analytical availability. To verify this hypothesis, a dialysis experiment was carried out. The dialysis bag containing 0.1 M HCl was submerged in a beaker containing a darunavir-polymer mixture and a reference experiment was carried out without addition of the polymer to the darunavir solution in the beaker. After equilibration, the darunavir concentration inside the dialysis bag and at the outside (in the beaker) were equal to 780 µM for the reference. However, when the beaker contained the darunavir-polymer mixture, the concentration at the inside dropped to 725, 276 and 693 µM for HPMC, HPMC AS and PVP respectively. Darunavir was adsorbed to the polymers and trapped in the

beaker because the polymer chains are too large to pass through the semi-permeable dialysis membrane. Consequently, the amount of molecules that was free to diffuse through the membrane was reduced. Adsorption was most notably observed for HPMC AS and this corresponds to the largest solubility drop in Fig 4.2A. The dialysis experiments thus support the adsorption hypothesis, but further investigation of the mechanism does not fall within the scope of this study.

Secondly, supersaturation experiments were carried out to investigate if concentrations higher than the equilibrium solubilities could be obtained when a highly concentrated organic solution of darunavir was added to the aqueous polymer solution. A representative example is shown in Fig 4.3, where the organic darunavir solution was added to a 0.6 % PVP solution (green) or to the blank acidic medium (blue). Since the aqueous medium acts as an anti-solvent, darunavir started to precipitate immediately but a supersaturated concentration could be maintained for at least two hours. Similar results were obtained in all supersaturation experiments with the other polymers and are represented as supersaturation factors in Table 4.1. The supersaturation factors for the media with the polymers in pH 1 (the first row of the table) are not significantly different from the reference without polymer (2.0), except for 0.15 % HPMC and 0.6 % PVP. Although at long term the equilibrium solubility of darunavir was lower when polymers were added (Fig 4.2A), all supersaturation factors were higher than two. For pH 7.5, almost all supersaturation factors are significantly higher than the reference. Darunavir is less soluble and the positive effect of the polymers on the supersaturation is more pronounced. Overall, supersaturation levels could be reached and maintained and the polymers are thus suitable for the preparation of the ASD.

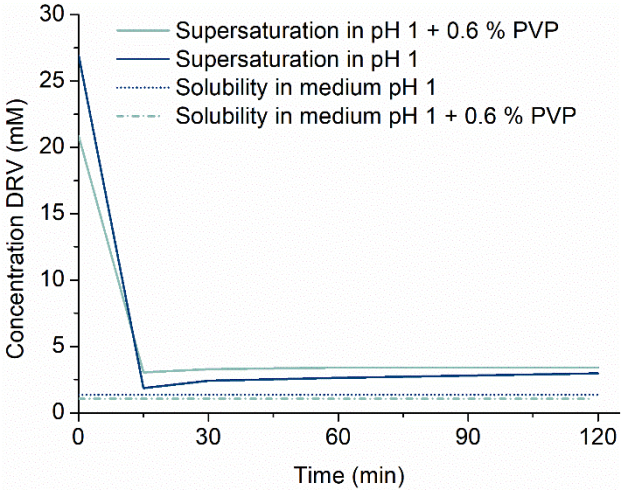

Figure 4.3. Example of a supersaturation experiment. A highly concentrated organic solution of darunavir in DMF was added to 0.1 M HCl (blue) or a solution of 0.6 % PVP in 0.1 M HCl (green). The darunavir concentration was measured over a time period of two hours.

*Table 4.1. Results of the supersaturation experiments expressed as supersaturation factors. This factor is the ratio between the $AUC_{(15\text{-}120\ min)}$ of the supersaturated curve and the $AUC_{(15\text{-}120\ min)}$ of the equilibrium concentration in both plain medium (first row) and medium spiked with the polymers (second row). * Supersaturation factors significantly higher than the value obtained without polymer (2.0 and 2.6 for pH 1 and pH 7.5 respectively).*

	without polymer	**HPMC 0.15 %**	**HPMC 0.6 %**	**HPMC AS 0.15 %**	**HPMC AS 0.6 %**	**PVP 0.15 %**	**PVP 0.6 %**
Medium pH 1	2.0	2.4*	2.2	2.1	2.1	2.3	2.2*
Medium pH 1 + polymer	/	4.1	4.3	4.1	5.8	3.0	2.9
Medium pH 7.5	2.6	2.7	2.8*	2.8*	3.2*	2.9*	3.0*
Medium pH 7.5 + polymer	/	3.9	4.0	8.0	8.5	3.3	3.1

Knowing that HPMC, HPMC AS and PVP are adequate polymers, ASDs were prepared via electrospraying and spray drying following the protocol mentioned in the *"Materials and Method"* section. Spray dried formulations were prepared as a reference, because this method is considered as a golden standard in ASD manufacturing. The choice of solvent, polymer concentration and the operational settings were based on previous studies carried out by our research group[65,142]. After a post-drying step in the vacuum oven, the formulations were characterised. As can be observed in the thermograms (Fig 4.4), all formulations were fully amorphous and showed only one single T_g, suggesting a one phase amorphous system, given the spatial resolution limits of DSC. The value of this T_g shifted to the T_g of darunavir (48 °C) with increasing drug loading. The diffractograms in Fig 4.5 confirm these results because amorphous halos without any Bragg peaks were observed for all spray dried and electrosprayed samples.

Since the API and polymer were originally dissolved in ethanol and/or dichloromethane and possibly not all of the solvent was evaporated during the spraying process, the residual solvent in the final formulations was determined. This determination was based on the percentage of mass loss due to evaporation of the residual solvent when the formulations were heated to 120 °C during TGA analysis. Table 4.2 provides an overview of the residual solvent levels. These residual solvent levels were similar for the formulations prepared with both techniques. Due to the different phenomena leading the atomization and evaporation in the two methods, a difference in residual solvent was expected but most likely, this was cancelled out by the post-drying step. Even though this post-drying step was applied, the residual solvent levels were relatively high, especially for the formulations with PVP.

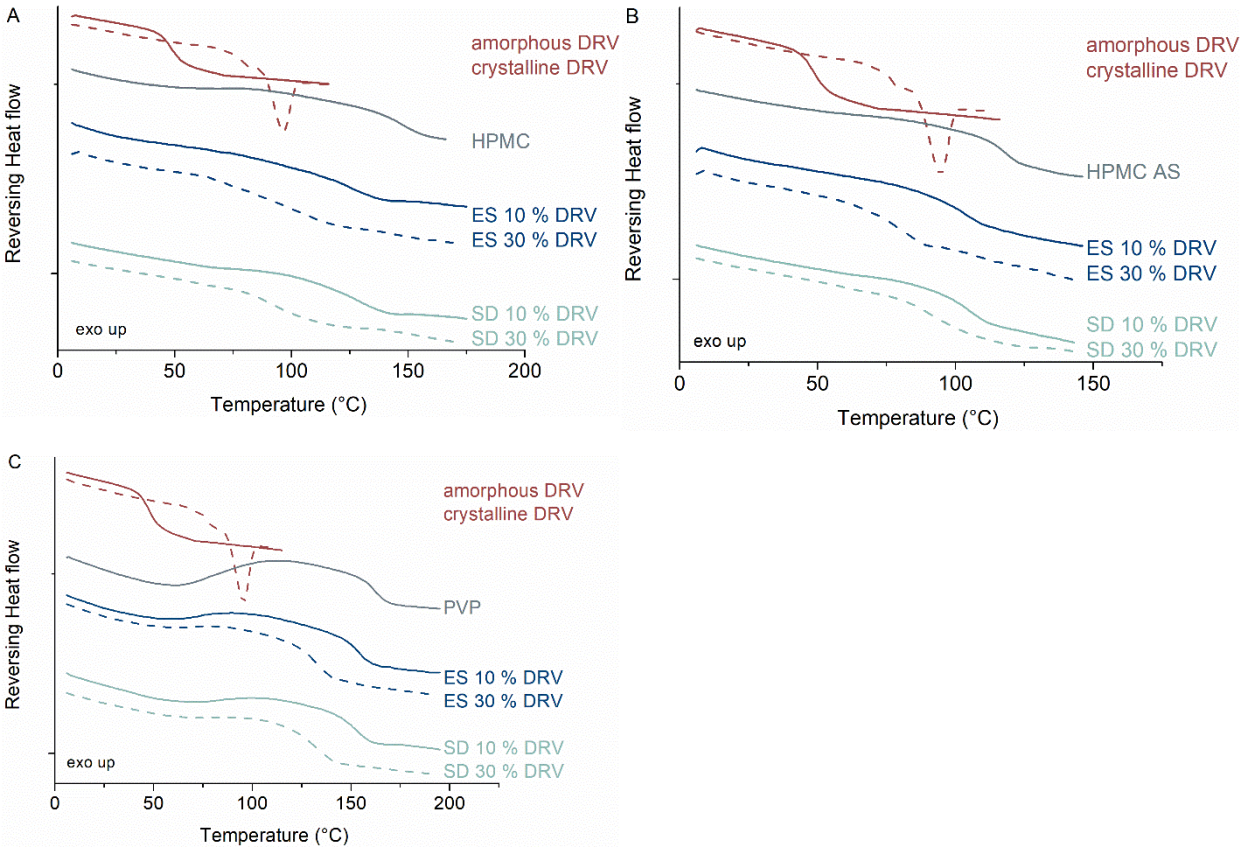

Figure 4.4. Thermograms acquired with mDSC. A: Formulations with HPMC and darunavir. B: HPMC AS and darunavir. C: PVP and darunavir. ES: Electrosprayed formulation with 10 or 30 % drug loading. SD: Spray dried formulation with 10 or 30 % drug loading. Endothermic signals are pointed downward.

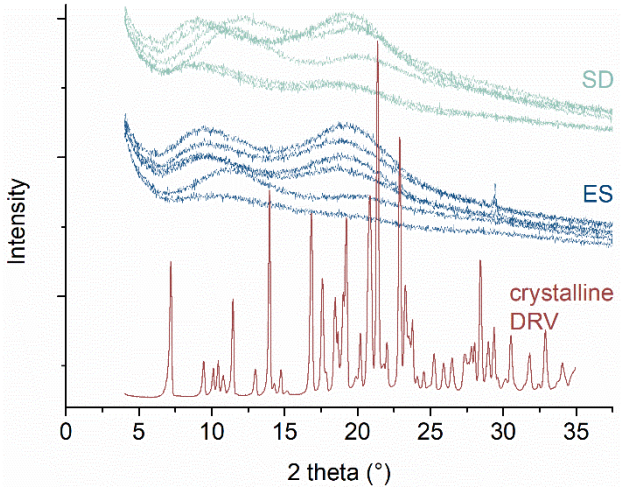

Figure 4.5. Diffractograms of unproccesed crystalline darunavir (DRV), the six electrosprayed (ES) and the six spray dried formulations (SD).

Table 4.2. Residual solvent of the electrosprayed and spray dried formulations based on the percentage of mass loss when heated to 120 °C during TGA analysis.

Residual solvent (%)	Electrosprayed	Spray dried
HPMC 10 % DRV	3.6	3.0
HPMC 30 % DRV	2.2	2.5
HPMC AS 10 % DRV	1.7	1.8
HPMC AS 30% DRV	1.9	1.7
PVP 10 % DRV	11	8.1
PVP 30 % DRV	9.4	7.1

To investigate the morphology and the particle size distributions of the ASDs, SEM images were recorded. The six spray dried formulations exhibited the typical collapsed morphology, irrespective of the polymer used, but the different polymers yielded different morphologies during electrospraying (Fig 4.6). The electrosprayed particles prepared with HPMC were rather flat and the ones with HPMC AS had a rough surface. The ethanol dichloromethane mixture used to prepare the polymer-API solution is possibly not the best solvent for HPMC AS. Polymer-polymer interactions are more favourable than polymer-solvent interactions which favours the polymer chains to fold up into a coil. This coil formation suppresses entanglement of the polymer chains leading to a less smooth surface[143]. On the other hand, the particles with PVP were smooth and spherical. A possible explanation is the fact that for the PVP systems, ethanol was used, a solvent in which this polymer is very soluble. Ethanol evaporates slower than the mixture with dichloromethane, giving the polymer chains more time to diffuse and entangle. On top of that, a solution with a higher polymer concentration of 10 % was used (HPMC and HPMC AS only 1.5 %) which also facilitates the entanglement of the polymer chains and increases the visco-elastic forces.

Fig 4.7 depicts the particle size distribution of the ASD particles, the corresponding Dv_{50} and span values are provided in Table 4.3. The Dv_{50} is the median diameter of the distribution and the span is defined as $(Dv_{90} - Dv_{10})/Dv_{50}$ with 90 and 10 % of the distribution lying under the Dv_{90} and Dv_{10} diameter respectively. The spray dried particles were larger than the electrosprayed ones and their particle size distributions were broader. However, one has to be careful when interpreting these results because neither the operational setting used for spray drying, nor the ones used for electrospraying were optimized in this explorative part of the project. Still, the results indicate that electrospraying can produce nearly monodisperse particles as previously mentioned in literature[59,73]. Nevertheless it is apparent that the PVP particles were larger than the particles produced with HPMC or HPMC AS. Again this can probably be explained by the higher solids concentration used for the particles with PVP. Charged droplets are ejected from the cone-jet during electrospraying and in these droplets the electric and visco-elastic forces compete with each other. Hence, when the visco-elastic forces are stronger owing to the higher polymer concentration and improved entanglement, the droplets are more resistant against Coulomb fission.

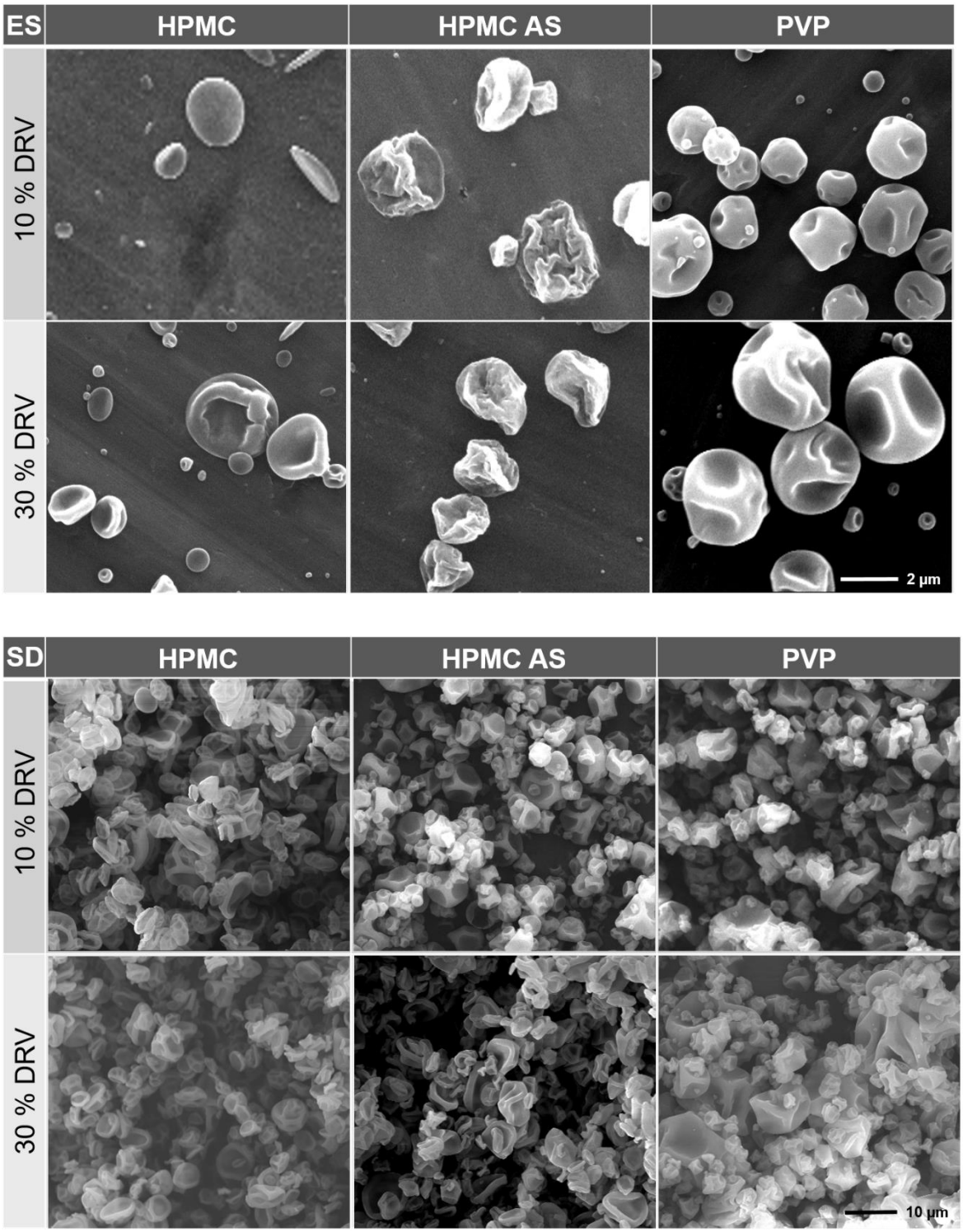

Figure 4.6. SEM images of the electrosprayed (ES) ASD particles and spray dried (SD) ASD particles. The first row depicts the particles with 10 % drug loading and the second row the particles with 30 %.

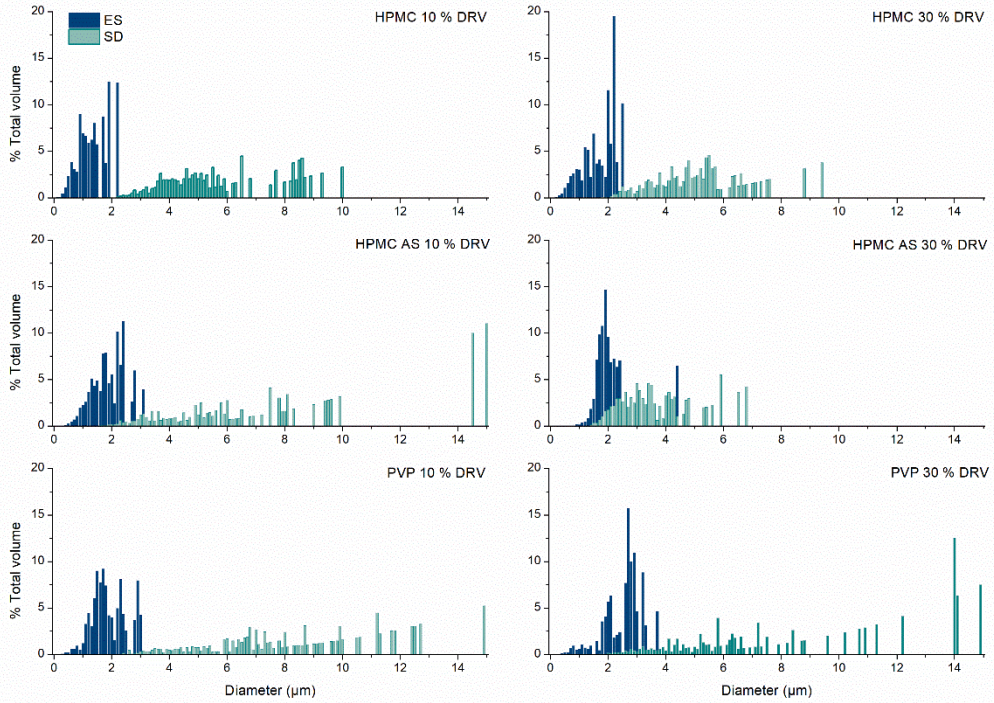

Figure 4.7. Particle size distributions of the ASD particles with low drug loading in the left column and higher drug loading in the right column. The dark blue bars represent the electrosprayed particles and the green bars the spray dried ones.

Table 4.3. Dv_{50} and span values of the electrosprayed and spray dried ASD particles prepared with the three different polymers and 10 or 30 % drug loading.

Electrosprayed			**Spray dried**		
	Dv_{50} (µm)	Span (µm)		Dv_{50} (µm)	Span (µm)
HPMC 10 % DRV	1.3	1.1	HPMC 10 % DRV	5.5	0.9
HPMC 30 % DRV	1.9	0.9	HPMC 30 % DRV	5.1	0.8
HPMC AS 10 % DRV	1.9	0.8	HPMC AS 10 % DRV	7.4	1.6
HPMC AS 30% DRV	1.9	0.5	HPMC AS 30% DRV	3.4	1.1
PVP 10 % DRV	1.7	0.9	PVP 10 % DRV	8.5	0.9
PVP 30 % DRV	2.7	0.5	PVP 30 % DRV	8.1	1.2

Despite the diversity in particle sizes obtained with the two methods, the release profiles for the same polymer were comparable (Fig 4.8). Apparently the dynamics during the dissolution balanced out the particle size and shape differences. Darunavir was quickly released from the formulations with HPMC and PVP and a higher concentration was reached after two hours compared to the unprocessed darunavir. During the supersaturation experiments (Table 4.3) it was observed that the supersaturation factors were not significantly higher when polymers were present compared to blank medium. This suggests that the improved dissolution is mainly due to amorphization.

The extent of release for the formulations containing HPMC AS was decreased, because HPMC AS is insoluble in the acidic medium. Interestingly, a higher concentration was observed for the HPMC AS formulation with the 30 % drug loading. This is in contradiction to the expectations: normally the highest release is obtained for the lowest drug loading[22]. When the drug loading is low, more polymer

is available for less API molecules which promotes the dissolution. We hypothesized that the enhanced solubility of darunavir in the acidic medium underpinned this discrepancy. Supplementary dissolution tests were performed with the HPMC AS formulations in phosphate buffer at pH 7.5. In this neutral medium HPMC AS dissolves easily, but darunavir is not protonated anymore and it becomes less soluble. It is apparent from the graph in Fig 4.9 that at this neutral pH, a lower drug loading does indeed generate a higher release. The release is "carrier-driven" and as a consequence a higher polymer to drug ratio facilitates the dissolution. However, in the acidic medium HPMC AS is insoluble but darunavir is better soluble, leading to an "API-driven" release mechanism where higher concentrations are observed with higher drug loadings, as observed during the original experiments[144]. To validate this hypothesis, ASDs of darunavir and another insoluble polymer, ethyl cellulose, were prepared and the release in acidic medium was monitored. The release profiles showed the same trend as the profiles from HPMC AS in acidic medium, conforming the suggested "API-driven" release mechanism.

The above mentioned results clearly point to the equivalency between electrospraying and spray drying in the case of ASD of darunavir and commonly used carriers like PVP, HPMCAS and HPMC. All formulations were amorphous and the dissolution of darunavir improved.

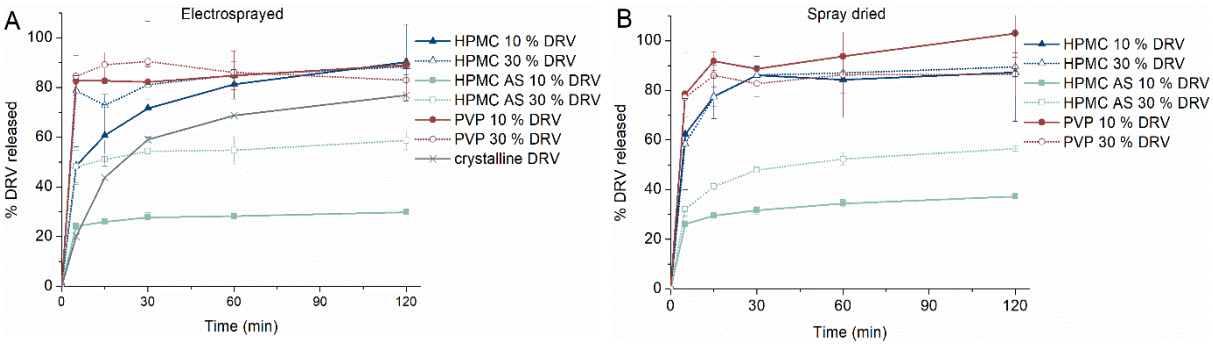

*Figure 4.8. Concentration-time profiles of the dissolution tests carried out in 0.1 M HCl. A: Electrosprayed formulations. B: Spray dried formulations. (*n *= 3)*

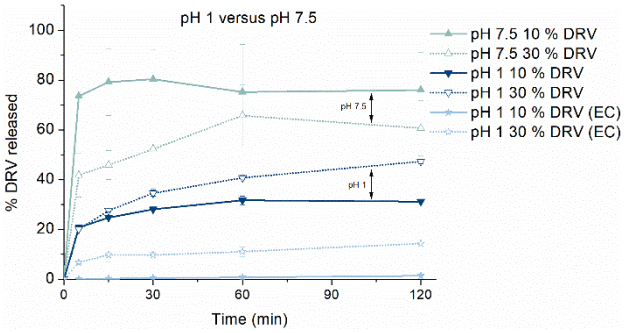

*Figure 4.9. Extra dissolutions tests with the spray dried HPMC AS formulations in phosphate buffer pH 7.5 (upward triangle), HPMC AS formulations in 0.1 M HCl pH 1 (downward triangles) and formulations with ethyl cellulose (EC) in pH 1 (stars). (*n *= 3 for EC and* n *= 6 for HPMC AS)*

4.4.2. Influence of process and formulation parameters in electrospraying

As electrospraying was proven to be a suitable method for the preparation of ASDs of darunavir, the process was studied in more detail. More precisely, a screening DoE was set up to investigate the impact of two process and two formulation parameters on various properties of the final ASDs. To date it is not evident to select the right formulation and operational settings for electrospraying as explained in the introduction. The influence on the formation of the cone-jet mode and the characteristics of the final particles is not completely understood yet. Nonetheless it is of great importance to work in the cone-jet mode. Only in this mode particles can be manufactured reproducibly, and even a small change in the settings can cause a shift to another mode. Already by using a different solvent, the conductivity, viscosity and surface tension of the solution can change and will affect the spraying mode. Often time-consuming empirical experiments need to be carried out to find out the appropriate settings and this hampers the use of electrospraying as a general method on a larger scale. When using a coaxial setup for the manufacturing of core-shell structures, complexity will only increase.

Different arguments led to the choice of darunavir-PVP as a model system for this study. In the first place, particles that are more spherical were obtained when using PVP (Fig 4.6) but secondly and more important, a higher polymer concentration without the addition of dichloromethane, a class 2 solvent, could be used. For the HPMC and HPMC AS systems, the polymer concentration was limited to 1.5 %. Because the feed flow rate during electrospraying is rather slow (<1 mL/h), this low concentration reduced the production rate remarkably. Furthermore, a broader polymer concentration range can be explored in the DoE when higher concentrations are possible, hence it will be easier to pick up the influence of this parameter.

To evaluate the influence of the two process (feed flow rate and tip-to-collector distance) and two formulation (total solids concentration and the drug loading) parameters on the characteristics of final particles, a full factorial experimental design (2^4) was used. This means that the particles were electrosprayed and characterised at all possible combinations of the four parameters, considering that each parameter can take its high or low value/level. Consequently, 2^4 or sixteen batches were prepared and apart from these sixteen batches at the upper and lower level, three centre point batches were prepared to check if any deviation occurred in the intermediate region. By testing the centre point in triplicate, the reproducibility of the process was tested. Using this type of design is more efficient than evaluating one parameter at the time and also allows to study possible interactions between the parameters. To select the limits for the upper and lower level, the workable parameter ranges were explored, guided by our previous study on electrospraying of polymer solutions, where the cone-jet window was mapped out[65]. In the following, the total solids concentration will be expressed in terms of the PVP concentration; the darunavir concentration was adapted correspondingly to obtain the desired drug loading. The limits for the PVP concentration and drug loading were set at 5-10 % and 10-30 % respectively. Solutions with these PVP concentrations and drug loadings were tested by increasing the tip-to-collector distance and feed flow rate until the cone-jet mode could no longer be observed. By doing so, the limits for the distance were specified at 6 and

12 cm and for the feed flow rate at 0.2 and 0.9 mL/h. After the preparation of the batches, the eight responses were measured and an overview of all data concerning the DoE can be found in Table 4.4. This table also mentions the applied voltage for each batch. Although the voltage is an important parameter as well, it was not included as a factor in the DoE, because the voltage cannot be changed independently. When changing the feed flow rate and tip-to-collector distance, the strength of the electric field will change, therefore the voltage was correspondingly adapted to ensure that the electrospraying process runs in the cone-jet mode.

Table 4.4. Overview of the four factors (parameters) and eight responses of the full factorial DoE (2^4). The voltage, which is a process parameter, was not included as a factor, but was optimized for each batch to ensure a stable cone-jet during the electrospraying process.

N°	Flow rate	Distance	PVP concen-tration	DRV loading	Voltage	Crystal-linity	Width T_g	Residual solvent	Dv_{50}	Span	Tailing	DRV released 5 min	AUC 120 min
	mL/h	cm	%	%	kV	%	°C	%	µm	µm	%	%	% . min
1	0.2	6	5	10	14	0	40	9.3	1.1	0.59	0	71	10296
2	0.9	6	5	10	19	0	37	8.0	2.5	1.2	63	83	9904
3	0.2	12	5	10	20	0	36	8.8	1.3	0.60	0	56	9815
4	0.9	12	5	10	22	0	40	9.9	4.5	1.1	23	65	9187
5	0.2	6	10	10	12	0	36	9.6	1.5	0.77	0	83	9803
6	0.9	6	10	10	17	0	35	11	2.5	1.8	15	85	10880
7	0.2	12	10	10	20	0	36	8.8	1.5	0.35	0	82	10160
8	0.9	12	10	10	22	0	39	9.0	2.7	0.81	0	61	9863
9	0.2	6	5	30	13	0	52	8.0	1.3	0.93	0	63	9846
10	0.9	6	5	30	16	0	52	6.7	4.5	1.0	21	55	10287
11	0.2	12	5	30	19	0	48	8.1	1.6	0.79	0	65	9636
12	0.9	12	5	30	25	0	53	6.7	2.5	1.4	11	63	9725
13	0.2	6	10	30	12	0	47	6.9	1.5	0.93	0	60	8977
14	0.9	6	10	30	15	0	51	7.4	3.5	0.68	0	63	10457
15	0.2	12	10	30	19	0	42	7.3	1.7	0.80	0	57	9434
16	0.9	12	10	30	20	0	38	7.8	2.7	1.3	0	52	9804
17	0.55	9	7.5	20	18	0	42	7.5	2.1	1.1	0	53	9085
18	0.55	9	7.5	20	18	0	42	8.1	2.2	0.83	0	64	9770
19	0.55	9	7.5	20	18	0	42	7.9	1.8	0.82	0	70	9668

The impact of the parameters on the responses was evaluated using multiple linear regression and Fig 4.10 shows the coefficient plots of the developed models. The factors represented in grey had a significant effect and the ones in white were not significant. Though, it was favourable in terms of model quality to keep this insignificant factors in the model. The percentage of darunavir released after 5 min as well as the AUC and the span were not included in the figure. The variability for these responses was too high and led to models of insufficient quality. A large deviation between the replicates in a dissolution experiment is not uncommon. Upon contact with the dissolution medium, the polymer starts to swell and this easily leads to a less reproducible response, especially at the first time point of 5 min. The crystallinity was also not included in Fig 4.10 because a fully amorphous system was observed for all 19 batches. This means that the four factors did not influence the amorphicity within the tested parameter ranges, a positive aspect for a manufacturing method of ASDs. For the four responses depicted in Fig 4.10 significant models could be obtained.

Starting with the impact of the two process parameters, the tip-to-collector distance had no influence on the properties of the ASDs; at least not within the range tested. This in contrast with the feed flow rate, which had a significant influence on the diameter and the morphology of the ASD particles. More

specifically, the particles became larger and more tailed when the flow rate was increased. The SEM images in Fig 4.11 illustrate this effect. The effect on the particle size is in line with the predictions based on different scaling laws, which correlate the size of the droplets emitted from the jet with the feed flow rate. The higher the flow rate the larger the droplets and consequently, the larger the particles[76]. Although it was not possible to create a qualitative model describing the influence of the factors on the span, it can be assumed from the data in Table 4.4 that a broader particle size distribution was obtained with higher flow rates. Reason is the fact that with increasing flow rate not only the droplet size but also the current through the jet will increase, leading to more instabilities and Coulomb fission, resulting in droplets with various sizes[73]. For the largest droplets, it was observed that the solvent was not completely evaporated when the particles hit the collector, creating the large spots on the aluminium foil.

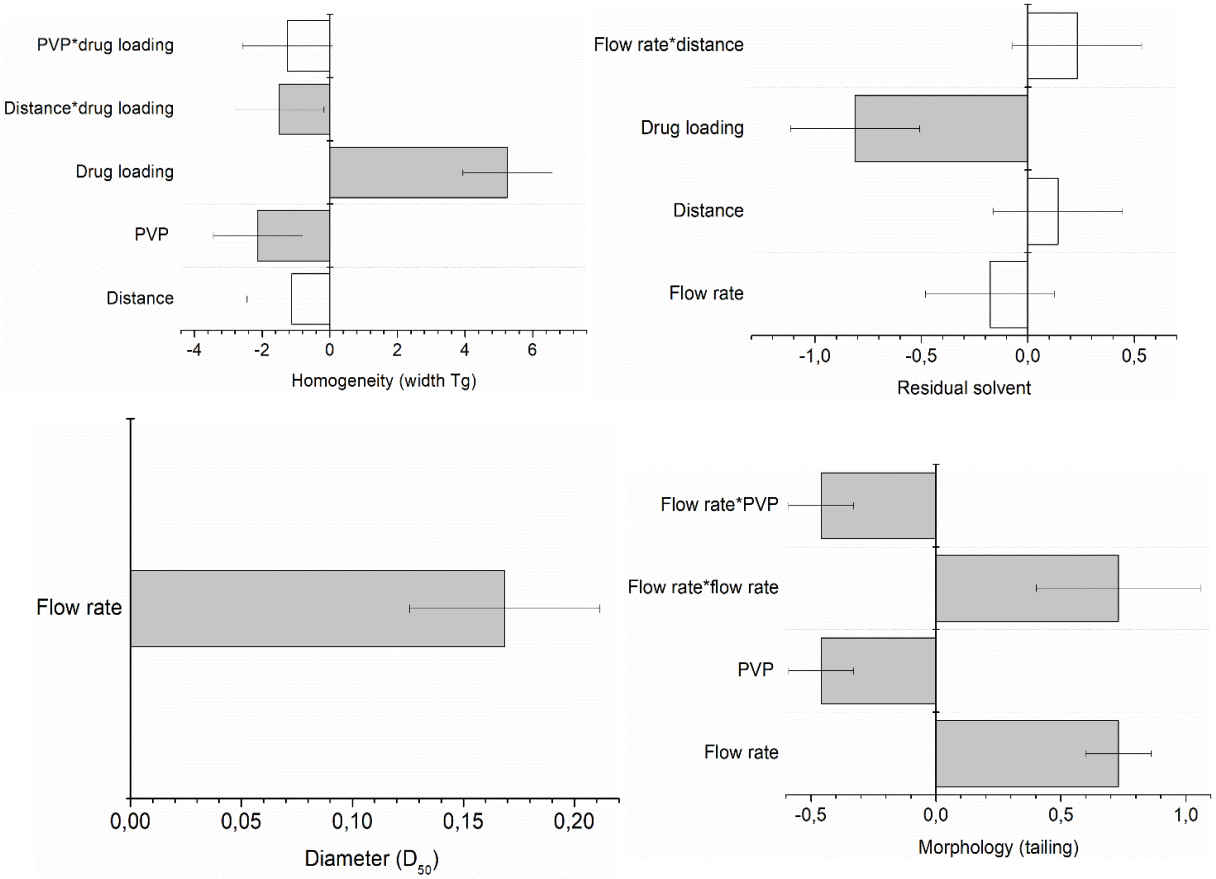

Figure 4.10. Coefficient plots of the models developed for the width of the T_g, the residual solvent, the diameter (Dv_{50}) and the morphology of the ASD formulations. Grey bars represent a signifcant effect of the factor on the response, white bars a non-significant effect. The coefficients are scaled and centered as predicted with the MODDEpro software package.

Likely, the instabilities and Coulomb fission are also the reason for the deviating morphology when the highest flow rate was applied. Almeria *et al*. reported the formation of elongated particles using high flow rates[72]. Due to the increased electric stress, the charge on the droplets becomes too high when the solvent evaporates and the droplets split up (Coulomb fission). However, when this fission occurs when the solvent is almost fully evaporated and the polymer chains are already entangled to a certain extent, the droplet is pulled apart but cannot completely split into two parts. Consequently,

the system freezes in the elongated formation. Furthermore, it can be inferred from Table 4.4 that a higher potential difference was applied for the batches produced at a higher flow rate. This could also be a reason for the observed deformation, because particles are typically more elongated when using a higher voltage[64,68]. A higher voltage to obtain the cone-jet mode was also necessary for the upper level of the tip-to-collector distance and the lower level of the PVP concentration. The latter is due to the lower conductivity of the solutions with less PVP and in case of the distance, a higher voltage is required to compensate for the weakening of the electric field when the distance between the two poles (nozzle and collector) is larger.

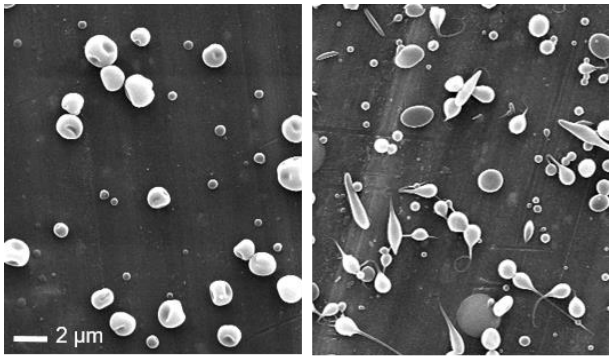

Figure 4.11. Left: SEM image of batch n°5 produced at low feed flow rate (0.2 mL/h). All particles are spherical (0 % tailing). Right: batch n°2 produced at high flow rate (0.9 mL/h). More than half the particles are elongated or have a fibrous protuberance (63 % tailing).

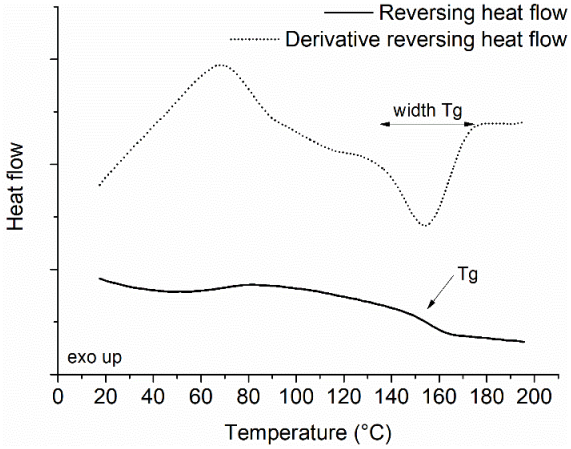

Figure 4.12. Thermogram of batch n°1 of the DoE to illustrate how the width of the T_g was measured.

The two formulation parameters had a significant impact on the ASDs as well. Formulations with a low drug loading were more homogeneous and contained more residual solvent. The homogeneity was evaluated based on the width of the T_g, calculated in the derivative reversing heat flow signal (Fig 4.12). The broader this event, the less homogenous the system is. At the lower level of the drug loading, less darunavir molecules needed to be dispersed as compared to the upper level. Hence the darunavir molecules were easier and more homogeneously dispersed between the polymer chains, yielding lower values for the width of the T_g. On the other hand, lowering the drug loading affected the residual solvent in a negative way since solvent evaporation is more difficult from polymer rich particles which can lock up the solvent. Finally, the second formulation parameter, the PVP concentration, had a significant impact on the homogeneity and the morphology. The influence on the homogeneity can be explained as follows: less solvent was used to prepare a solution with a high PVP concentration in comparison to a solution with a low PVP concentration. Because there was less solvent available, the darunavir molecules were forced to disperse in the polymer, resulting in a more homogeneous system (lower values for the width of the T_g). Increasing the PVP concentration was also advantageous for the morphology as it prevented the formation of tailed particles. As mentioned earlier, the entanglement and visco-elastic forces are larger for higher concentrated PVP solutions, which counterbalances the detrimental impact of the electric stress in the deformation of the particles.

4.5. CONCLUSION

The possibility to use electrospraying as a manufacturing method for amorphous solid dispersions of darunavir was evaluated and compared with spray drying. It was shown that electrospraying was equivalent to spray drying regarding the characteristics and pharmaceutical performance of the produced amorphous solid dispersions. The preparation of amorphous solid dispersions with both HPMC and PVP as a carrier improved the rate and extent of the dissolution. The extent of the dissolution for the ASD with HPMC AS was suppressed as expected when using this enteric polymer. In a second part of the study, it was demonstrated that the feed flow rate, the total solids concentration and the drug loading had a significant effect on the electrosprayed formulations, more specifically on the residual solvent, the homogeneity, particle size and the morphology. This knowledge opens perspectives for future exploration and optimization of the use of coaxial electrospraying to coat the amorphous solid dispersion particles of darunavir and obtain a dosage form for delayed release.

Acknowledgements

Het Fonds voor Wetenschappelijk Onderzoek-Vlaanderen (FWO, project G0A3916N) is acknowledged for financial support. In addition, the authors want to thank Bernard Appeltans as well as Nico Coenen for the practical support in the lab and Annouschka Laenen for the statistical advice

Chapter 5
Gastro-resistant encapsulation of amorphous solid dispersions containing darunavir by coaxial electrospraying

Results of this chapter are based on:

Gastro-resistant encapsulation of amorphous solid dispersions containing darunavir by coaxial electrospraying. ***Annelies Smeets and Robin Koekoekx*,*** *Wouter Ruelens, Mario Smet, Christian Clasen and Guy Van den Mooter. Accepted by the International Journal of Pharmaceutics.*

****joint first authorship***

5.1. ABSTRACT

The relatively simple technique of coaxial electrospraying allows to produce core-shell microparticles with potentially high encapsulation efficiencies. In this study, amorphous solid dispersions of a hydroxypropyl methylcellulose or polyvinylpyrrolidone based polymer matrix containing the active pharmaceutical ingredient darunavir were coated with a gastro-resistant shell polymer that does not dissolve at lower pH present in the stomach, but only later at a higher pH in the small intestine. A multitude of shell polymers were tested with the aim to identify a material that limits the drug release to less than 10 % after two hours at a pH of 1 to comply with the European Pharmacopoeia regarding gastro-resistant formulations. In parallel, the core-shell structure of the particles was determined with confocal imaging and their surface morphology with scanning electron microscopy. While the structural analysis revealed significant differences between the different formulations, all investigated shell polymers exhibited a burst drug release followed by a slow release for the remainder of a two hour period. Ultimately, the shell copolymer poly(methacrylic acid-co-methyl methacrylate), in particular for a monomer ratio 1/2, resulted consistently in darunavir release below the 10 % upper limit compared to the other tested polymers where such low releases were inaccessible. Further investigation of this shell polymer revealed that both the monomer ratio of methacrylic acid to methyl methacrylate in the copolymer and the utilized solvent are determining factors in the release performance of the final particles.

5.2. INTRODUCTION

Over the past years, the amount of new active pharmaceutical ingredients (APIs) that suffer from low aqueous solubility or low dissolution rate and hence a low oral bioavailability, has been growing increasingly. As a result, multiple novel formulation strategies have been developed to increase oral bioavailability[14], including the application of cyclodextrines[145], co-crystals[146], lipid-based systems[147], silica-based systems[148], particle size reduction[149] and amorphous solid dispersions (ASDs)[18] . The last strategy mentioned will be of particular interest for this work. In an ASD, the API is dispersed in an inert (polymeric) matrix at molecular level lacking any long range order, which leads to a higher free energy and thus improved solubility and dissolution rates[18]. Usually, ASDs are formulated as immediate release solid dosage forms, in order to release the API instantaneously after oral intake. However, in some specific cases a more delayed release can be favourable e.g. for site specific targeting in the gastrointestinal tract[150], for powders for reconstitution[151], or for a sustained release of the API in order to prevent fast precipitation of the supersaturated drug, which should maintain supersaturated levels over a longer time period[90].

ASD particles can be tableted and if needed, subsequently coated with polymers to reach the optimal release profile[48]. Still, tablets are limited in their applicability for a growing majority of patients with swallowing disabilities like elderly and young children. It is thus desirable to deliver the poorly soluble API in an easy-to-swallow dosage form while retaining the delayed release kinetics. A stable powder (with diameters in the lower micrometre range) that consists of coated particles containing the necessary API in the core and that can be reconstituted into an oral suspension prior to administration, would prove to be an excellent solution. However, there is limited experience and scientific knowledge, if at all, on how to tune the release profile of such individual solid dispersion microparticles.

Electrohydrodynamic atomization or electrospraying is of particular interest in this context, since this method is able to produce monodisperse nano- and microsized ASD particles[71]. This process is an emerging technique in drug delivery and can be categorized under the solvent-based ASD manufacturing methods. Moreover, different research groups have proven that this technique is able to produce coated nano- and microsized ASD particles with a wide variety of polymers, APIs and solvents in a facile continuous one-step process, when using a coaxial setup[78,84,106,120,152,153]. As depicted in Fig 5.1, a core solution containing the API plus the inert ASD carrier is pumped through the inner needle of a coaxial nozzle, while the shell solution is concurrently pumped through the outer part. A high potential difference over the nozzle and collector creates a strong electric field, leading to the formation of a Taylor cone-jet which breaks up into an aerosol of very fine drops. These falling drops undergo forthwith a phase transition to the solid state due to solvent evaporation, yielding dry and coated ASD particles on the collector. Not only a broad range of monodisperse particle sizes and morphologies can be achieved, but the process can also run at ambient conditions without the need of a secondary drying step[64,73]. These advantages and the unique core-shell structures produced make it worthwhile exploring this novel method, despite the rather limited expertise and available literature

in comparison to manufacturing methods like spray drying or hot melt extrusion, which are already well established in the pharmaceutical industry[18,71].

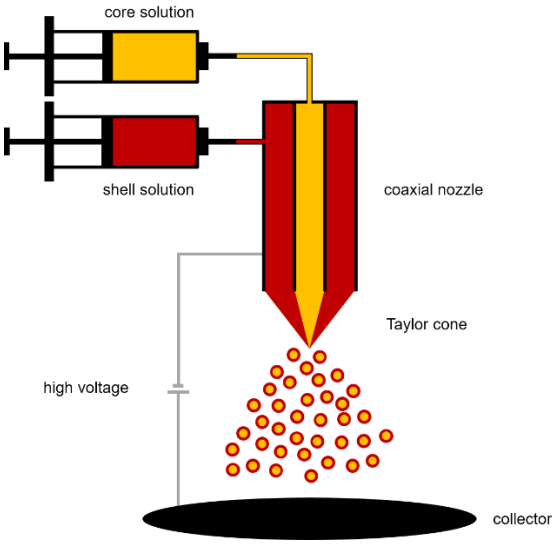

Figure 5.1. Schematic representation of the coaxial electrospraying setup.

This study focusses on electrospraying ASD particles containing the HIV-protease inhibitor darunavir as a model drug, encapsulated within an enteric polymer. The enteric polymer needs to exhibit a pH dependent dissolution behaviour to achieve specific targeting of the API in the gastrointestinal tract. For the current work, the product should resist the acidic environment in the stomach, so that an optimal release at the higher pH further down the gastrointestinal tract is obtained. According to the European Pharmacopoeia (Ph. Eur.) for gastro-resistant formulations, a maximal drug release of 10 % after two hours is allowed at low pH levels for gastro-resistant formulations[154].

Some proof-of-concept studies are already published, demonstrating the value of coaxial electrospraying in the manufacturing of these enteric-coated ASD particles[78,84]. However, contradictory observations remain unexplained, for example, in a previous study of our research group a high burst release of the model API darunavir in acidic medium was observed (above the amount that is allowed by the Ph. Eur.), despite the fact that high encapsulation efficiencies were obtained[78,154]. While previous literature mainly proved electrospraying being an effective method for the production of particles with a specific core and shell combination, our goal goes beyond this first aim of producing coated ASD darunavir particles to obtain formulations in compliance with the Ph. Eur. limits. Indeed, during our initial experiments on darunavir ASDs with different commercially available coating polymers, a significant variability in coating efficiency was observed, which points to the lack of a fundamental understanding of the film coating formation during coaxial electrospraying. Hence, the novelty of our approach lies not only in the fact that a broad range of commercially available enteric polymers was compared for the production of the coated particles, but we also aim to reveal the underlying physicochemical phenomena governing the coating process. The burst release

and significant differences in coating efficiency gave rise to the hypothesis that darunavir can migrate to a certain extent through the core-shell particle and question is how this is influenced by the different formulations parameters like type and composition of the polymer, concentration and solvent.

5.3. MATERIALS AND METHODS

5.3.1. Materials

Polymers: polyvinylpyrrolidone K-30 (PVP) was acquired from BASF® ChemTrade GmbH (Ludwigshafen, Germany), hydroxypropyl methylcellulose 2910 5 mPa·s (HPMC) from Colorcon (Dartford, UK), hydroxypropyl methylcellulose phthalate grade 50 (HPMC P) from Acros Organic (Geel, Belgium), hydroxypropyl methylcellulose acetate succinate grade HF 3 mPa·s (HPMC AS) from Shin-Etsu Chemical Co. (Ohtemachi, Japan), poly(methacrylic acid-co-ethyl acrylate) 1/1 (P(MAA/EA)), poly(methacrylic acid-co-methyl methacrylate) 1/1 (P(MAA/MMA)) (1/1)) and poly(methacrylic acid-co-methyl methacrylate) 1/2 (P(MAA/MMA)) (1/2)) from Evonik Röhm GmbH (Darmstadt, Germany), and cellulose acetate phthalate Mw 2 500 g/mol (CAP), poly(methyl vinyl ether-alt-maleic anhydride) Mw 216 000 g/mol (P(MV/MA)) and poly(methyl methacrylate) Mw 120 000 g/mol (PMMA) from Sigma-Aldrich Co. (St-Louis, USA).

Organic solvents: absolute ethanol (EtOH) and chloroform ($CHCl_3$) were purchased from VWR (Leuven, Belgium), acetonitrile (ACN), dichloromethane (DCM) and 1M hydrochloric acid (HCl) from Fisher Chemical (Loughborough, UK), methanol (MeOH) from Arcos Organic (Geel, Belgium), acetone (ACE) from Chemlab (Zedelgem, Belgium) and anhydrous dimethyl sulfoxide (DMSO) and hexadeuterodimethyl sulfoxide (DMSO-d_6) from Sigma-Aldrich Co. (St-Louis, USA). All solvents were of HPLC or analytical grade.

Reagents: NaH_2PO_4 was obtained from Honeywell, Fluka (Seelze, Germany), formic acid from Chemlab (Zedelgem, Belgium) and 1,1,3,3-Tetramethylguanidine (TMG), methyl iodide (CH_3I), Na_2HPO_4, phenolphthalein and sodium hydroxide (NaOH) from Sigma-Aldrich Co. (St-Louis, USA). The dyes used for confocal imaging were rhodamine B for visualisation of the core and fluorescein isothiocyanate isomer 1 (FITC) for the shell, both from Sigma-Aldrich Co. (St-Louis, USA). Darunavir ethanolate (DRV) was a kind gift from Cilag AG (Schaffhausen, Switzerland) and de-ionized water (Maxima Ultra-Pure Water, Elga Ltd., Wycombe, England) was used in all experiments.

5.3.2. Preparation and characterization of the solutions

The core solutions were prepared by dissolving either PVP or HPMC in a DCM/EtOH 1/1 (V/V) mixture at a concentration of 1 % (m/V) and darunavir was added to obtain a drug to polymer ratio of 1/2. Additionally, a higher concentrated core solution with 5 % (m/V) PVP was prepared without changing the darunavir to polymer ratio of 1/2. For the shell solutions, the different enteric polymers were dissolved in the appropriate solvents at different concentrations as can be found in Table 5.1, and subsequently the physicochemical properties of the solutions were determined. The chemical structures of the polymers can be consulted in Annex 1. First, the kinematic viscosity was measured using an Ubbelohde capillary viscometer with a type I capillary (iVisc capillary viscometer, Lauda, Lauda-Königshofen, Germany) and multiplied by the density of the solutions, which was determined with a glass pycnometer (Blaubrand, Brand GmbH, Wertheim, Germany), to calculate the dynamic viscosity. Secondly, the conductivity of the solutions was determined with a steel 2-electrode conductivity cell (Orion 150Aplus, Thermo Fisher Scientific, Massachusetts, USA) and lastly, a Modular

CAM 200 (KSV Instruments Ltd, Helsinki, Finland) was used to measure the surface tension of the solutions via the pendant drop method. All measurements were performed in triplicate.

5.3.3. Production of the core-shell particles

The core-shell particles were prepared in a single step via electrospraying using a two-concentric stainless steel nozzle (coax_2disp, Linari Engineering, Pisa, Italy) in a climate controlled electrospinning apparatus (EC-CLI, IME Technologies, Geldrop, The Netherlands) at 25 °C and 20 % relative humidity. The core and shell solutions were pumped through the inner part of the nozzle at 0.3 mL/h and through the outer part at 1.2 mL/h respectively, using two syringe pumps (PHD 4400, Harvard Apparatus, Massachusetts, USA). When the shell solution contained chloroform, the distance between the tip of the nozzle and the collector was set at 15 cm, while the distance was 6 cm for all other shell solutions. In general, a potential difference of 20-25 kV was applied, but the exact voltage was slightly varied within this range for each core/shell combination to ensure a stable cone-jet mode. The particles were collected on a glass petri dish that was placed on top of the copper collector plate.

5.3.4. Morphology of the core-shell particles

Scanning electron microscopy (SEM) was used to study the morphology and size of the obtained core-shell particles. To prepare the samples, the glass petri dish on the copper collector of the electrospraying setup was replaced by aluminium foil and the samples were directly electrosprayed onto this foil, after which they were coated with platinum (SCD-030 Balzers Union sputter-coater, Balzers, Liechtenstein). The particles were then visualised with a Phillips XL30 SEM-FEG (Philips, Eindhoven, The Netherlands) including a Schottky emission electron gun. A beam of 20 kV and a conventional Everhart-Thornley type detector was used.

5.3.5. Verification of the core-shell structure

An inverted laser scanning confocal microscope Leica TCS SP8 (Leica, Mannheim, Germany) with a magnification lens of 63x was utilized to visualise the core-shell structure of the particles. Fluorescein isothiocyanate (FITC) and rhodamine B were added to the core and shell solutions respectively. After electrospraying, the produced core-shell particles were brought into paraffin oil for visualisation under the microscope. The excitation laser wavelength utilized for FITC was 488 nm and for rhodamine B 552 nm, while the fluorescence emission was acquired between 517-546 nm and 600-726 nm respectively.

The assessment of the miscibility of the core and shell polymers was based on the glass transition temperature(s) (T_g) of polymeric blends, determined via modulated differential scanning calorimetry (mDSC). For this purpose, the core and shell polymer were co-dissolved at different ratios in a common solvent mixture, namely DCM/MeOH 1/1 (V/V), to obtain a solid content of 5 %, and subsequently thin films were cast. The films were dried for two days in a vacuum oven at 25 °C to ensure maximal solvent evaporation. Aliquots from the films were accurately weighed in standard aluminium pans (TA Instruments, Brussels, Belgium) and transferred to the Q2000 mDSC calorimeter (TA Instruments, Leatherhead, UK), where they were heated under a dry nitrogen flow at a heating rate of 2 °C/min with a superposed modulation of +/- 0.64 °C per 40 seconds. The samples were consecutively cooled

to room temperature and heated again in the same conditions as during the first heating cycle. The assessment of the T_g was based on the reversing heat flow signal and its temperature derivative, which was processed with a Savitsky−Golay smoothing (region width 5 min). Likewise, the electrosprayed core-shell particles were analysed using the same mDSC procedure.

5.3.6. *In vitro* drug release

Prior to the *in vitro* drug release tests, the drug loading or relative amount of darunavir present in the core-shell particles was determined by dissolving an accurate amount of the particles in either methanol or phosphate buffer pH 7.5, depending on the solubility properties of the shell polymer. Subsequently, the concentration of darunavir was quantified via HPLC-UV (Hitachi LaChrom system, Merck, Darmstadt, Germany) equipped with a L-7420 UV-VIS detector an ODS Hypersil C18 column, 4.6 x 250 mm, d_p = 5 µm (Thermo Scientific, Massachusetts, USA). Analyses were run at room temperature, the injection volume was 20 µL, the wavelength of detection was 278 nm and the flow rate of the mobile phase was 1 mL/min. The mobile phase itself consisted of 50/50 (V/V) acetonitrile/10 mM formic acid in water, adjusted to pH 3.2. The details of the method validation can be consulted in Annex 2. For particles with a HPMC AS shell, the acidic buffer was replaced by a 20 mM phosphate buffer pH 6.8.

To evaluate the gastro-resistance of the core-shell particles, an exact amount of the particles was weighed in test tubes containing 0.1 M HCl, simulating a dose of 600 mg darunavir in 900 mL of gastric fluid. The test tubes were placed in a rotary mixer (Labinco BV, Breda, The Netherlands) and after two hours, a sample was taken and filtered through a 0.1 µm polytetrafluoroethylene syringe filter (Whatman, GE Healthcare, Buckinghamshire, UK). The filtrate was diluted with mobile phase and the darunavir content quantified with the above described HPLC method. This way, the drug release was calculated by dividing the amount of free darunavir in the dissolution medium by the total amount that was present in the particles, taking the actual drug loading into account. All experiments, both the drug loading and release experiments, were conducted in triplicate.

5.3.7. Investigation of P(MAA/MMA) with different monomer ratios

P(MAA/MMA) copolymers were synthesized based on a methylation method described by Qianbiao Li *et al*[155]. Commercially available P(MAA/MMA) (1/1) was used as the start product and dissolved in anhydrous DMSO to reach a concentration of 43 mg/mL (0.25 mmol acid groups). Next, 31.5 µL TMG (0.25 mmol) per mL solution and either 12.5 µL CH_3I (0.2 mmol) to synthesize P(MAA/MMA) (1/9), or 3 µL CH_3I (0.05 mmol) to synthesize P(MAA/MMA) (1/1.5), was added and the mixture was stirred for two hours at room temperature, after which the solution was neutralized with HCl. The newly methylated polymers were purified multiple times by dissolving them in acetone followed by precipitation in acidified water and finally dried in a vacuum oven. To evaluate the purity and the exact monomer ratio of P(MAA/MMA), the synthesized polymers were dissolved in DMSO-d_6 and proton nuclear magnetic resonance (NMR) spectra were recorded (Bruker Avance 300, Bruker, Billerica, Massachusetts, USA). The ratio was determined by the ratio of the area under the peak at δ = 3.62 ppm (methoxyl proton of MMA unit) versus the peak area at δ = 0.5-1.2 ppm (methyl protons of the

MMA unit). Complementary, the ratio was also confirmed based on the acid value performing an acid base titration with 0.01 M NaOH and phenolphthalein as pH-indicator. Subsequently, the newly methylated P(MAA/MMA) polymers were used as shell polymers for the production of core-shell structured particles and the drug release from these particles was determined as described above.

5.4. RESULTS

5.4.1. Preparation and characterization of the solutions

The viscosity, conductivity and surface tension of the solutions were determined and listed in Table 5.1, as they are known to influence the electrospraying process[64,73]. It has been shown that a higher polymer concentration in the core or shell solution results in final particles with a more spherical shape and a smoother surface with less pores respectively[156]. Accordingly, the concentration of each shell polymer was increased until clogging of the nozzle was observed, except for the P(MAA/MMA) solutions, where electrospinning and thus fibre formation occurred below the clogging concentration. The polymer concentrations mentioned in Table 5.1 are the highest and thus theoretically optimal concentration for the production of spherical, well-encapsulated particles found for these polymer/solvent combinations. The viscosity and conductivity increased with increasing polymer concentration, while the surface tension was barely affected by addition of the polymers (surface tension of ethanol 22 mN/m, chloroform 27 mN/m and acetone 23 mN/m)[157]. As for the conductivity, the concept of a 'driving liquid' was proposed in literature, which postulates that a cone-jet can be achieved more easily if the conductivity of the inner solution is higher than that of the outer one[58]. However, it was also stated that this concept is less critical when the inner and outer solvents are miscible, which is confirmed by our results (conductivity of the core solution containing HPMC was 14.3 µS/cm and 7.6 µS/cm for the one with PVP).

*Table 5.1. Properties of the shell solutions ± standard deviation. *specifications of the supplier.*

Shell polymer	Concentration (% m/v)	Solvent	Surface tension (mN/m)	Conductivity (µS/cm)	Viscosity (mPa·s)	Molecular weight (g/mol)*
P(MAA/MMA) (1/1)	3.0	EtOH	22.4 ± 0.1	15.55 ± 0.06	3.06 ± 0.01	125 000
P(MAA/MMA) (1/2)	3.0	EtOH	22.6 ± 0.4	17.90 ± 0.00	2.40 ± 0.01	125 000
P(MAA/EA)	3.0	EtOH	22.3 ± 0.2	23.25 ± 0.06	4.98 ± 0.01	250 000
CAP	1.5	EtOH/ACE	22.5 ± 0.2	21.20 ± 0.44	1.12 ± 0.01	2 500
P(MV/MA)	5.0	ACE	22.5 ± 0.2	5.00 ± 0.72	1.23 ± 0.01	126 000
HPMC AS	4.0	$CHCl_3$	25.8 ± 0.3	<0.1	6.76 ± 0.13	18 000
HPMC P	4.0	$CHCl_3$	25.6 ± 0.6	<0.1	6.36 ± 0.09	n.a.

5.4.2. Production of the core-shell particles

In order to study the influence of the formulation parameters as described above, the process parameters during electrospraying were kept constant for the production of all formulations. The choice of these process parameters was based on previous studies performed in our research groups and adapted where necessary to obtain a stable cone-jet and subsequently a dry powder[65,78]. This way, the tip-to-collector distance was set at 6 cm. However, when working with the chloroform based shell solutions, a polymeric film rather than a powder was collected, even at an increased tip-to-collector distance of 9 cm, which was confirmed via SEM images (Fig 5.2A). The particles produced with a chloroform shell solution were larger and, due to incomplete evaporation of the solvent, they were not completely dry when reaching the collector, which led to fusion and formation of a film. For

this reason, the tip-to-collector distance was increased to 15 cm, which lengthens the period for evaporation and leads to the formation of single dry particles (Fig 5.2B).

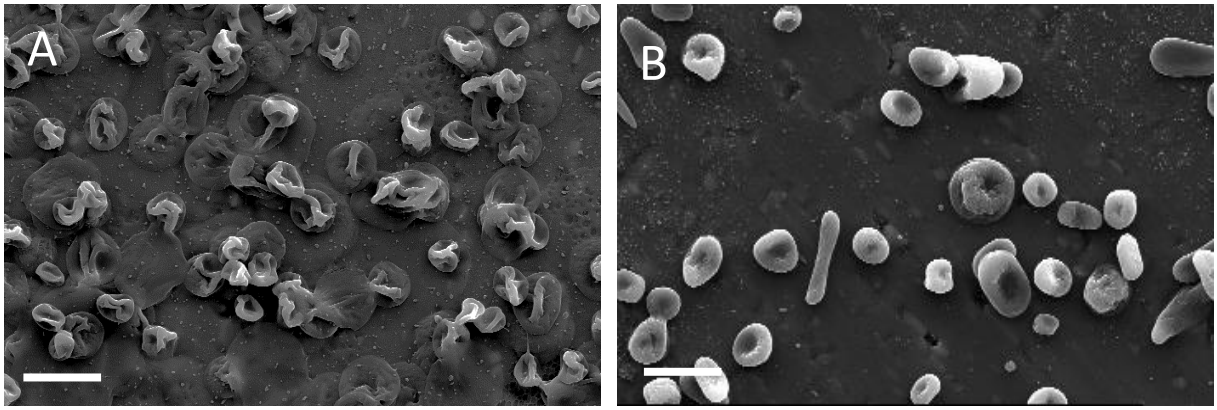

Figure 5.2. Effect of tip-to-collector distance during the production of core-shell particles with a HPMC-DRV core and HPMC AS shell (chloroform). A: 9 cm, B: 15 cm. The scale bar indicates 10 µm.

The ratio between the core and shell feed flow rate is another process parameter of interest; mainly, the shell flow rate should be higher than the core flow rate to ensure proper encapsulation and prevent blending of the two fluids[106,113,158]. We previously found that increasing the shell/core flow rate ratio from 1/0.8 to 1.2/0.3 suppressed the release of darunavir in acidic medium from 43 % to 18 %, due to an increase of the shell thickness[78,152]. A further increase in the ratio was investigated, but increasing the shell flow rate eventually led to an unstable cone-jet regime, while decreasing the core flow rate resulted in inadequate drug loading. Thus, the flow rate of the core solution was set and kept at 0.3 mL/h and the shell flow rate at 1.2 mL/h for all experiments.

5.4.3. Morphology of the core-shell particles

SEM was used to image the different particle morphologies. Fig 5.3 shows the particles obtained by coaxially electrospraying the shell solutions from Table 5.1, with image A till G representing the particles with a HPMC-DRV core and image H and I the ones with a PVP-DRV core. When using this PVP-DRV core, only a limited amount of shell polymers, namely HPMC AS and HPMC P, yielded core-shell particles that could be tested. The other polymers resulted in the formation of a gel at the tip of the nozzle, which cannot be electrosprayed, and that can be attributed to the formation of a complex with PVP upon contact due to a cooperative formation of hydrogen bonds between acid and base groups[159,160].

While the HPMC-DRV particles with the three derivatives of PMAA (image A, B and C) as well as the ones with P(MV/MA) (image E) measure about 1-2 µm, the size of the CAP containing particles is much smaller. This can be explained by the low molecular weight of CAP (Table 5.1) leading to less polymer chain entanglements and weaker viscoelastic forces to counterbalance the impact of the electric field. Hence, the system is more prone to Coulomb fission and this results in the end in smaller and irregular shapes[73]. The particles consisting of HPMC AS and HPMC P are on the contrary much larger, around 5-10 µm. Scaling laws predict that the droplet size is inversely proportional to the conductivity, thus the

larger particle size for the chloroform based solutions is most likely resulting from the lower conductivity (Table 5.1)[73].

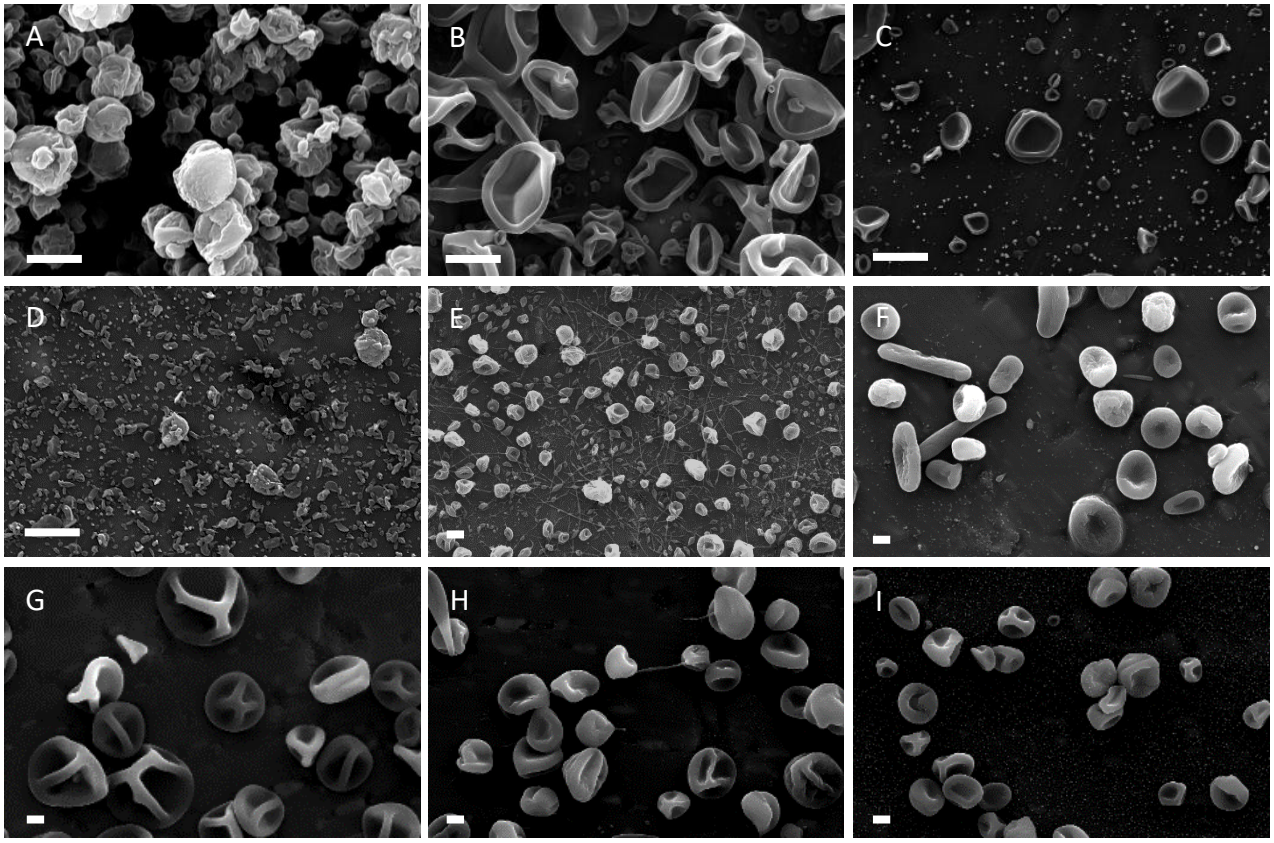

Figure 5.3. SEM images of the core-shell particles with different shell polymers, produced with the highest concentrated shell solutions from Table 2. A: P(MAA/MMA) (1/1), B: P(MAA/MMA) (1/2), C: P(MAA/EA), D: CAP, E: P(MV/MA), F: HPMC AS, G: HPMC P, H: HPMC AS, I: HPMC P. A-G particles with a HPMC-DRV core, H-I: PVP-DRV core. The scale bar indicates 2 µm.

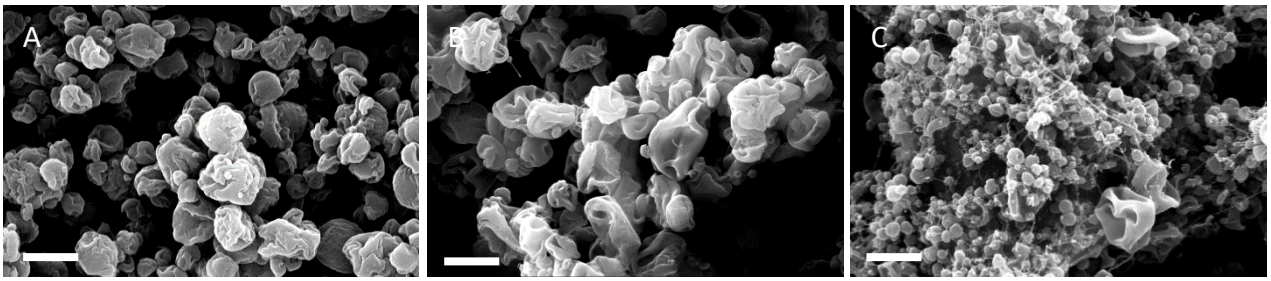

Figure 5.4. Effect of increasing core polymer concentration. A: 1 % HPMC, B: 4 % HPMC, C: 8 % HPMC. All particles were produced using a P(MAA/MMA) (1/1) shell solution of 3 %. The scale bar indicates 2 µm.

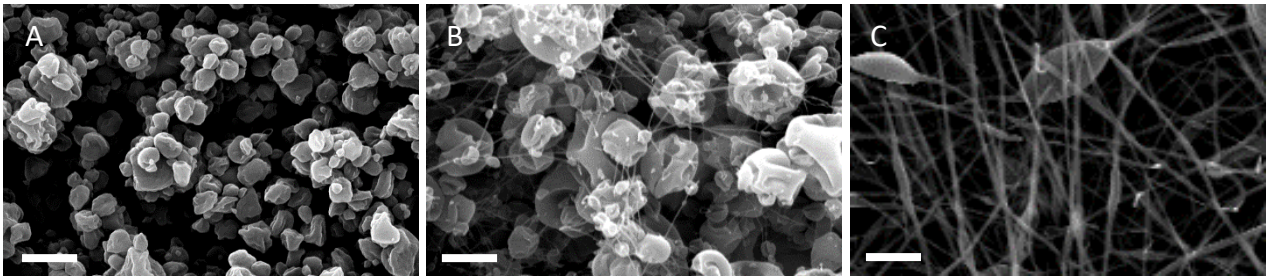

Figure 5.5. Effect of increasing shell polymer concentration. A: 1.5 % P(MAA/MMA) (1/1), B: 5 % P(MAA/MMA) (1/1), C: 9 % P(MAA/MMA) (1/1). All particles were produced using a HPMC core solution of 1 %. The scale bar indicates 2 µm.

Apart from the differences in size, all particles have roughly the same wrinkled and collapsed morphology as a result of the fast evaporation of the solvent[71]. Literature shows that the use of a less volatile solvent like dimethylformamide enhances the sphericity, because there is more time for the polymer chains to diffuse to the centre of the drying droplet and form a dense particle[161,162]. However, in our case there was incomplete evaporation and film formation on the collector when using dimethylformamide (data not shown). Adjusting the process parameters like tip-to-collector distance did not result in completely dry particles. Other studies reported a shift to more spherical particles for various types of polymers during electrospraying when the concentration of the polymers in the core or shell solution was increased[156,163,164]. For this reason, also HPMC - P(MAA/MMA) (1/1) particles with an increasing concentration of HPMC in the core were produced, however, also those particles kept their collapsed morphology as visualised in Fig 5.4.

Similar, the effect of increasing the concentration of the shell polymer P(MAA/MMA) (1/1) was studied. Above a concentration of 3 % not only particles, but also small polymer fibres were created (Fig 5.5). Solely focusing on the increase of the shell polymer concentration, this phenomenon can be correlated to the magnitude of the actual polymer concentration relative to the overlap concentration c* of the respective polymer[32] (Fig 1.6). At c*, the solution transitions from the dilute region, where separate P(MAA/MMA) chains do not interact with each other in the solution, to the semi-dilute unentangled region, where the polymer chains start to overlap, resulting in a pronounced increase in viscoelastic material functions of the system beyond c*. Eventually this increase reaches a level that is sufficient to stabilise the emerging jet, preventing it to break up into a spray of fine droplets so that polymer fibres will be created. Gupta *et al.* showed that for lower molecular weight polymers a combination of particles and fibres is created once c* is reached[67]. If the concentration is increased even further, the entanglement concentration c_e for the polymer/solvent system will be reached, entering the semi-dilute entangled region where solely polymer fibres are produced. Since only spherical particles need to be created for the application in mind, c* forms the upper concentration limit if no clogging of the nozzle is occurring at lower concentrations. As an example, the different concentration regimes for P(MAA/MMA) (1/1) in EtOH were determined by measuring the kinematic viscosity of the solvent (ν_s) and of the different polymer solutions (ν) with an Ubbelohde viscometer, and calculating the specific viscosities η_{sp} from their ratio and the known densities of the solutions (Fig 5.6).

$$\eta_{sp} = \nu\rho/\nu_s\rho_s - 1 \quad \text{(Eq 5.1)}$$

According to the evolution of η_{sp} over the concentration regimes, an overlap concentration c* = 3.65 wt% could be determined, which is in good agreement with the experimental electrospraying results. These limits on the concentration range restrain the possibility to alter the morphology via the concentration of the shell polymer.

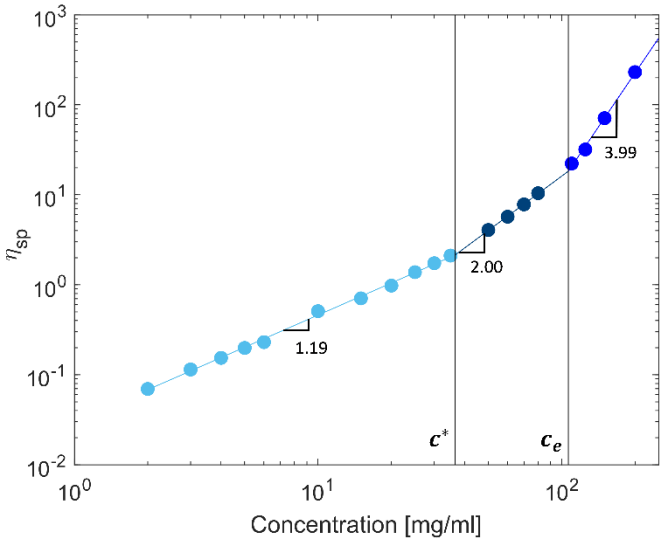

Figure 5.6. Specific viscosity as a function of concentrations of P(MAA/MMA) (1/1) in EtOH. The dilute regime below the overlap concentration c^* shows a scaling with a power of 1.19, while the semi-dilute unentangled regime between c^* and c_e exhibits a scaling of 2.00 and the semi-dilute entangled regime after c_e scales with an exponent of 3.99.

5.4.4. Verification of core-shell structure

Confocal images were obtained to verify the core-shell structure of the different formulations (Fig 5.7). Confocal imaging allows to visualise different sections along a primary axis (the z-axis) of the particles, and thus to verify the internal structure of the particles. Particles containing for example P(MAA/MMA) (1/2) as the shell (Fig 5.7B) generally exhibited a spherical morphology with a core in the centre of the particle. On the other hand, when HPMC AS was used as enteric coating, a higher fraction of particles with more irregular shapes were produced (Fig 5.7A), which corresponded in form to the external shape seen on the SEM images. Still, the internal core-shell structure is clearly maintained in the majority of the particles.

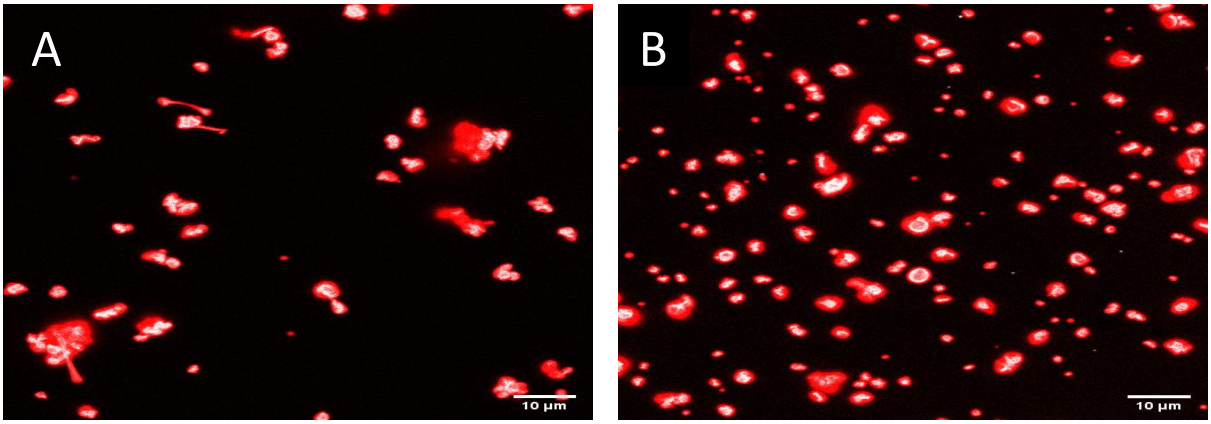

Figure 5.7. Confocal images of a cross section of core-shell particles consisting of HPMC-DRV amorphous solid dispersion and A: a HPMC AS shell (a), B: a P(MAA/MMA) (1/2) shell.

In addition to the visualisation of the core-shell structure with confocal imaging, mDSC was applied to determine the degree of polymer blending at the core and shell interface. Fig 5.8A shows the thermograms of films consisting of a miscible system: a single T_g was observed for each core to shell ratio and the value of this T_g changed with changing composition. Similar results were obtained for all the other combinations of core and shell, except for the combinations with HPMC AS (namely PVP-HPMC AS and HPMC-HPMC AS). The thermograms for the HPMC-HPMC AS combination can be found in Fig 5.8B, and it is clear that, for the 50-50 and 75-25 core to shell ratio, the two distinct T_g's of HPMC and HPMC AS remained unchanged even after fast cooling and a second heating cycle (data not shown). For the combinations with CAP, no conclusions could be drawn from the thermograms since the T_g of CAP and PVP/HPMC overlap. Leaving CAP aside, all enteric polymers, except for HPMC AS were miscible with the core polymers. However, this does not necessarily mean that blending at the interface does happen, as can be seen in the thermogram of the coated HPMC-DRV particles (Fig 5.9). For example, particles coated with P(MAA/MMA) (1/1) clearly show two different glass transition events (Fig 5.9A). The first event at 102 °C corresponds to the glass transition of the HPMC-DRV core and is in correspondence with the theoretical value of the mixture (108 °C) as calculated with the Gordon-Taylor equation (Eq 5.2)[165].

$$T_g = \frac{w_1 T_{g1} + k_{GT}(1 - w_1) T_{g2}}{w_1 + k_{GT}(1 - w_1)} \quad \text{(Eq 5.2)}$$

with $w =$ weight fraction, $k_{GT} = \frac{\rho_1 T_{g1}}{\rho_2 T_{g2}}$, $\rho =$ density, $T_{g1} = T_g$ of the component with the lowest T_g and $T_{g2} = T_g$ of the component with the highest T_g.

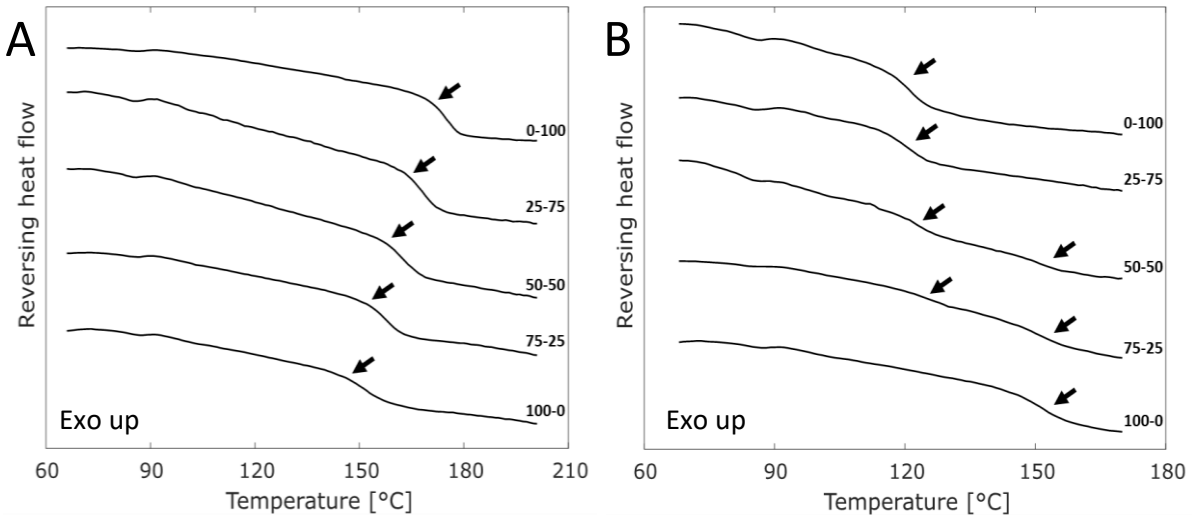

Figure 5.8. Thermogram A: The miscible system HPMC-P(MAA/MMA) (1/2) showing one Tg that shifts following the polymer blend composition. Thermogram B: The immiscible system HPMC-HPMC AS showing two Tg events, one for each polymer of the blend.

The second event corresponds to the glass transition of P(MAA/MMA) (1/1), which indicates that the core and shell polymers are not blended. A likely explanation is that the evaporation of the solvent during electrospraying happens on time scales shorter than the diffusion, an effect that is further

enhanced by the viscosity increase with solvent evaporation, which further slows down the diffusion of the polymers. Similar thermograms were obtained for particles coated with P(MAA/MMA) (1/2) and P(MV/MA), but only one broad T_g was observed for the particles coated with the other shell polymers, most likely because the difference between the T_g of these shell polymers and the T_g of the core mixture is not high enough to be resolved by mDSC (Fig 5.9B).

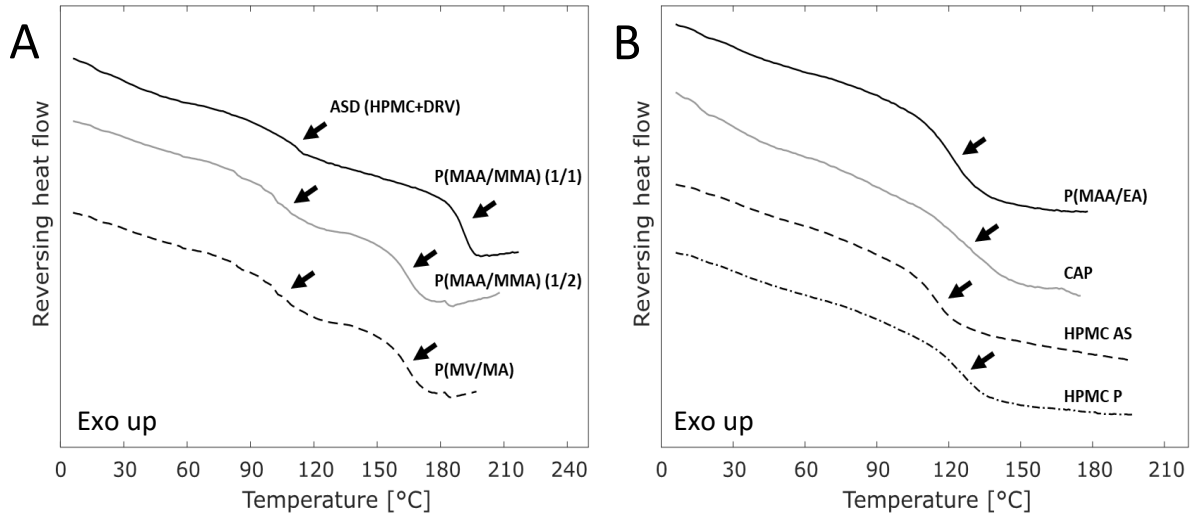

Figure 5.9. Thermograms of the coated HPMC-DRV particles. A: Core-shell combinations showing two different glass transition events. The first event at 102 °C corresponds to the T_g of the HPMC-DRV core and the second event corresponds to the T_g of the shell polymer. B: Core-shell combinations showing only one T_g. The difference between the T_g of these shell polymers and the T_g of the core mixture is probably not high enough to be resolved by mDSC.

5.4.5. *In vitro* drug release

The results of the drug release experiments after two hours in acidic medium are listed in Table 5.2. As mentioned in the previous section on morphology, particles with a PVP-DRV core could only be coated with HPMC AS or HPMC P. Comparing the results obtained with the PVP core versus the HPMC core, one can observe a remarkable difference: the particles with PVP released almost twice the amount of darunavir. Since this could be due to the nature of the polymer itself or to overloading at higher concentrations (5 %), particles with only 1 % PVP in the core were tested and showed a similar release (24.2 %) as the HPMC core (25.4 %). Besides the selection of an optimal polymer concentration for the core solution, also the shell polymer concentration showed to be of importance. Increasing the concentration of the polymer in the shell solution supressed the drug release. For example, the release decreased from 45.1 to 21.6 % for particles coated with 1 and 3 % P(MAA/EA), respectively.

Nevertheless, P(MAA/MMA) (1/2) was the only polymer yielding a formulation in compliance with the Ph. Eur. limits of maximum 10 % release after two hours in acidic medium[154]. A complete drug release profile of the best performing formulation (P(MAA/MMA) (1/2) shell) and one that performed worse (HPMC AS shell), are shown in Fig 5.10. Additionally, the release profile of crystalline darunavir and the uncoated core, made of an HPMC based solid dispersion of DRV prepared by electrospraying as studied in our previous work, were also included in this graph[166]. The profiles show that the relatively low dissolution rate of crystalline DRV can be improved significantly by producing an HPMC based solid

dispersion of the API (= uncoated core). As expected, the release of darunavir is eminently supressed in the coated particles, though for both formulations an initial burst release was observed during the first minutes with barely any increase during the following two hours. Still, the amount of burst release was significantly different between particles coated with HPMC AS or P(MAA/MMA) (1/2). The formulation with P(MAA/MMA) (1/2) was produced multiple times at different days to check the reproducibility of the system and batches with comparable release characteristics were obtained, as displayed in Table 5.1 (indicated with *).

*Table 5.2. Results of the drug release experiments after two hours in acidic medium for the formulations with different shell polymers in different concentrations for particles with either a HPMC core (1 %) or PVP core (5 %). *Three different batches of this formulation were made to check the reproducibility of the system. **A concentration of 1 % PVP was used for the core instead of 5 %.*

Shell polymer	Concentration (% m/v)	Shell solvent	Drug release (%) ± SD HPMC core	Drug release (%) ± SD PVP core
P(MAA/MMA) (1/1)	3.0	EtOH	12.8 ± 0.7	/
P(MAA/MMA) (1/2)	3.0	EtOH	5.5 ± 0.2; 6.6 ± 0.1; 7.5 ± 0.1*	/
P(MAA/EA)	1.0	EtOH	45.1 ± 0.1	/
P(MAA/EA)	3.0	EtOH	21.6 ± 0.6	/
CAP	1.5	EtOH/ACE	28.7 ± 0.3	/
P(MV/MA)	2.5	ACE	27.9 ± 0.2	/
P(MV/MA)	5.0	ACE	18.6 ± 1.2	/
HPMC AS	2.5	$CHCl_3$	25.4 ± 0.5	55.4 ± 3.0; **24.2 ± 0.8
HPMC AS	3.0	$CHCl_3$	20.5 ± 0.7	/
HPMC AS	4.0	$CHCl_3$	19.9 ± 1.8	51.6 ± 3.7
HPMC P	1.5	$CHCl_3$	58.4 ± 0.6	/
HPMC P	2.5	$CHCl_3$	41.6 ± 3.7	78.7 ± 2.2
HPMC P	4.0	$CHCl_3$	/	64.0 ± 2.7

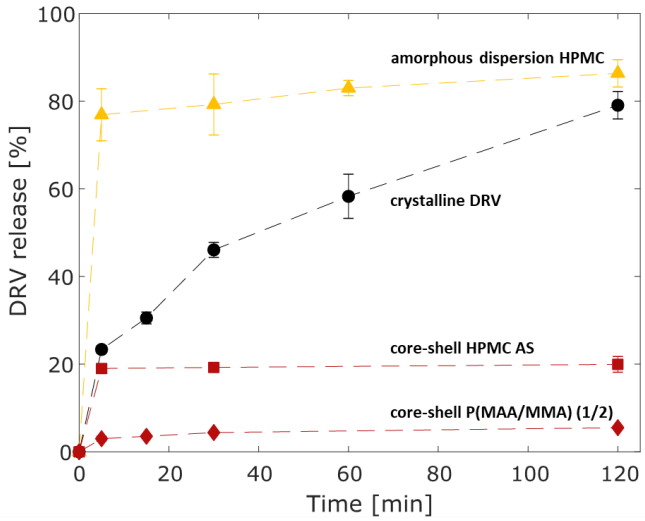

Figure 5.10. In vitro drug release results of the amorphous solid dispersion with HPMC-DRV = uncoated core (orange ▲), crystalline DRV (black ●), core-shell particles with HPMC AS as shell polymer (red ■) and P(MAA/MMA) (1/2) (red ♦).

5.4.6. Investigation of P(MAA/MMA) with different copolymer ratios

Despite the fact that the first goal (producing enteric coated ASD particles with less than 10 % of darunavir release in acidic medium) was successfully reached, the reason for the different performance of the coating polymers remained unclear. Consequently, the P(MAA/MMA) copolymer system was studied in more detail. From Table 5.2 one can see that a shell with P(MAA/MMA) (1/1), which has an equal amount of free and methylated carboxylic groups, displayed a burst release of 12.8 %, while a shell with P(MAA/MMA) (1/2), which has in comparison a higher ratio of methylated carboxylic groups, had a maximum release of 7.5 %. This gave rise to the hypothesis that the methylated groups are beneficial for the formation of an adequate enteric coating and to test this, additional copolymers with different monomer ratios were synthesized (other ratios are not commercially available, and both literature and our own mDSC analysis demonstrated that blends of the 1/1 ratio, 1/2 ratio, and pure PMMA are not miscible on the molecular level[167]). The newly synthesized copolymers were used as the shell polymer during coaxial electrospraying, and subsequently drug release experiments were performed with the results presented in Table 5.3. Indeed, the release decreased with an increasing amount of MMA units. However, the 1/9 ratio was no longer soluble in ethanol and hence it was tested by using chloroform as a solvent. This resulted in a drug release of 11.8 ± 0.5 %, which was much higher than hypothesized because it was expected to be less than the 6.5 % obtained with the 1/2 ratio. To rule out any possible influence of the used solvent, a common solvent system (a mixture of EtOH/$CHCl_3$ 1/1 (V/V)) was applied to dissolve the copolymers and a clear relationship between the degree of methylation and the drug release was observed (Table 5.4). However, with this solvent mixture the release of the 1/2 ratio, which was below 10 % when using ethanol (Table 5.3), was raised to 12.5 %, illustrating the strong influence of the interplay between the polymer and the chosen solvent during the formation of the coating shell.

*Table 5.3. Drug release experiments of core-shell particles, all consisting of a HPMC-DRV core but a different type of P(MAA/MMA) was used for the shell. *This is the average of the three different batches tested.*

Ratio P(MAA/MMA)	Solvent	Drug release (%) ± SD
1/1	EtOH	12.8 ± 0.7
1/1.5	EtOH	11.2 ± 0.2
1/2	EtOH	6.5 ± 0.8*
1/9	Not soluble in ethanol	/

*Table 5.4. Drug release experiments of core-shell particles, all consisting of a HPMC-DRV core but a different type of P(MAA/MMA) was used for the shell, though a common solvent mixture (EtOH/$CHCl_3$ 1/1 (V/V)) was used to dissolve all the different ratios. *This batch could not be electrosprayed because it was not possible to create a cone-jet.*

Ratio P(MAA/MMA)	Solvent	Drug release (%) ± SD	***Ra***
1/1	EtOH/$CHCl_3$	/*	6.37
1/1.5	EtOH/$CHCl_3$	12.7 ± 0.6	6.72
1/2	EtOH/$CHCl_3$	12.5 ± 0.2	7.03
1/9	EtOH/$CHCl_3$	8.5 ± 0.3	8.62
0/1	EtOH/$CHCl_3$	6.8 ± 0.2	9.44

The role of the utilized solvent for the final drug release properties can also be seen in Table 5.3 and Table 5.4, where for example particles coated with P(MAA/MMA) (1/2) showed a drug release of 12.5 % in case the shell is formed from a EtOH/$CHCl_3$ 1/1 (V/V) mixture, but only 6.5 % when pure EtOH is used. The solvent quality for a certain polymer is known to have an important impact on the chain conformation and interaction during drying and thus final particle morphology[143]. An indication of solvent quality can be derived from the intrinsic viscosity [η] of the polymer/solvent combination as well as from Hansen solubility factors[168,169]. The latter is based on the "like dissolves like" principle and defines each component with three Hansen parameters, which represent a point in a three dimensional or Hansen space. The smaller the distance in Hansen space Ra between two components, the closer they are in the space and the more alike. Thus both a higher [η] and a lower distance in Hansen space R_a correspond to a better solvent where the polymer chains are in a more expanded form due to favourable interaction between polymer and solvent, and are thus expected to generate a more smooth surface with more dense properties[143].

To investigate the influence of solvent quality on the final drug release, the polymer P(MAA/MMA) (1/2) is kept the same, but different ratios for the EtOH/$CHCl_3$ solvent system are applied and the drug release is tested (Table 5.5). Both the intrinsic viscosity and the Hansen solubility parameter calculations exhibit the same trend, a higher fraction of $CHCl_3$ results in a better solvent system for P(MAA/MMA) (1/2). On the other hand, the *in vitro* release tests generally showed an increase in drug release for the core-shell particles when more $CHCl_3$ was present. Thus, a better solvent system does not automatically result in a better encapsulation of the final particles. Similar results are found for the reverse case, where a polymer consisting of varying amounts of the different monomers are electrosprayed in the same solvent of EtOH/$CHCl_3$ 1/1 (V/V) as is reported in Table 5.4. As it was proven in Table 5.5 that both [η] and R_a give the same trends for the solvent quality, only theoretical calculations for the Hansen solubility factors were applied to evaluate the solvent quality in this case. Again, similar results are found, for systems where the solvent quality is worse for the shell polymer (higher R_a values), less drug release was found.

Table 5.5. Drug release experiments of core-shell particles, all consisting of a HPMC-DRV core and a P(MAA/MMA) (1/2) shell, but where different ratios of the solvent system EtOH/$CHCl_3$ were used. [η] and Ra represent the solvent quality that was present for the shell system.

Ratio EtOH/$CHCl_3$	Drug release (%) ± SD	[η] (ml/mg)	R_a
1/0	6.5 ± 0.8	0.0164	11.92
1/0.33	6.2 ± /	0.0365	9.00
1/1	11.9 ± 0.7	0.0554	7.03
1/3	11.0 ± 0.2	0.0566	6.87

5.5. DISCUSSION

Electrospraying is a relatively novel, but acknowledged production method not only for amorphous solid dispersions (ASDs), but also for the production of coated ASDs in a coaxial setup. In our previous work, ASDs consisting of darunavir as a model drug and PVP or HPMC, both water soluble carriers commonly used for the manufacturing of ASDs, were successfully prepared in a single nozzle setup[22,47,166]. Moreover, it was shown that HPMC and PVP are suitable polymers to formulate ASDs of darunavir and that the particles displayed proper solid state characteristics and pharmaceutical performance. Consequently, for the selection of the formulation parameters in this work, the same solvent combination, polymers (both HPMC and PVP), drug loading and total solids content was applied to formulate the core. Regarding the shell solutions, a variety of commercially available gastro-resistant coating polymers[52,53] were selected for study (Table 5.1). Despite their broad range of characteristics, all utilized polymers have free carboxylic groups, resulting in pH dependent aqueous solubility profiles. However, due their different characteristics, different organic solvents were necessary to prepare clear solutions.

The final coating performance is highly dependent on multiple formulation parameters like the type of gastro-resistant polymer, the polymer concentration and solvent used for the solutions during electrospraying. Initially, the solution properties were studied as they are known to influence the electrospraying process (Table 5.1)[73]. Interestingly, no clear correlations could be found between these polymer solution properties like the conductivity, surface tension and viscosity and the final product performance (Table 5.2). Also, the molecular weight of the polymers showed not to be a factor of high impact. Xu *et al*. concluded that the use of a polymer with a higher molecular weight did not yield a thicker shell layer[156]. Similarly in our experiments, P(MAA/EA) with a significant higher molecular weight of 250 000 g/mol than for example P(MAA/MMA) (1/1) with 125 000 g/mol did not result in a lower drug release (21.6 versus 12.8 % respectively).

Nevertheless, the polymer concentration in solution does play a major role, since the highest possible shell polymer concentration, where no nozzle clogging is occurring and solely particles are created, results in more complete encapsulation of the core and thus the lowest *in vitro* drug release. This can be explained by the formation of a thicker and more complete shell and concurs with the work of Xu *et al.* who developed a model to predict properties like shell thickness of PDLLA coated PLGA particles[156]. Unfortunately, the concentration cannot be raised infinitely, because the increasing viscosity will lead to clogging of the nozzle or the increasing viscoelasticity due to chain entanglements will result in the formation of fibres[68,131]. These limits on the concentration range restrain the possibility to alter the particle structure via the concentration of the shell polymer.

Contrarily, a higher solids content in the core increases the drug release as was the case for the PVP-HPMC AS particles with a 5 % PVP core. Lowering the PVP concentration in the core solution to 1 % resulted in a lower extent of the release, comparable to the release of HPMC-HPMC AS particles. The higher release observed for the first formulations with 5 % PVP was thus due to overloading, proving that both polymers are useful if low concentrations are applied. Since the SEM images in Fig 5.4 did

not show any improvement in sphericity for higher concentrations, a low polymer concentration of 1 % in the core is considered the best alternative. In the end, a perfect spherical particle is not necessarily a prerequisite to obtain an adequate gastro-resistant profile, as shown by the particles coated with P(MAA/MMA) 1/2 (Fig 5.3B). Furthermore the small difference in size between the particles coated with the different polymers is not expected to be the main factor causing the distinct extent of burst release (Fig 5.3 and Table 5.2). After all, the particles coated with HPMC AS are slightly larger, but the burst release is higher, which is contra-intuitive if only the size versus release rate would be taken into account (as smaller particles will give a faster release).

Despite the difference in the extent of the release after two hours in acidic medium when using different coating polymers (Table 5.2), the coated formulations showed a burst release during the first five minutes with only a small increase in release over the two following hours (Fig 5.10). This burst release can be explained by two different phenomena as depicted in Fig 5.11. The fact that for all the formulations an initial burst release was observed might indicate that a certain percentage of particles is produced with incomplete or defected encapsulation. Moreover, non-spherical particles will possibly have a higher chance to have an incomplete, non-homogeneous coating or a coating containing more defects. Their core will therefore be able to directly interact with the environment and immediate dissolution of the amorphous solid dispersion can occur, which could explain the observed burst release. However, various arguments contradict this first hypothesis. Firstly, the lack of a flawless spherical external morphology did not necessarily influence the coating performance in a negative way. After all, the HPMC-P(MAA/MMA) (1/2) particles which performed the best, had a very wrinkled morphology (Fig 5.3). Secondly, the presence of a proper core-shell internal structure was confirmed and visualised by confocal microscopy (Fig 5.7), while mDSC confirmed a low state of mixing of the two polymers in the electrosprayed particles. Lastly, the reproducibility of the burst release contradicts the hypothesis, since it is highly unlikely that the process generates every time the same percentage of badly coated particles.

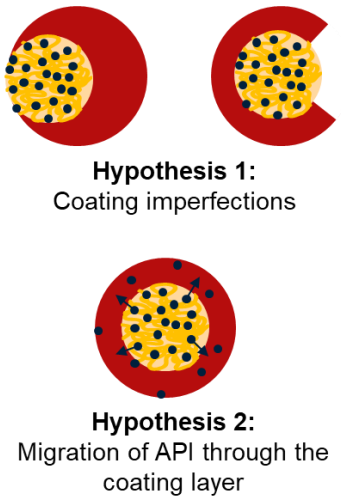

Figure 5.11. Schematic representation of the two hypotheses that can explain the observed burst release for the electrosprayed core-shell particles. The dark blue dots are DRV molecules, the orange chains are HPMC molecules and the red layer is the shell polymer.

A second and probably more reasonable explanation for the burst release might be found in the diffusion of the API through the shell solution during the droplet/particle formation in the electrospraying process. The API molecules that have migrated towards the surface of the particle, will be easily released by diffusion through the coating during the dissolution tests in the acidic medium. Depending on the polymer type and solvent used, the rate of diffusion and hence the extent of the burst release might be different. After all it was shown that the type of polymer in the shell was the determining factor for release from the electrosprayed product. Especially P(MAA/MMA) consistently resulted in drug releases well below the upper limit of 10 %, while this was not attainable for other shell polymers. A more in-depth investigation of this polymer was therefore performed, where different monomer ratios in the copolymer P(MAA/MMA) were synthesized. This revealed that the monomer ratio but also the utilized solvent plays an important role in the final drug release characteristics of the particles. A higher MAA content resulted in a higher darunavir release for the same solvent system and concentration, which was especially clear when $CHCl_3$/EtOH 1/1 (V/V) was used as solvent system. Even for the particles coated with pure PMMA (insoluble in the aqueous medium) a burst release of 7 % was observed, which can indeed be explained by the fact that the API is present at the surface. Complementary, the effect of the solvent quality was evaluated by using different ratios of the $CHCl_3$/EtOH mixture. The fact that a better solvent should produce more smooth particles with better surface properties and thus better retains drug molecules in the particles seems to be invalid in this study, even the opposite trend was demonstrated.

A better understanding of all the important factors that lead to a specific degree of burst release for the different formulations should be attained for an improved prediction of the performance of electrosprayed core-shell particles *a prior*. Hence, a more specific study is currently being performed, to validate the hypothesis postulating that the diffusion of the API towards the surface of the particle causes the burst release, and to elucidate the reason why certain shell polymers exhibit significant lower drug release than other similar formulations as well as the impact of the solvent quality on the coating performance.

5.6. CONCLUSION

This study proves the viability of coaxial electrospraying for the production of gastro-resistant microparticles containing an amorphous solid dispersion in the core. Core-shell particles were created that comply with the Ph. Eur. specifications for delayed release dosage forms, i.e. a drug release in acidic medium lower than 10 % after two hours. A multitude of different formulation parameters were investigated, revealing specifically the major impact of polymer concentration in the core and shell solutions, polymer/solvent interaction during particle formation and the type of shell polymer on the final performance of the product. Nevertheless, all the formulations exhibited burst release of DRV in the acidic medium, followed by minimal release in the remainder of the two hours. In this work, it is hypothesized that this phenomenon results from the fact that during the formation of the microparticles the DRV can diffuse towards the surface of the particles becoming readily available for rapid dissolution. Further investigation is necessary to verify this hypothesis and to reveal what is occurring in reality, and which factors influence the degree of burst release.

Acknowledgements

The Fonds voor Wetenschappelijk Onderzoek-Vlaanderen (FWO, project G0A3916N) is acknowledged for financial support. In addition, the authors want to thank Bernard Appeltans and Nico Coenen for the practical support in the lab.

Chapter 6
Fixed dose combinations for cardiovascular treatment via coaxial electrospraying: coated amorphous solid dispersion particles

Results of this chapter are based on:

Fixed dose combinations for cardiovascular treatment via coaxial electrospraying: coated amorphous solid dispersion particles. Annelies Smeets, Ida Lo Re, Christian Clasen and Guy Van den Mooter. Submitted to International Journal of Pharmaceutics.

6.1. ABSTRACT

As a result of an aging population, the need for fixed dose combinations in the treatment of cardiovascular diseases, that are easy to swallow and administer, has been growing remarkably. In this work, the feasibility of coaxial electrospraying (CES) was investigated to manufacture in one single step, a powder of individually coated particles containing atenolol (ATE), lovastatin (LOV) and acetylsalicylic acid (ASA). To improve the dissolution rate of the poorly water soluble LOV, an amorphous solid dispersion (ASD) of LOV with Soluplus® (SOL) was formulated and Eudragit® S100, an enteric copolymer that only dissolves above pH 7, was applied as coating to avoid LOV hydrolysis in acidic medium. Furthermore, ATE was added to the inner ASD compartment and the acidic ASA was embedded in the coating layer. With regard to the uncoated ASD particles, which were prepared with single nozzle electrospraying, the rate and extent of the LOV dissolution was increased, even to an extent of 100 % for the 1/1/6 (ATE/LOV/SOL) ratio. Hence, this ratio was selected and coated particles with proper release of the three APIs could be successfully produced via CES. However, a peculiar behaviour of the coating performance was observed. Regarding LOV, the enteric layer of the particles performed as expected in acidic medium and supersaturation was obtained after the switch to a neutral pH, but in contrast, over 50 % of ATE was released after 90 min in acidic medium. Nonetheless, hardly any ATE was released under acidic circumstances from ATE tablets that were, as a benchmark, manually dip-coated with Eudragit® S100. Two different model APIs, namely paracetamol (well soluble) and fenofibrate (poorly soluble) were tested as well, revealing similar discrepancy in the coating performance. The coating layer formed during CES is most likely less dense as compared to the layer produced with tablet coating and consequently, more permeable for highly soluble APIs, but not for the poorly soluble compounds.

6.2. INTRODUCTION

According to the World Health Organization (WHO), almost 18 million people died worldwide in 2016 due to cardiovascular complications. As a consequence, cardiovascular events such as heart attack or stroke, are the main cause of death worldwide[170]. Nonetheless, the risk to suffer from such a cardiovascular event can be reduced by 80 % when implementing a healthy lifestyle in combination with a well-monitored pharmacological treatment, consisting of a combination of antihypertensive drugs (beta-blocking agents and angiotensin converting enzyme inhibitors), lipid lowering drugs (statins) and antiplatelet drugs[171,172]. Unfortunately, a large meta-analysis published by Naderi *et al.* revealed that in general only 57 % of the patients is adherent to their therapy, leading to an enormous amount of death cases that could have been avoided with the currently available drug therapy[172]. The medicines are after all off-patent and widely available at a low cost[173]. One of the reasons for the low adherence rate is the complexity of the treatment regime. This can be simplified by the use of fixed dose combinations (FDCs), where different active pharmaceutical ingredients (APIs) are combined in one single dosage form hence, lowering the pill burden for the patient[173]. It was proven by the UMPIRE clinical trial that the adherence of patients on FDCs improved remarkably as compared to patients taking the conventional therapy[174]. On top of the improved simplicity for the patients, the costs for the manufacturing and distribution of FDCs are generally lower and the benefits of FDCs are not limited to the cardiovascular area. Their use has also been recommended in the treatment of other diseases where polytherapy is necessary as for the treatment of malaria, HIV and tuberculosis[175].

Besides these undeniable advantages, the production of FDC entails a considerable list of challenges. To start, combining multiple APIs with different physicochemical properties can lead to both physical and chemical instabilities as they can interact with each other and additionally, they can have a different stability profile as such[176]. Secondly, the aqueous solubility of the APIs can be different and co-administration can even influence their mutual solubility, which is especially problematic for poorly water soluble drugs[176]. Nguyen *et al.* reported for example the decreasing solubility of ritonavir and darunavir upon combination[93]. Furthermore, the optimal release kinetics and specific site in the gastrointestinal tract to deliver the API can vary, as one API may require a fast release whereas for another a delayed or prolonged release is more suited. To conclude, in case the combined APIs require different dosing, a uniform distribution of the low dosed API in the higher dosed API needs to be assured[176].

Various formulation technologies can be applied to tackle the above defined challenges, like multi-layered tablets or multi-particulate systems[175]. Different studies can be found in literature proposing state-of-the-art manufacturing methods, for instance, a coextrusion setup was tested in a study by Andrews *et al*. to manufacture a bi-layered system of simvastatin and acetylsalicylic acid and Khaled *et al.* used 3D extrusion printing for the production of a compartmentalized tablet containing five APIs[177,178]. However, the innovative approach in our study is profiled in the focus on the convenient administration of the FDC, an important feature that is often neglected within the conventional formulation strategies. Many elderly, which form the vast majority of the patients with cardiovascular

diseases, suffer from dysphagia and encounter difficulties swallowing tablets or capsules, which will again negatively affect the adherence rate[88]. Splitting and crushing of the dosage form is often not an option, as it will cause a loss of the special functionalities of the formulation. Hence, there is a need for FDCs in the treatment of cardiovascular diseases that are more conveniently to administer.

In this work, the formulation of an easy-to-swallow FDC containing the beta-blocking agent atenolol (ATE), the anti-platelet drug acetylsalicylic acid (ASA) and lovastatin (LOV), a lipid-lowering compound, is studied (Fig. 6.1). However, the use of the latter raises three main concerns. First, LOV is a lactone prodrug that is hydrolysed *in vivo* to the active β-hydroxy acid form (LOVh). This form inhibits HMG-CoA reductase and thus the endogenous cholesterol synthesis in the liver[179]. Acids catalyse the hydrolysis of the lactone group and premature conversion to the active form will occur in the acidic gastric fluid. LOV should thus be protected from the gastric medium, for example by adding an enteric coating layer to ensure maximal conversion in the liver, the target organ, and reduce the risk of side effects[180]. Moreover, LOV should be physically isolated from the acidic ASA by using different compartments in the dosage form, avoiding conversion during storage. Secondly, the drug is extensively metabolized by the CYP3A4 enzymes, which are, besides in the liver, abundantly present in the mucosa of the small intestine[179]. Still, these enzymes are mostly expressed in the proximal regions, with a decline towards the ilium[181]. This leads to a choice of enteric polymers which only dissolve at a pH corresponding to the more distal intestinal region in order to bypass any release and possible CYP3A4 metabolism in the proximal region. Examples of these enteric polymers are poly(methacrylic acid-co-methyl methacrylate) in a monomer ratio of 1/2 (commercially available as Eudragit® S100) or hypromellose acetate succinate HF[52,182]. Lastly, LOV is a poorly water soluble API, which causes, together with the extensive CYP metabolism, an oral bioavailability of less than 5 %[179,183]. One of the options to overcome this low solubility is the implementation of an amorphous solid dispersion (ASD), which implies that lovastatin needs to be molecularly mixed within a hydrophilic amorphous carrier such as hypromellose or polyvinyl caprolactam-polyvinyl acetate-polyethylene glycol graft copolymer, commercially available as Soluplus® (SOL), to form a homogenous amorphous system. The amorphous solid state entails a higher free energy as compared to the crystalline state, which results in an improved solubility and dissolution rate and consequently, a higher oral bioavailability[18]. The most common production technologies are spray dying and hot melt extrusion.

In order to combine all these features to improve the bioavailability of LOV into one easy-to-swallow dosage form, coaxial electrospraying (CES) is proposed in this work to manufacture an inventive FDC in the form of a powder for reconstitution of coated ASD particles that can be mixed with beverages of food upon administration (Fig 6.2). The particles consist of an ASD of LOV with the hydrophilic carrier Soluplus® and ATE. To protect LOV from the gastric medium and enzymatic degradation, the coating layer consists of Eudragit® S100 and ASA is as well added to this outer layer. The reason to choose for CES over a conventional method like spray drying, is the fact that ASD particles can be produced which are individually coated. As a consequence, there is no need for down-stream processing like tabletting and coating to achieve the requested release kinetics. However, it must be

noted that the throughput of electrospraying is very low compared to the conventional manufacturing methods and effort is currently made regarding the upscaling, for example with the use of a multi nozzle setup[64].

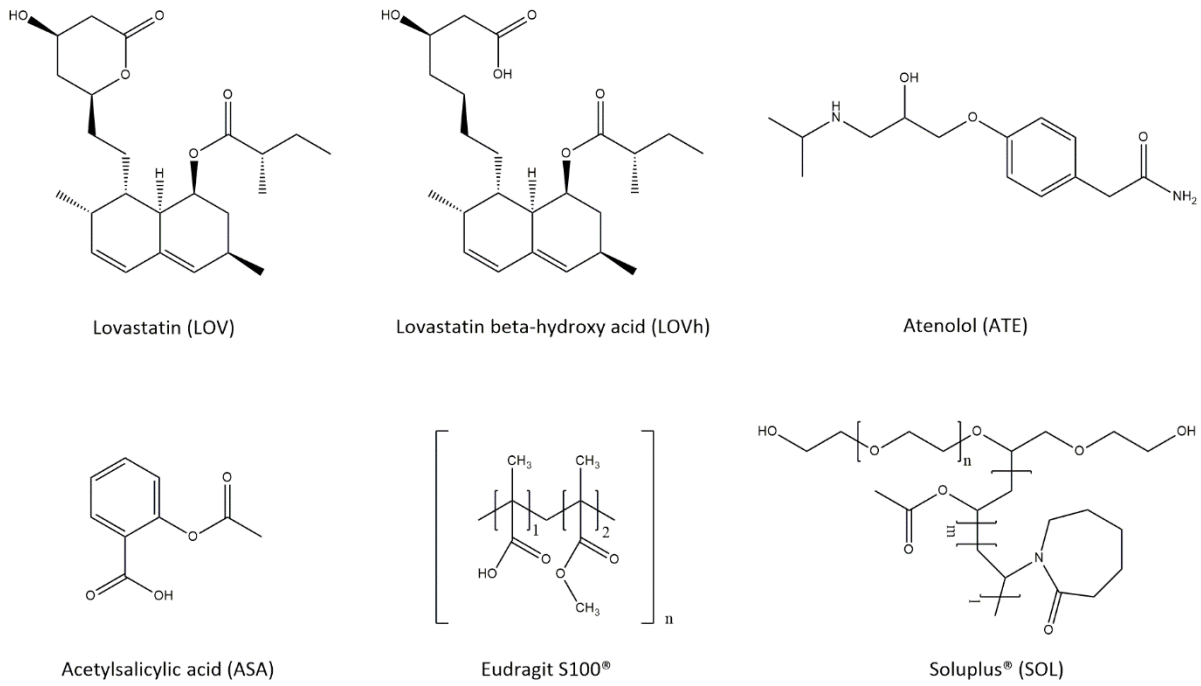

Figure 6.1. Structural formula of the APIs and polymers, designed with ChemDraw® (PerkinElmer Informatics).

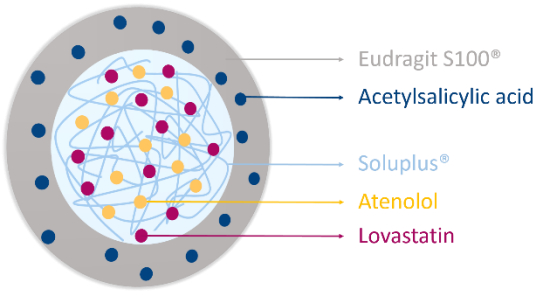

Figure 6.2. Design of the coated ASD particles. The core exists of Soluplus®(SOL), atenolol (ATE) and lovastatin (LOV), while the coating layer exists of Eudragit® S100 and acetylsalicylic acid (ASA).

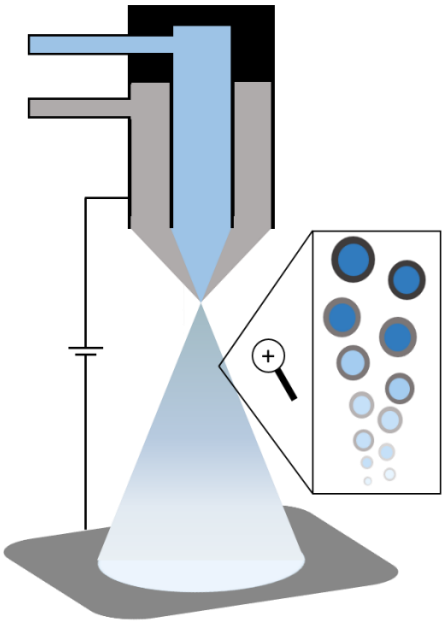

Figure 6.3. Schematic representation of a coaxial electrospray setup.

A schematic representation of the used CES setup is given in Fig 6.3. Briefly, the core and shell solutions are prepared by dissolving the different APIs and polymers in an appropriate organic solvent and accordingly pumped through the internal and external channel of the coaxial nozzle. By applying a strong electrical field over the nozzle and collector, the solutions are deformed into a Taylor cone-jet and subsequently atomized into tiny droplets. As the solvent rapidly evaporates from these droplets, coated particles are created in one single manufacturing step. Due to the fast evaporation of the solvent, amorphous material is obtained. In literature, the usefulness of CES has been demonstrated for the production of coated ASD particles as well as particles containing multiple APIs. As an example, Nguyen *et al.* used CES to produce enteric coated particles of darunavir, while a sustained release of budesonide and theophylline from PLGA particles was investigated by Yeh and Chen[78,184]. In contrast, the novel and added value of our work on CES lies in the combination of the different formulation strategies, namely the use of an ASD, an enteric coating and compartmentalization to formulate no less than three APIs in the form of a powder for convenient administration.

The electrospraying process however, is a complex interplay between various parameters. One has to consider process parameters like the electric field strength and the feed flow rate, as well as variable formulation parameters e.g. the viscosity, conductivity and surface tension of the solutions used[64]. Hence, a bottom-up approach was applied, starting with the analysis of the solid state and *in vitro* release kinetics of the uncoated ASD with different levels of drug loading. This core was manufactured via single nozzle electrospraying, which is identical to the setup shown in Fig 6.3, except that the coaxial nozzle is replaced by a one-channel needle. Subsequently, the CES production and characteristics of the coated particles were investigated. During these experiments, an unexpected performance of the coating was observed with regard to the different APIs because a gastro-resistant profile was not obtained for all compounds. With this in mind, the coating performance was studied into more detail by applying a conventional dip-coating method of tablets as a benchmark and examining the behaviour of two extra model APIs, namely paracetamol and fenofibrate.

6.3. MATERIALS AND METHODS

6.3.1. Materials

Lovastatin (LOV) and fenofibrate (FEN) were purchased from Hangzhou APIChem Technology Co. (Zhejiang, China), atenolol (ATE), phosphorus pentoxide and sodium phosphate tribasic dodecahydrate (Na_3PO_4) from Acros Organic (Geel, Belgium), acetylsalicylic acid (ASA) from Sigma-Aldrich Co. (St-Louis, USA), salicylic acid from VWR (Leuven, Belgium), paracetamol (PAR) from Fagron (Nazareth, Belgium) and sodium hydroxide (NaOH) from Merck (Darmstadt, Germany). Polyvinyl caprolactam-polyvinyl acetate-polyethylene glycol graft copolymer (Soluplus® or SOL) was obtained from BASF ChemTrade GmbH (Ludwigshafen, Germany), poly(methacrylic acid-co-methyl methacrylate) in a monomer ratio of 1/2 (Eudragit® S100) from Evonik Röhm GmbH (Darmstadt, Germany) and microcrystalline cellulose from Fagron (Nazareth, Belgium). Acetonitrile (ACN), dichloromethane (DCM) and 1M hydrochloric acid (HCl) were purchased from Fisher Chemical (Loughborough, UK), methanol (MeOH) from Arcos Organic (Geel, Belgium), phosphoric acid from Chemlab (Zedelgem, Belgium) and absolute ethanol (EtOH) from VWR (Leuven, Belgium). In all experiments, ultrapure water was used, prepared with a Maxima Ultra Pure Water system (Elga Ltd., Wycombe, England).

6.3.2. Electrospraying

Amorphous solid dispersion particles

A DCM/MeOH solvent mixture (1/1, V/V) was used to dissolve ATE, LOV and SOL in order to obtain four different solutions with increasing polymer content, more specifically in the m/m/m ratios of 1/1/1, 1/1/3, 1/1/6 and 1/1/8 (ATE/LOV/SOL). The solids concentration of SOL was fixed at 48 mg/mL and correspondingly, the concentration of ATE and LOV was adapted to obtain the desired ratios. One by one, the solutions were electrosprayed in a climate controlled electrospinning apparatus (EC-CLI, IME Technologies, Geldrop, The Netherlands) at 25 °C and a relative humidity of 20 %, applying a potential difference of 23-25 kV over the nozzle and collector. A syringe pump (PHD 4400, Harvard Apparatus, Massachusetts, USA) was used to pump the solutions at a flow rate of 0.4 mL per hour through the one-channel nozzle and the distance between the tip of this nozzle and the copper collector plate measured 6 cm. A glass petri-dish was placed on top of the plate to collect the produced particles.

Coated amorphous solid dispersion particles

The same electrospinning apparatus and operation parameters were used to produce the coated particles, except for the nozzle, which was replaced by a two-concentric-(coaxial)-channel stainless steel nozzle (coax_2disp, Linari Engineering, Pisa, Italy) and the tip-to-collector distance, which was enlarged to 9 cm. Six types of coated particles were electrosprayed starting from the solutions whose composition are defined in Table 6.1. The solutions were prepared by using a DCM/MeOH solvent mixture (1/1, V/V) for the core and EtOH for the shell. Two separate syringe pumps were connected to the system in order to pump the core at 0.3 mL per hour and the shell solution at 1.2 mL per hour through the internal and external channel of the coaxial nozzle, respectively. The choice of solvent,

solids concentration and process parameters was based on previous electrospraying experiments performed in our research groups[65,78]. All electrosprayed particles were stored at -20 °C over phosphorous pentoxide before further analysis.

Table 6.1. Composition of the core and shell solutions used during coaxial electrospraying. EtOH was used as solvent for the shell solution and a DCM/MEOH solvent mixture (1/1, V/V) for the core solution.

Batch	API 1 mg/mL	API 2 mg/mL	SOL mg/mL	Eudragit® S100 mg/mL	ASA mg/mL
		Core solution		Shell solution	
C-S1	1.67 ATE	1.67 LOV	10	30	0
C-S2	1.67 ATE	1.67 LOV	10	30	1.36
C-S3	3.33 ATE	0	10	30	0
C-S4	0	3.33 LOV	10	30	0
C-S5	3.33 PAR	0	10	30	0
C-S6	0	3.33 FEN	10	30	0

6.3.3. Solid state analysis

Modulated differential scanning calorimetry (mDSC)

The mDSC analysis of the electrosprayed particles was performed using a Q2000 differential scanning calorimeter (TA instruments, Brussels, Belgium) connected to a RCS 90 cooling system. The cell was continuously purged with dry nitrogen at a flow rate of 50 mL per minute. Prior to analysis the samples were dried in a Mazzali vacuum oven (MSL, Lissone, Italy) at 25 °C and the DSC system was calibrated for the enthalpy with indium and the temperature with indium, octadecane and tin as standards. Furthermore, the heat capacity was calibrated with sapphire. An amount of particles in the range of 1 to 3 mg was accurately weighted into standard aluminium DSC pans (TA instruments, Brussels, Belgium), after which they were analysed at a heating rate of 2 °C per minute superimposed by a sinusoidal temperature oscillation with an amplitude of 0.212 °C and a period of 40 seconds. The thermograms were compiled and processed with the Universal analysis 2000 software version 4.5. Similarly, pristine ATE, LOV and SOL were scanned as a reference. Furthermore, amorphous reference material of ATE and LOV was *in situ* prepared by heating the APIs above their melting temperature. They were subsequently cooled at 20 °C/min and subjected to a second heating cycle to record the thermograms of the amorphous APIs.

X-Ray Powder Diffraction (XRPD)

To perform the XRPD analysis, the X'pert PRO diffractometer (PANalytical, Almelo, The Netherlands) fitted with a copper X-ray source was used, applying an acceleration voltage of 45 kV and current of 40 mA. Scanning of the samples was performed in transmission mode by placing the electrosprayed particles between two Kapton films (Kapton polyimide thin films, PANalytical, Almelo, The Netherlands), and programming the following instrumental parameters: angle 2ϑ of 4 to 40°, step size of 0.0167° and count time of 400 s. Data were collected and analysed with the X'Pert Data Collector software. As a reference, the diffractograms of pristine (crystalline) ATE and LOV were recorded.

6.3.4. Scanning electron microscopy (SEM)

The morphology of the electrosprayed particles was assessed using a FEI XL30 FEG microscope (Philips, Eindhoven, The Netherlands) with a field emission electron gun and secondary electron detector. Particles for SEM analysis were electrosprayed directly onto aluminium foil instead of collection on the glass petri dish. Next, the aluminium foil was mounted with double-coated adhesive carbon tape (Ted Pella Inc., California, USA) onto the SEM stubs and platinum coated under vacuum by the use of a SCD-030 Balzers Union sputter-coater (Balzers, Liechtenstein). Images were recorded using an acceleration voltage of 20 kV and spot size of 3.

6.3.5. Solubility and *in vitro* dissolution test

Solubility test

The solubility of pristine ATE, LOV, PAR and FEN in acidic (0.1 M HCl) and neutral medium (0.1 M HCl adjusted to pH 7.5 with 0.4 M Na_3PO_4) was determined. To this end, an excess of API was added to test tubes containing the specified medium and the tubes were placed in a rotary mixer (Labinco BV, Breda, The Netherlands). Regarding LOV, extra test tubes containing 0.5 % SOL in the medium were prepared as well to study the influence of the polymer on the solubility of LOV. After 72 hours, the content of the test tubes was filtered using a 0.1 µm Whatman polytetrafluoroethylene syringe filter (GE Healthcare, Buckinghamshire, UK) to remove the undissolved fraction and the concentration of the dissolved APIs was measured with HPLC as described below. Adsorption of the APIs to the filter was tested upfront and only observed for LOV. Consequently, filters were saturated before use with an aqueous saturated LOV solution. All experiments were performed in triplicate.

HPLC

For the HPLC analysis, a LaChrom system (Merck-Hitachi, Darmstadt, Germany) equipped with a L-7420 UV-VIS detector was used and the analyses were run on an ODS Hypersil C18 column, 4.6 x 250 mm, d_p = 5 µm (Thermo Scientific, Massachusetts, USA). Chromatograms were analysed with the D-7000 HPMC System Manager Software version 4.1. For the simultaneous analysis of ATE, LOV and ASA, a gradient elution was installed as described in Table 6.2, with the organic phase being ACN and the aqueous phase being 0.1 % phosphoric acid. Since LOV and ASA are prone to hydrolysis, their corresponding acids, LOVh and salicylic acid, were quantified as well. In order to obtain a LOVh standard, hydrolysis of LOV was performed with NaOH at room temperature, following neutralisation after 1h with HCl[180]. The flow rate of the mobile phase was set at 1 mL per minute, the injection volume at 20 µL, the analyses were run at room temperature and the wavelength for detection was varied throughout the analysis to ensure maximal absorbance of the different APIs (Table 6.2). Prior to analysis, the method was validated and the details are shown in Annex 2.

For the separate analysis of PAR and FEN, an isocratic method was selected instead with mobile phase compositions of respectively 85/15 and 10/90 (V/V) 0.1 % phosphoric acid in water/ACN. Finally, the wavelength was changed to 245 nm (PAR) and 286 nm (FEN).

Table 6.2. Detailed overview of the HPLC gradient method for the separation of ATE, LOV, LOVh, ASA and salicylic acid.

Time (min)	Aqueous phase (%)	Organic phase (%)	Time (min)	Wavelength (nm)
0	83	17	**0**	194
2	83	17	**7.5**	200
9	10	90	**12.5**	239
15	10	90		
16	83	17		
20	83	17		

***In vitro* dissolution test**

A two-stage pH shift method was selected to assess the release kinetics of the APIs from the electrosprayed particles. An accurate amount of the electrosprayed particles was weighted into test tubes containing 0.1 M HCl, equivalent to a dosage of the API in 500 mL gastric fluid. The applied dosage was 25 mg for ATE and LOV and 100 mg for ASA. For each time point of the dissolution test, three test tubes were prepared in order to perform the experiment in triplicate. All test tubes were placed in a rotary mixer and after 5, 15, 30, 60 and 90 minutes, the content of the three corresponding test tubes was filtered with a 0.1 µm syringe filter. The samples were diluted with ACN to avoid precipitation of the potentially supersaturated LOV during analysis. At 90 min, the pH of the remainder test tubes was adapted to 7.5 by adding 0.4 M Na_3PO_4 and samples were taken at 100, 120, 150, 240 (and 300) minutes, filtered and properly diluted. All samples were quantified using HPLC-UV as described above, and the actual drug loading, determined by dissolving the electrosprayed particles in MeOH following HPLC analysis, was taken into account to compile the dissolution profiles. As a reference, the dissolution profiles of pristine ATE and LOV were recorded, with and without addition of SOL to the medium.

6.3.6. Coated atenolol tablets

25 mg ATE and 75 mg microcrystalline cellulose were blended with mortar and pestle and subsequently, the mixture was manually tabletted using a 13 mm die (PerkinElmer, Beaconsfield, UK), applying 186 MPa with a bench press (Rodac International, Sittard, The Netherlands). Subsequently, the tablets were dip-coated in a 150 mg/mL Eudragit® S100 solution in EtOH. Three coating layers were applied to ensure a proper enteric coating layer. Furthermore, both coated and uncoated tablets were subjected to an *in vitro* dissolution test using the same dissolution media and time points as described above. However, a USP 2 apparatus was used (Hanson SR8-plus dissolution test station, Hanson Research Corporation, California, USA) and at each time point, 3 mL of sample was taken from the vessel, filtered and quantified with HPLC. After each sampling, the withdrawn medium was replenished and the dissolution tests were performed in triplicate.

6.4. RESULTS AND DISCUSSION

6.4.1. Amorphous solid dispersion particles

As discussed in the introduction, a step-by-step approach was applied in order to control the complexity of the coaxial electrospraying principle. To formulate an ASD, different water soluble polymers are commercially available, for example polyvinylpyrrolidone, hypromellose and Soluplus®[22]. The latter was proven to be a good choice to manufacture an ASD of LOV as high supersaturation levels were seen during the preliminary experiments. Consequently, particles containing an increasing amount of SOL compared to LOV and ATE (whose ratio was kept constant at 1/1, m/m) were synthesized via single nozzle electrospraying and analysed with mDSC and XRPD in order to determine the highest drug loading that still led to an amorphous system (Fig 6.4). Fig 6.4A shows the thermograms of the reference compounds: pristine ATE melts at 154 °C and LOV at 172 °C. Additionally, amorphous ATE and LOV were prepared *in situ* by cooling in the DSC, but ATE crystallised already during cooling from the melt, as a consequence, only the glass transition temperature (T_g) of LOV could be determined as 25 °C. Lastly, SOL is an amorphous polymer with a T_g of 75 °C. Regarding the electrosprayed particles, Fig 6.4B displays the thermograms of the samples with decreasing drug loading. The combination 1/1/1 (m/m/m, ATE/LOV/SOL) has a glass transition event at 47 °C which is an indication of a homogenous amorphous mixture between the polymer and one or both of the APIs.

However, the system is not fully amorphous because a melting event shows up at 130 °C. Since it is reported that ATE has a high crystallisation tendency and a melting temperature closer to 130 °C than LOV, this peak corresponds most likely to the melting of crystalline ATE[185]. Moreover, the peak shifts to lower values with an increasing polymer content, which can be explained by an increasing effect of melting point depression when more polymer is present in the mixture. To verify this assumption, XRPD was performed and indeed, only Bragg peaks corresponding to ATE were observed, indicated with the arrows in Fig 6.4C-D. This confirms together with the absence of a LOV melting peak in the thermograms, that LOV is amorphous in the core formulation. ATE in contrast does not become fully amorphous during the electrospraying process, or it does immediately crystallise during storage, even at low drug loadings (1/1/8 ATE/LOV/SOL). Since ATE is highly water soluble, it will not need the enabling effect of the ASD to obtain an appropriate dissolution profile as will be illustrated in the next paragraph. Nevertheless, with respect to the physical stability of the ASD, one should be aware that ATE could form seeds that might induce crystallisation of LOV.

To evaluate the pharmaceutical performance of the ASD core particles, the 1/1/3 and 1/1/6 combinations were subjected to a dissolution test in which the low pH of the stomach was mimicked during the first 90 min and subsequently switched to a neutral pH. Before conducting this test, first the dissolution profile of pristine ATE and LOV as well as their solubility in the dissolution media were recorded (Fig 6.5A-B). As can be deduced from Fig 6.5B, the solubility of the basic compound ATE (pKa 9.4) is highly dependent on the pH[186]. Still, the solubility of ATE in both media is very high (39 and 17 mg/mL in acidic and neutral medium, respectively), resulting in ATE being instantaneously and completely dissolved (Fig 6.5A). In contrast, LOV is a neutral compound whose solubility is not

influenced by the pH of the medium, but it is very poorly soluble. Consequently, almost none of the pristine LOV is dissolved after five hours. Addition of SOL to the media doubled the solubility of LOV, but nevertheless, the addition of SOL did not improve the dissolution behaviour (Fig 6.5A-B).

In contrast to this, testing now the dissolution of the combinations, supersaturation of LOV was observed for the 1/1/3 ASD core particles (Fig 6.5C). Additionally, the 1/1/6 combination was also tested, and in this case a higher release rate with even 100 % release of LOV after four hours was achieved (Fig 6.5D). It is well known from literature that decreasing the drug loading in the ASD is beneficial to obtain supersaturation of the API, however, a lower drug loading also increases the pill burden[22]. Since in this study a powder is envisaged that should be mixed with food or drinks, the use of more excipients in not a major drawback. All in all, single nozzle electrospraying proved to be a valid method for the production of the ASD core particles with SOL, leading to a fast and complete release of both ATE and LOV.

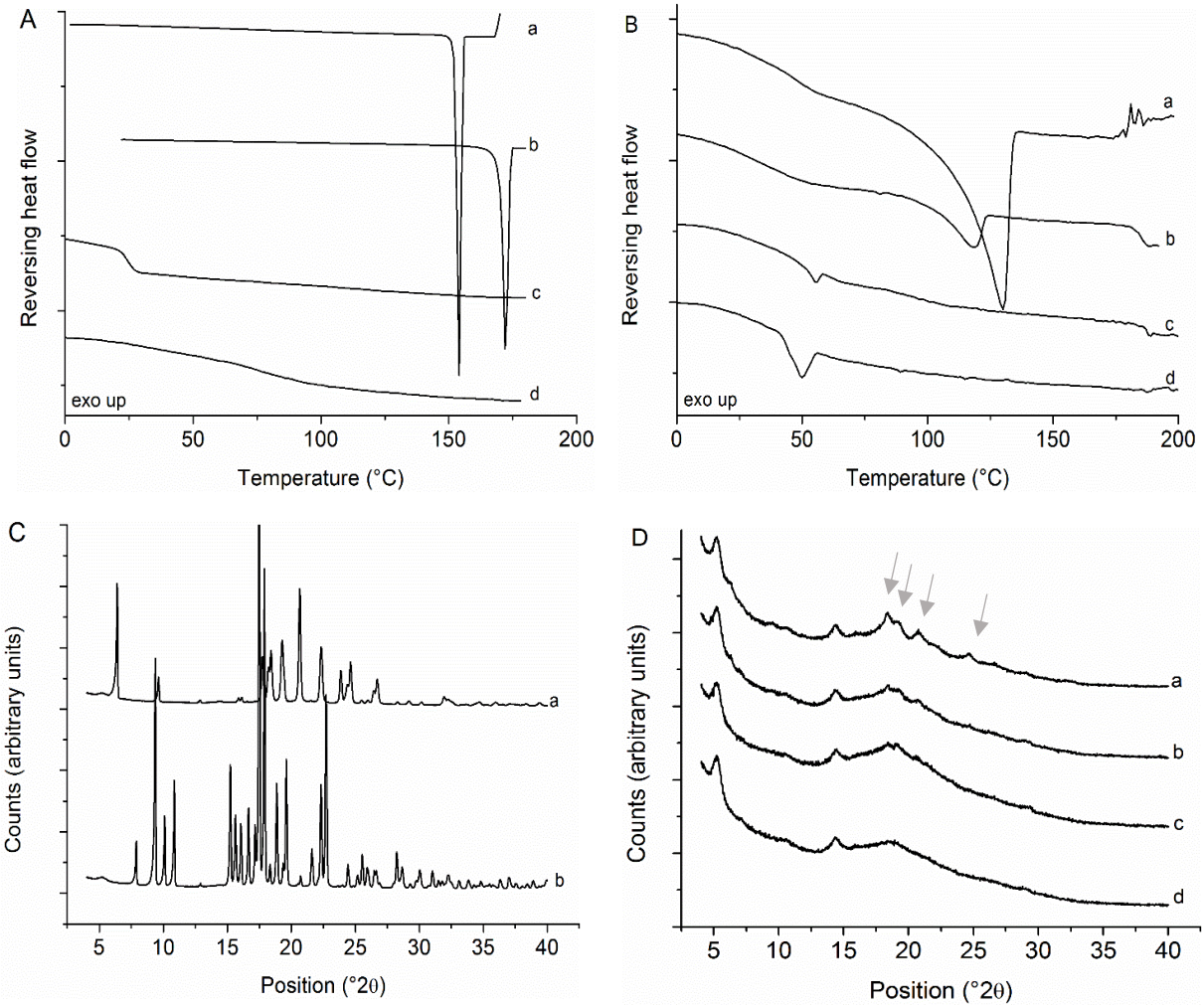

Figure 6.4. A: Thermogram of pristine ATE (a) pristine LOV (b) amorphous LOV obtained via in situ formation in the DSC (c) SOL (d). B: Thermogram of core particles containing ATE/LOV/SOL in different m/m/m combinations of 1/1/1 (a) 1/1/3 (b) 1/1/6 (c) 1/1/8 (d). Endothermal signals are facing downwards. C: XRPD profiles of pristine ATE (a) pristine LOV (b). D: XRPD profiles of core particles containing ATE/LOV/SOL in different combinations 1/1/1 (a) 1/1/3 (b) 1/1/6 (c) 1/1/8 (d). The arrows indicate the characteristic peaks of ATE.

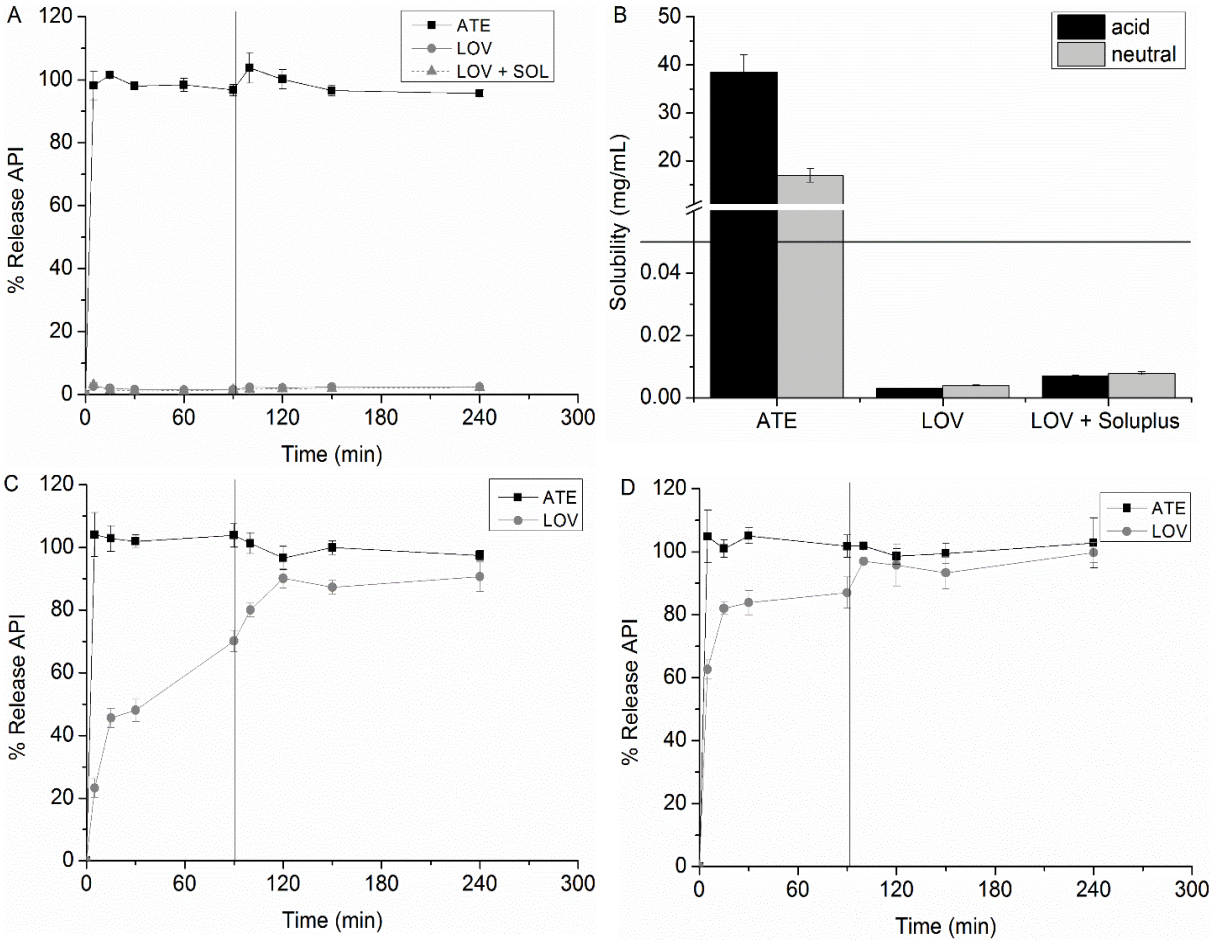

Figure 6.5. A: Dissolution profiles of pristine ATE (solid black) LOV (solid grey) and LOV for which SOL was added upfront to the dissolution medium (dashed grey). The vertical line in the dissolution profiles indicates the time point of the switch from acidic to neutral medium. B: Solubility values in acidic (black) and neutral (grey) media for ATE, LOV and LOV for which SOL was added to the media. The solid horizontal line depicts the concentration if 100 % release of the APIs would be achieved during the later dissolution tests from ASD core particles. C: Dissolution profile of ASD core particles with 1/1/3 (ATE/LOV/SOL). D: Dissolution profile of ASD core particles with 1/1/6 (ATE/LOV/SOL).

6.4.2. Coated amorphous solid dispersion particles

To coat the ASD particles with an enteric polymer, a CES setup was used in which the core solution (containing ATE, LOV and SOL) and the shell solution (containing the enteric polymer and ASA) were simultaneously pumped through the inner and the outer part of the coaxial nozzle, respectively. The shell solution was pumped through the nozzle at a higher volumetric flow rate compared to the core solution, ensuring proper encapsulation. In our previous work on the production of coated particles with CES, it was found that coating with the copolymer Eudragit® S100 yielded gastro-resistant particles in compliance with the guidelines of the European Pharmacopoeia regarding gastro-resistant formulations, stating that the release of the API after two hours in acidic medium should be less than 10 %[154], while this was not succeeded with other coating polymers. Apart from the type of polymer, the influence of different formulation parameters like the polymer concentration and choice of

solvent were investigated in the same study. When using EtOH and higher polymer concentrations, less burst release in acidic medium was observed compared to using other solvents. However, with regard to the polymer concentration, the limit was found to be 30 mg/mL as will be discussed in more detail in one of the following paragraph. Based on these results, it was thus decided to select Eudragit® S100 as coating polymer for this FDC and more specifically, a 30 mg/mL solution in ethanol was applied. Moreover, it was observed that particles are easily overloaded, resulting in a high burst release of the API in acidic medium. Hence, a low solids content of maximum 10 mg/mL SOL was preferable for the core solution.

Taking these considerations regarding the formulation parameters into account, ASD particles coated with solely Eudragit® S100 were prepared (Table 6.1: C-S1) to evaluate the coating performance. Afterwards a second batch was prepared with ASA added to the coating solution (Table 6.1: C-S2). To analyse the morphology and solid state as well as to have an estimate about the dimensions of the coated particles, SEM was conducted, and pictures of C-S1 and C-S2 are represented in Fig 6.6A and B/C respectively. The coated particles without ASA (C-S1) are in the size range of a few micrometres, while the ones with ASA (C-S2) are slightly smaller. By adding an extra compound to the shell solution, in this case ASA, the conductivity probably increases, which leads in general to smaller particles[64]. Looking at the morphology, the C-S1 particles have the typical collapsed morphology of a particle formed by rapid solvent evaporation, as also often observed for spray drying. The C-S2 particles are in contrast remarkably smooth and spherical. Subsequently, the solid state of the coated particles was investigated with mDSC and XRPD (Fig 6.7). The thermograms show a clear T_g at 160 °C, which corresponds with the T_g of Eudragit® S100. On the other hand, the T_g of the SOL-LOV ASD is less clear and no melting peaks or Bragg peaks in the XRPD profiles were observed. However, based on the solid state experiments of the uncoated core, ATE can be expected to be (partially) crystalline in the coated particles as well, but the drug loading in these coated particles is very low and detection of a crystalline fraction falls most likely below the detection limit of the equipment.

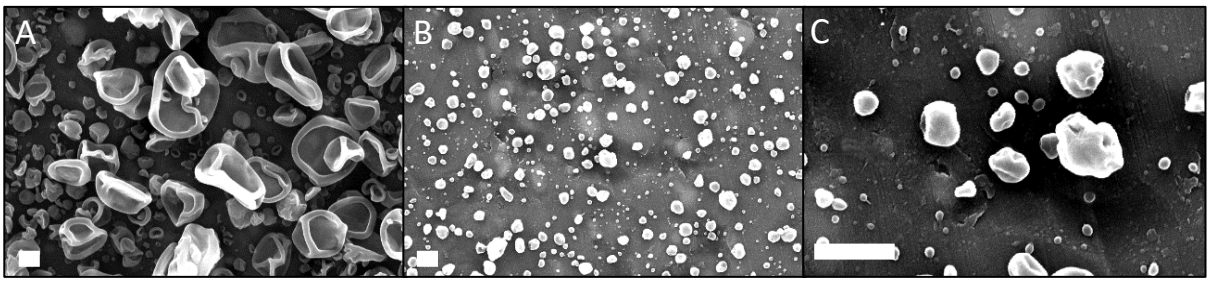

Figure 6.6. Scanning electron microscopy images of A: C-S1 particles with 6 500 x magnification. B: C-S2 particles with 6 500 x magnification. C: C-S2 particles with 25 000x magnification. The scale bars indicate 1 µm.

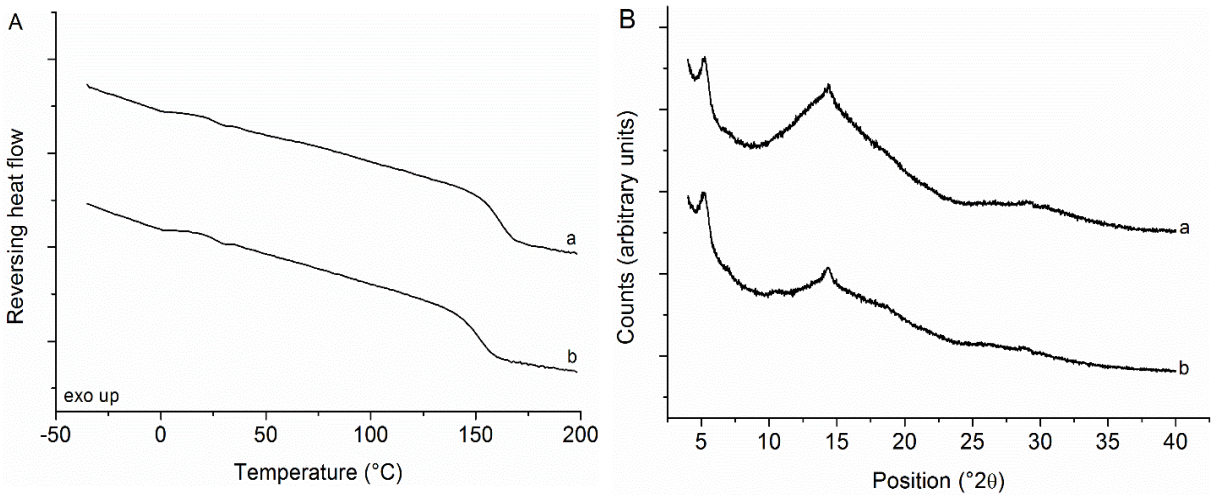

Figure 6.7. A: Thermograms of C-S1 particles (a) and C-S2 particles (b). Endothermal signals are facing downwards. B: Diffractograms of C-S1 particles (a) and C-S2 particles (b).

Next, the coated particles were subjected to a dissolution test, shown in Fig 6.8A-B. To start, the C-S1 particles were tested to evaluate the gastro-resistant performance of the pure Eudragit® S100 coating (Fig 6.8A). A discrepancy in the release of ATE and LOV from the coated particles was observed during the 90 min time period in acidic medium. For LOV, the coating performed well with only minor release of the API, while 60 % of ATE was released in the acidic stage, far above the 10 % limit of the European Pharmacopoeia. After the switch to the neutral pH at 90 min, the coating dissolved completely and supersaturation of LOV was achieved, comparable to the release from the uncoated core; also ATE reached the level of 100 % release. When adding ASA to the shell solution (Fig 6.8B), similar release profiles were obtained. Since ASA is present in the shell and not in the core, release of ASA in acidic medium was expected, still not as much as almost 50 % within the first five min. Gastro-resistance was expected to some extent when ASA is formulated in a Eudragit® S100 matrix[52]. All in all, the premature release of ATE is not problematic regarding the FDC which is aimed for, since ATE is not acid-labile and does not necessarily need to be delivered in the distal intestinal region. Still, the underlying reason was further researched in order to get a better understanding concerning the performance of a coating generated during the coaxial electrospraying process.

To eliminate the fact that the inadequate coating performance for ATE would be due to the co-formulation of LOV and ATE, coated particles with only ATE and SOL (C-S3) or only LOV and SOL in the core (C-S4) were prepared and tested. Again a flawless gastro-resistant behaviour was observed for LOV, followed by complete release of LOV in the neutral medium. However, for ATE still a similar apparent coating failure as for CS-1/2 was observed (Fig 6.9A-B).

The apparent coating failure for ATE can either be explained by the fact that the coating layer itself is not sufficient to retain the highly soluble ATE, or that the particles have an impaired core-shell structure. However, the latter can be countered by the reproducibility and the observations made for LOV and ASA. Indeed the optimal release kinetics of LOV, without any release in the acidic stage and complete release in neutral medium, indicates the presence of a coating layer that can at least retain the ASD of LOV. In addition to that, the more gradual release of ATE that was observed in comparison

to that of ASA, suggests that the APIs are localised in a different layer of the particles (Fig 6.8). Furthermore, it can be expected from previous research that a proper core-shell structure can be obtained with this setup. Confocal imaging performed in our own research group in the past, demonstrated the core-shell structure for electrosprayed enteric coated ASD particles. This is supported by other published studies where confocal and transmission electron microscopy were applied to visualise the core and coating layer of particles composed with similar polymers and APIs[121,152]. Thus, the explanation for the coating failure should probably be found in the properties of the electrosprayed coating layer itself. However, the small dimensions of the particles limit the use of conventional methods used to study coating layers.

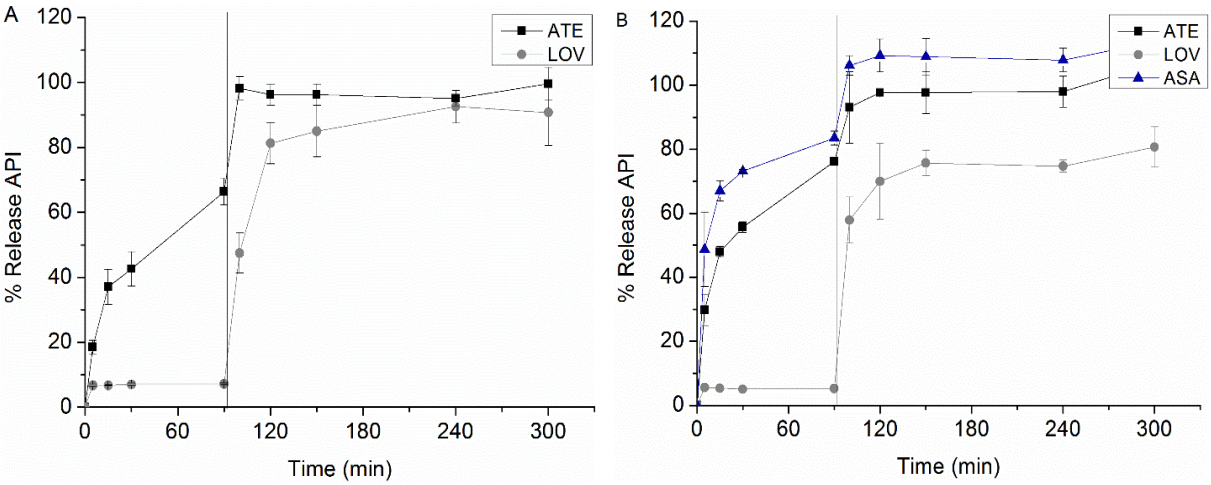

Figure 6.8. Dissolution profile of A: C-S1 particles and B: C-S2 particles for ATE (black), LOV (grey) and ASA (blue). The vertical line indicates the time point of the switch from acidic to neutral medium.

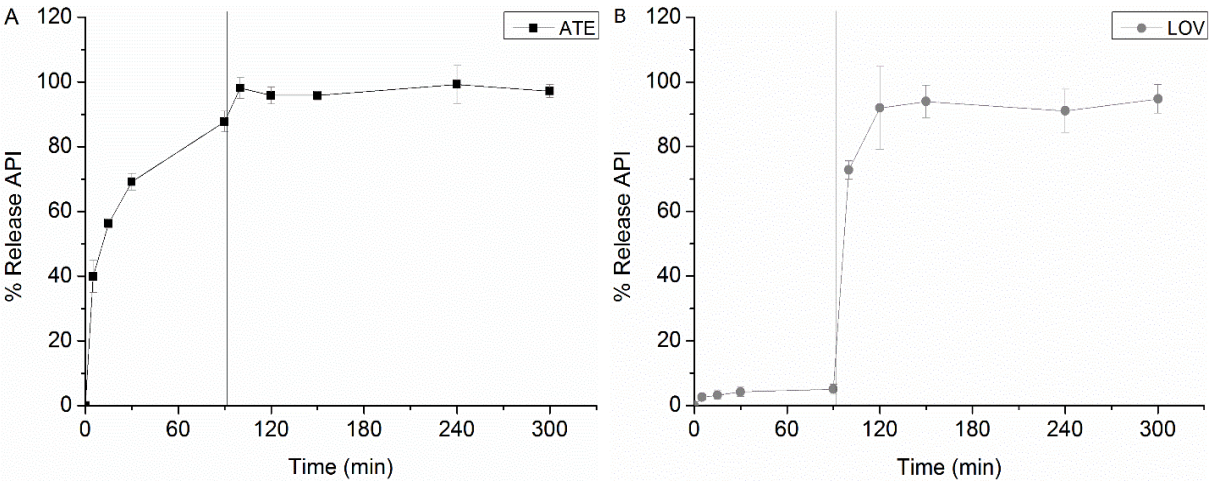

Figure 6.9. Dissolution profile of A: C-S3 particles and B: C-S4 particles with ATE (black) and LOV (grey). The vertical line indicates the time point of the switch from acidic to neutral medium.

6.4.3. Benchmarking with a conventional coating process

In order to further elucidate the discrepancy in coating performance between ATE and LOV, coaxial electrospraying was compared to conventional tablet coating. After all, Eudragit® S100 is generally accepted as an enteric polymer and it is highly unlikely that it would not be suitable to retain ATE in acidic medium. ATE was mixed with microcrystalline cellulose and compressed into tablets. Subsequently, the tablets were manually dip-coated in a concentrated Eudragit® S100 solution and the ATE release was determined. In addition, the release kinetics of the uncoated tablets was measured to have an idea about the disintegration profile of the bare tablets; the ATE tablets dissolved in less than 15 min (Fig 6.10). For the coated tablets, practically no ATE dissolved in the acid stage and the tablets only started to disintegrate after the pH switch.

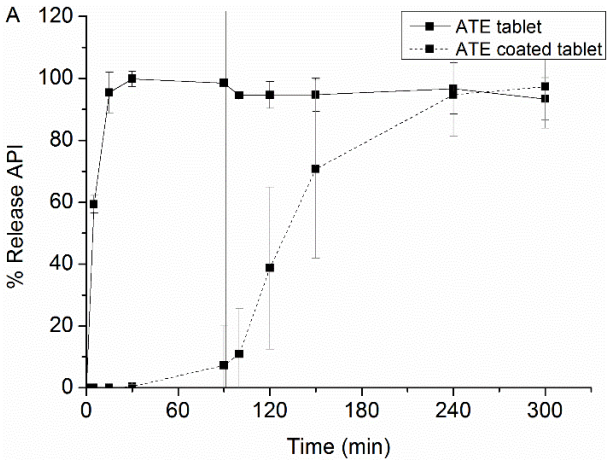

Figure 6.10. Dissolution profile of uncoated ATE tablets (solid black line) and coated ATE tablets (dashed black line). The vertical line indicates the time point of the switch from acidic to neutral medium.

6.4.4. Poorly versus highly water soluble

Comparison with the manual coating method proved that Eudragit® S100 can successfully be used for an enteric coated formulation containing ATE when a proper film is applied. This suggests that regarding the electrospraying process a coating with insufficient thickness and/or chain entanglements is produced during electrospraying. In order to increase the shell thickness, a higher concentrated Eudragit® S100 solution could be used. However, there is a maximal concentration that can be applied as the process will shift from electrospraying to electrospinning with increasing polymer concentration. During electrospinning, the jet at the tip of the cone is stabilised and does not split up anymore into an aerosol of droplets, consequently, fibres instead of particles are produced. This shift from spraying to spinning can be related for lower molecular weight polymers to the critical overlap concentration of the polymer (c*)[64,73,187]. The concentration region below c* is called the dilute region and no chain overlap will occur. At concentrations above c*, in the so-called semi-diluted unentangled regime, the polymer chains begin to overlap. At even higher concentrations, the chains will properly entangle, which is then called the semi-diluted entangled regime. In this regime the extensional viscosity of the system is strongly increasing with concentration and hence the jet will be stabilised. The applied Eudragit® S100 concentration for the shell should thus be low enough, allowing

the jet to be atomized into droplets. Previously, the concentration limit was determined in our research group to be around 3-4 % based on SEM images and viscosity measurements. Apart from the coating polymer concentration, the ratio of the shell to core feed rate at which the solutions are pumped through the coaxial nozzle could be increased to obtain a thicker shell layer. Both options were explored but it did not drastically reduce the ATE release and even more, the release of LOV in neutral medium was negatively influenced.

The observation that ASA was almost instantaneously released from the shell layer in which it was embedded in the Eudragit® S100 polymer, gave rise to the hypothesis that the coating layer is more porous compared to a film coating produced with the manual coating method. Due to this porosity, a certain amount of water can penetrate through the otherwise integer coating layer and, for compounds with high solubility like ATE and ASA, selectively dissolve those, while compounds with low solubility like LOV are not affected and remain undissolved in the core. To validate this hypothesis, coated particles with either another highly soluble API, namely paracetamol (Table 6.1, C-S5) or another poorly soluble API fenofibrate (Table 6.1, C-S6) were electrosprayed following the same procedures as for particles C-S3 and C-S4, and subjected to a dissolution test. The same dissolution trend could be observed as depicted in Fig 6.11. PAR with a high solubility of 14 mg/mL was quickly released in the acidic media, while FEN (solubility of 0.0002 mg/mL) showed barely any, if at all, release. Interestingly, after the pH switch a FEN release of 40 % was achieved, which is extremely well for an ASD of FEN because supersaturation for this very lipophilic API is hard to achieve[188]. This observation points again to the viability of electrospraying as a production method for ASDs. After 150 min, the concentration of FEN dropped again due to the increased precipitation propensity of the highly supersaturated FEN.

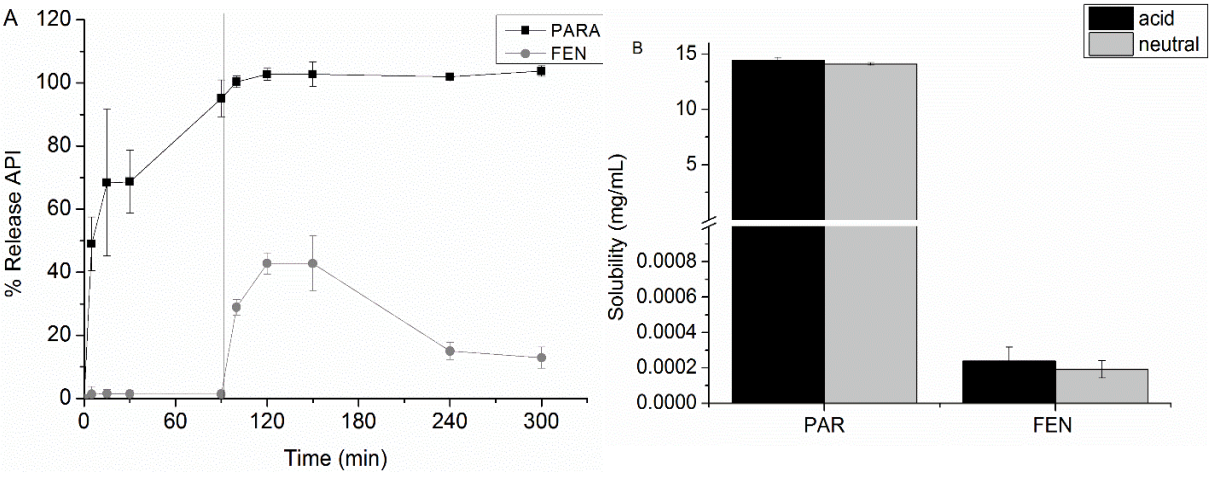

Figure 6.11. A: Dissolution profile of CS-3 particles (black) and CS-4 particles (grey). The vertical line indicates the time point of the switch from acidic to neutral medium. B: Solubility of PAR and FEN in acidic (black) and neutral (grey) medium.

Interestingly, in a study from Alhnan *et al*. that investigated the release in acidic conditions of APIs with different physicochemical characteristics embedded in Eudragit® S microparticles, the burst release from these matrix particles was correlated to the molecular weight of the APIs rather than the solubility[189]. Although in this work, coated particles instead of matrix particles are covered and the described correlation is not fully fulfilled, the molecular weight of ATE and PAR is lower than that of LOV and FEN, which possibly can favour diffusion. Another aspect, that is especially clear for the release of LOV, is that fact that already at the first time point, the maximal concentration in acidic medium is reached and does not change for the remaining 90 min. This suggested that a certain amount of LOV is readily available for dissolution and present at the surface, what would mean that during the droplet drying process, the API probably migrated to the shell layer as this is highly unlikely to happen in the solid state. Consequently, it would be deeply interesting for further research to elucidate how the different APIs are exactly distributed through the core-shell particles, although this will be challenging given the small dimensions of the particles.

6.5. CONCLUSION

In this work, the usefulness of coaxial electrospraying for the production of a fixed dose combination that contains three APIs and is easy to swallow, was demonstrated. Formulating lovastatin as an amorphous solid dispersion with Soluplus®, together with atenolol, led to fast and full dissolution of lovastatin. By using Eudragit® S100 as a coating polymer, the release of lovastatin from the particles was prevented in acidic medium; in contrast, the release of atenolol was only partially inhibited. Most likely, the coating layer produced during the coaxial electrospraying process is less dense and consequently too permeable for highly water soluble compounds like atenolol and paracetamol but not for less soluble compounds like lovastatin and fenofibrate. These observations form a foundation for further investigation of the coating performance. Future research will be necessary to overcome the observed limitations and evaluate whether coaxial electrospraying will be applicable to modify the release of a broad range of compounds.

Acknowledgements

The authors thank The Fonds voor Wetenschappelijk Onderzoek-Vlaanderen (FWO, project G0A3916N) for the financial support.

Chapter 7
General discussion

7.1. FROM POLYMERS TO FIXED DOSE COMBINATIONS

This research project revolved around the production of a powder for reconstitution consisting of enteric coated ASD particles. Despite the simplicity of the coaxial electrospraying setup, the complexity evolving from the large amount of variables for both core and shell solution as well as the selection of the process parameters, turns optimisation into a laborious process. Which polymers can be used? Which solvents are better? Which are the better process settings in order to easily obtain a cone-jet mode? These questions rise in twofold as two different solutions for core and shell are applied and are typically clarified via trial-and-error. Hence a step by step approach was applied in this PhD project, starting with single nozzle electrospraying and gradually adding compounds to eventually reach a core-shell structured fixed dose combination. A schematic overview of the different steps was illustrated in Fig 2.1 (chapter 2: Objectives).

Throughout the project, a variety of polymers and settings for the formulation and process parameters was used. The rational flow of the polymer selection is displayed in Fig 7.1 (the criteria that led to the selection of the other parameters will be handled in more detail in the next section). Various polymers were selected for the first project in order to cover a broad range of physicochemical characteristics and applications e.g. cellulose derivatives versus vinyl polymers or a polymer to manufacture ASDs versus one to be applied as coating. As it was seen that all polymers were suitable for electrospraying, all paths for the second project, the manufacturing of an ASD with darunavir, were open. Hence, to include some variety, the three most accessible polymers with diverse properties, namely HPMC, PVP and HPMC AS, were tested regarding their supersaturation potential on darunavir. This supersaturation experiment did not lead to a superior candidate, consequently, they were all three used in parallel for electrospraying.

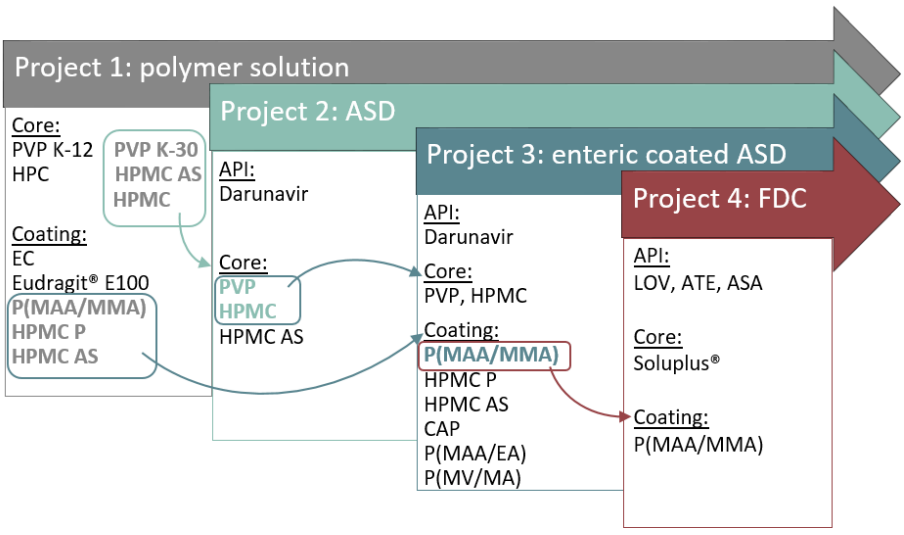

Figure 7.1. Flow of polymer selection throughout the four experimental parts of the thesis. For the meaning of the abbreviations and corresponding chemical structures of the polymers, the reader is referred to Annex 1.

Subsequently, the second project showed that electrospraying successfully produced ASDs of darunavir with the three polymers. Henceforth, a cellulose derivative (HPMC) and vinyl polymer (PVP)

were included to make the core of the core-shell structured particles in the third project. With regard to the shell, all the enteric polymers of the first project, plus even extra enteric polymers which were not touched upon yet, were here included to be able to learn as much as possible on the coating behaviour. A similar conclusion as in the first project could be drawn: all extra polymers were also suitable for electrospraying, yet resulting in particles with different pharmaceutical performance.

For the fourth and last project, darunavir was discontinued and a formulation for cardiovascular disease was investigated. The choice for this shift was twofold: in the cardiovascular area, diverse APIs with very different properties need to be combined and it would be interesting to see how APIs other than darunavir behave in the core-shell system. The choice for P(MAA/MMA) 1/2 as coating agent is a logical consequence of its outstanding performance in the third project as it was the only enteric polymer whereby particles could be produced that were in compliance with the Ph. Eur.. The choice for Soluplus® needs more explanation: PVP was eliminated as core polymer due to its incompatibility with P(MAA/MMA) 1/2 and supersaturation experiments with HPMC and lovastatin were not favourable. Other polymers thus needed to be tested for their supersaturation potential and Soluplus®, a polymer that was not electrosprayed before, performed extremely well, even so that 100 % release of the poorly soluble lovastatin was observed. Since in the previous projects no limitations for the polymers had been encountered, it was certainly worthwhile to test this polymer for the core as well.

7.2. POLYMER SOLUTIONS AS A GUIDE TOWARDS COATED ASD PARTICLES

When looking into literature in which electrospraying has been investigated as an ASD manufacturing method, it shows that PVP is a polymer that has been repeatedly used. Two studies used PVP K-30 to enhance the solubility of either fenofibrate and ketoprofen and Kawakami used on top Eudragit® E100 to make solid dispersions of the model APIs prednisolone and carbamazepine, while in another study the vinylpyrrolidone-vinyl acetate copolymer was applied to formulate coenzyme Q10[109,112,117,119]. Different polymers were thus already used before, but it would still be interesting to evaluate the applicability of a wide range of polymers and this in one experimental design. Consequently, the first goal of the first experimental project (chapter 3) was to elucidate which polymers that are generally used in ASD manufacturing and for coating purposes, can also be used in electrospraying and which are moreover the limitations regarding the molecular weight (especially for PVP). Interestingly, all polymers and tested molecular weights for PVP could be electrosprayed during the first project. This opens perspectives towards ASD manufacturing, as different polymer-API combinations can be screened with respect to the supersaturation potential and long-term stability, but also towards the coating materials that can be used to tune the release.

The impact of the first project was not restricted to the polymers itself because an evaluation of the different parameters was also incorporated in our study design. Despite the fact that probably in each published electrospraying study, an investigation (whether very brief or more elaborated) of the influence of the different parameters on the electrospraying mode has been performed in order to

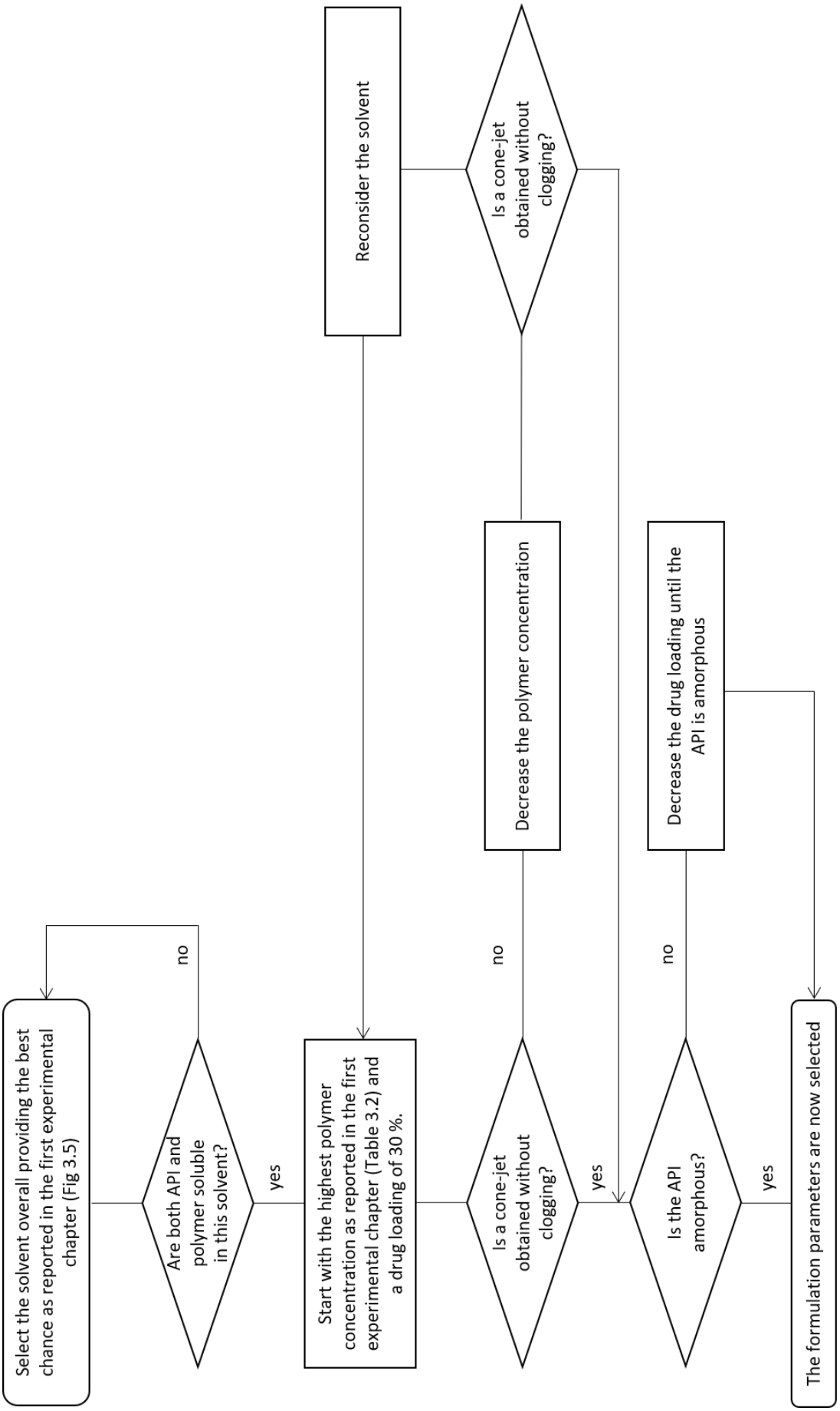

Figure 7.2. Flow chart to illustrate the selection process of the formulation parameters throughout the different projects.

work in a stable cone-jet regime, this is not always reported within the scope of the specific study. Still, papers have been published engaging this topic and for example in papers by Pareta *et al.* and Enayati *et al.*, studying respectively bovine serum albumin and polycaprolactone, the electrospraying regime resulting from the combination of the applied voltage and flow rate was mapped in a graph[135,162,190-193]. It could mainly be concluded that the cone-jet regime only existed for a narrow range of flow and voltage combinations and that this range shifted with the solute concentration. However, the characteristics of the applied compounds in these studies vary, which makes it difficult to correlate it to the solutions applied for ASD manufacturing.

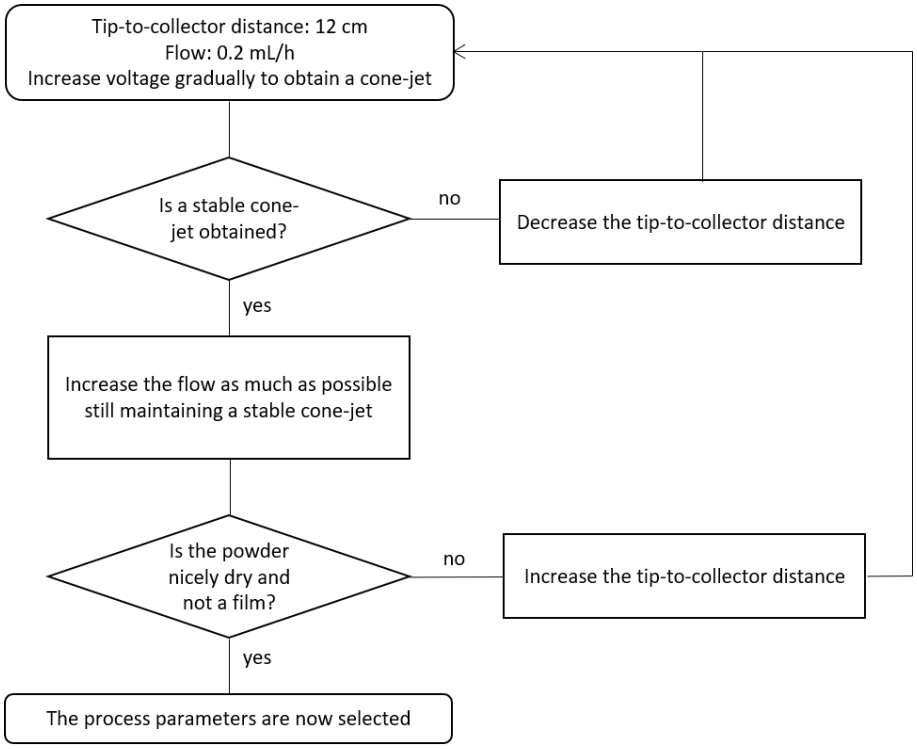

Figure 7.3. Flow chart to illustrate the selection process of the process parameters throughout the different projects.

In this work, by also changing solvent quality and polymer concentration (formulation parameters) and evaluating the influence of the voltage, flow rate and tip-to-collector distance (process parameters), the limits **for each polymer solution** regarding the working window, were determined. This information is highly valuable for the upcoming experimental projects. For example, if an ASD with HPMC needs to be manufactured, one knows immediately to look into which concentration range and which are the solvents that can be chosen from. Even more, the accompanying combination of process parameters that will most likely lead to a cone-jet, can readily be selected. This bypasses the demanding process to find the cone-jet window and ideal parameter settings every time a change to one of the formulation parameters is made.

The major constraint of the project's outcome was that no general correlations or limits could be determined. Changing the solvent and concentration of the polymer solution alters the viscosity and conductivity of the solution and they in turn influence the electrospraying process. Ideally, a

correlation would have been found between these solution properties and the formation of a cone-jet mode. In this work, one of the parameters was studied at the time but a more elaborated experimental design will be necessary to unravel the complex interplay between all process and formulation parameters and this at a broader interdisciplinary level so that the theoretical and physical principles can be linked to the more applied observations in this work.

Nonetheless, highly valuable conclusions could be drawn from the first experiments with regard to the parameter selection for the following projects. Similar to the polymer selection, the choice of the parameter settings might not always seem as logical at first sight. Why not always using isopropanol as a solvent or a high tip-to-collector distance as this was found to give the highest chance for a cone-jet mode? The answer lies in the fact that on top of the recommendations described in the first project, other issues like the solubility of the polymer and API need to be taken into account. Throughout the different projects, two flow charts were developed to be used as selection criteria. One concerns the formulation parameters (Fig 7.2) and the other one the process parameters (Fig 7.3). All in all, single nozzle electrospraying is a good starting point to develop a coaxial electrospraying method.

7.3. (COAXIAL) ELECTROSPRAYING IN THE ASD LANDSCAPE

The references made in the previous section to the different studies published to prepare ASD of poorly soluble compounds like fenofibrate, ketoprofen etc., point out that electrospraying is undoubtful an interesting manufacturing method for the production of ASDs. Indeed, high rate and extent of release were obtained during the dissolution test of the electrosprayed fenofibrate and ketoprofen particles[109,112]. From this point of view, the second project which focussed on electrospraying ASDs of darunavir is another confirmation of this already established application[109,110,112,117,119]. However, with the view of studying coated ASD of darunavir, this step could not be bypassed as a proper ASD core needed to be ascertained before further elaboration. Hence, to differentiate the project from the published work, the electrosprayed particles were directly compared to particles prepared by spray drying in order to evaluate the usefulness of electrospraying against a golden standard and roughly, the electrosprayed and spray dried particles were comparable. Recently, a study was published comparing ASDs of ketoprofen and different polyvinyl polymers prepared by both manufacturing techniques and generally the same conclusions could be drawn, however they also evaluated the flowability, which was less favourable for the electrosprayed powder[194]. Besides the comparison of the manufacturing methods for darunavir ASDs, a design of experiments was performed in our study to map the influence of different parameters on the characteristics of the produced particles. One could argue that a lot of research already focused on the latter and many articles can be found evaluating the effect of different parameters on the size and morphology of the obtained particles[108,161,163,195-200]. Most of them concern research on polymers like polystyrene, poly(lactic-co-glycolic acid) (PLGA) and polycaprolactone. Though, a similar effect of the feed flow rate on the size of the darunavir particles was observed as reported in two papers about PLGA, namely the size increased with increasing flow rate[161,200]. More unique to our approach was the

systematic evaluation of the effects on the ASD related parameters (amorphicity, homogeneity and drug release).

Nevertheless, from an industrial point of view, electrospraying might not have a tremendous impact at this moment in time due to the low throughput and limited expertise compared to the already well established industrial manufacturing methods. Still, it must be noted that besides ASDs, it has a great potential regarding the delivery of proteins[192,201-203], nucleic acids[204-206], cells[207-210] etc. and with the growing interest in nanotechnology, it can produce nanoparticles with a narrow particle size distribution[107,114,211-213]. Furthermore, it offers several advantages and the benefit of coaxial electrospraying for the production of coated particles regarding biomedical applications cannot be overestimated[58,214]. As an illustration, Beidokhti *et al.* coated methotrexate in folate conjugated chitosan for tumour targeted drug delivery and Xie *et al.* indicated the benefit of coaxial electrospraying to encapsulate proteins like BSA and lysozyme in PLGA[215,216].

The overall goal of this thesis project was the study of enteric coated microparticles. Applying an enteric coating layer is an approach that is already well established in the pharmaceutical industry in order to prevent the release of the API in the stomach. Examples of APIs that are typically coated are diclofenac, naproxen and omeprazole[217-219]. A spray dried ASD powder can be compressed into a tablet after which the coating is applied or it can be filled in an enteric capsule[220-222]. However, such a coated dosage form cannot be split or crushed as it will lose the coating functionality and this hampers its applicability for patients with a swallowing disability. While tablet/capsule coating is straight-forward, the production of individual coated powder particles that can serve as an easy-to-swallow powder for reconstitution is not that evident as discussed before and illustrated by the burst release observed in previous research[78,84].

One could argue that a powder with an enteric release profile could be more easily formulated with the API embedded in a gastro-resistant polymer. This is less complex than a coating approach and could be realized via simple electrospraying or even more conventional methods. It has indeed been proven that with the matrix concept a proper enteric release profile can be obtained. In fact, in a study by Alhnan *et al.* gastro-resistant microparticles that embedded different APIs were manufactured via an emulsion solvent technique. Others prepared particles with piroxicam via spray drying, with griseofulvin via single nozzle electrospraying and with cyclosporin via a quasi-emulsion solvent technique[110,189,223,224]. Although these formulations improved the dissolution, burst release in acidic medium was observed. However, when using a core-shell system, the options to tune the characteristics of the final particles and their release profile is more versatile. Furthermore, the advantage of the core-shell structured particles is the fact that it can be used as a platform for different kind of coatings e.g. protective, aesthetic, taste-masking and sustained release; not only limited to the enteric model exploited in this thesis. Besides, a core-shell structure can be interesting as a compartmentalized system for fixed dose combinations like investigated in the last experimental chapter (chapter 6), where the incompatible lovastatin and acetylsalicylic acid were physically separated in the core and shell layer.

7.4. CHALLENGES REGARDING COAXIAL ELECTROSPRAYING

The fact that enteric coated ASD particles with darunavir or lovastatin could be prepared that were in compliance with the Ph. Eur. guidelines, consolidates again the capability of coaxial electrospraying as demonstrated before in literature. Nonetheless, for atenolol the enteric coating layer did not perform adequately and significant differences in burst release regarding darunavir were observed for different shell solutions. Two hypotheses were considered to explain these discrepancies: the particles either lack a proper core-shell structure or the APIs migrate to the coating layer, whether or not coupled with the quality/permeability of the coating that leaves to be desired. As a matter of fact, proper validation was hampered by some limitations of our analysis techniques, merely to evaluate the internal structure and distribution of the different compounds throughout the particles. Yet not touched upon in detail, the control of the external morphology is another aspect that should be taken into consideration. Below, a critical analysis is made on the different challenges that need to be overcome to fully evaluate the fundamental culprit behind the burst release.

7.4.1. Evaluation of the coating layer

The first hypothesis is the most intuitively explanation and relates the burst release to the fact that the core is simply not homogeneously coated. This implies that either the core is not properly located in the centre of the particle and thus possible open at one side to the environment or that the coating is extremely thin or cracked at certain points. A first contra-argument against the coating imperfections is the fact that the burst release for a specific formulation is very reproducible and it is hard to believe that each time the exact same amount of imperfections is created. Withal, different options were approached to visualise the internal structure but the small dimensions of the particles entailed analytical difficulties.

When coating tablets or pellets with an enteric polymer via the traditional coating methods, the coating layer is generally a few dozens of µm thick[180,225]. Hence, scanning electron microscopy (SEM) is an accessible method to evaluate the coating layer. Tablets are crushed and the fractions can be analysed with SEM to create a cross-section image[226,227]. The coating layer can usually be clearly distinguished from the core tablet, allowing the evaluation of the thickness and for instance the porosity of the coating layer. Also transmission electron microscopy (TEM) has been used in other studies to differentiate between the core and shell layer in electrosprayed particles[106,113,193,228,229]. Example is a study that encapsulated a solid dispersion containing acyclovir in a shell of sucralose and sodium dodecyl sulphate. When the shell flow rate was increased, the SEM images nicely showed an increased shell thickness[106]. Unfortunately, when SEM or TEM were performed on the coated darunavir particles, no clear differentiation could be made.

Due to the numerous amount of publications successfully reporting the use of confocal microscopy to visualise the core-shell structures, this imaging method was investigated and indeed showed to be valuable as was demonstrated in chapter 5[121,152,164,230-232]. While in this chapter only the 2D images are shown, the technique also allowed to build a 3D representation of the particles by performing a scan along the z-axis. It became clear that the particles are homogeneously covered with the coating layer.

Despite the fact that confocal microscopy surely has a justified place for the evaluation of the core-shell structure, one needs to be critical about the fact that dyes need to be added and that consequently, it actually only visualises where the dyes are located and does not give any information on the structure of the polymer layers itself. It is for example possible that the differences in burst release obtained with the coating polymers as described in the 5th chapter are linked to differences in the porosity of the coating layer. Hence, an in-depth study of the particle structure would be explanatory. Moreover, it is possible that adding the dyes induces some deviations. Although electron and confocal microscopy are the two prominent methods in a lot of papers, it is necessary for further research to explore the applicability of other techniques.

With this in mind, the study by Roine *et al*. can be interesting because micro- and nanotomography X-ray imaging were used to investigate the core-shell structure of their microparticles[233]. The principle of this technique is similar to the typical computer tomography-scan used in clinical practice. The sample is irradiated with X-rays and the transmitted beams are detected, creating a cross-sectional image. By rotating the sample, a 3D structure can be build[234]. In the depicted study, the tomography technique visualised an intact coating layer but their particles were around 30 µm in diameter and the pixel resolution was 420-540 nm for the microtomography and 65 nm for the nanotomography imaging. In general, the best resolution that can be obtained with nanotomography is around 50 nm[235,236]. Knowing that the core-shell particles in this thesis were only in the range of a few micrometres, the resolution can be a limiting factor. Electron tomography, used for the imaging of intracellular structures and nanoparticles can possibly be an alternative[237].

7.4.2. Localisation of the API in the core-shell particles

The second hypothesis presumes a proper core-shell structure but proposes that the API migrates to the coating layer. Based on the confocal images, it can be assumed that the API, similar to the dye used for the core, would be immobilised in the core. However, when looking carefully to the release profile of darunavir in acidic medium, one can clearly observe a **burst** release, which means that a significant amount was already released at the first time point and the concentration barely increased during the remainder of the two hours. This suggests that at least some darunavir molecules are readily available to be released and are possibly not located in the core. From a theoretical point of view, this migration should happen during the droplet drying process. Bi-layered droplets are emitted from the cone-jet and due to their small dimensions the solvent forthwith evaporates. Once in the solid state, it is impossible that the API has enough mobility to migrate. Hence, the migration should take place during the small time frame of evaporation and it is then logical that the amount of migration is influenced by the solution composition like the solvent, polymer type and concentration.

Contrary, solely migration is probably not enough to describe all our observations, especially when looking at the lovastatin and atenolol system (chapter 6). For lovastatin, hardly any release was seen in the acidic medium, but for atenolol, after a first burst release, a gradual increase in the release was seen over time (unlike for darunavir) and this is an indication that it takes time for part of the atenolol molecules to diffuse through the particle. The discrepancy in burst release between lovastatin and

atenolol was related to their solubility by comparison with another poorly soluble (fenofibrate) and highly soluble (paracetamol) API. Probably due to atenolol's high solubility, it can permeate more easily through the coating layer. The permeability as such can be explained from a mechanistic point of view regarding the coating formation. When a tablet is coated in a traditional way, either by dip coating or pan coating as displayed in Fig 1.11B (Introduction) high polymer concentrations are used which leads to a dense network of polymer entanglement and a real coating film. During electrospraying, rather low polymer concentrations are used because the process will otherwise generate fibres. Hence, the applied concentrations are only around the critical overlap concentration, which probably creates a less dense coating film and consequently allows permeation of highly soluble compounds.

All things considered, it would thus be of high interest to track the API molecules in the core-shell particles as this information is essential for further research and to elucidate the remaining research questions. It would be useful to study a fluorescent API, for example by coupling a fluorescent dye to darunavir so the API itself can be visualised with confocal imaging and concurrently the drug release can be followed. Still, it must be noted that the fluorescent derivatisation will change the physicochemical characteristics of the API. Ideally the chemical composition of a cross section of the particles would be mapped. Due to the small dimensions of the particles it is not possible to manually prepare a cross-section. An option would be to embed the particles in a substance like epoxy-resins and subsequently cut slices of the resin. The obtained cross sections can then be analysed via electron microscopy coupled to an energy dispersive X-ray spectroscopy (EDX) detector that can provide information on the chemical composition. By analysing the X-ray photons emitted from the sample under influence of the electron beam, 'coloured' SEM images, in which each colour represents a different element, can be obtained. Via this method for example, the distribution of cisplatin in PLGA coated particles could be visualised[238]. Hence EDX was explored for the core-shell darunavir particles, but the analysis depth was probably too high to get any useful results.

To avoid this problem, X-ray photoelectron spectroscopy (XPS) was tested to investigate whether darunavir is located at the surface of the particles. XPS is based on the irradiation of the sample with X-rays, which will lead to the emission of photoelectrons just from the upper layer of the surface (around 10 nm in depth)[158,196]. By detection of the number and kinetic energy of these emitted electrons, the atomic composition of the surface can be determined. Darunavir has several nitrogen atoms and one sulphur atom that can be used for its detection, because the polymers (HPMC and P(MAA/MMA)) do not consist out of these two atoms. Unfortunately, the small amount of these characteristic atoms in darunavir formed a limitation. The surface contained an extremely small amount of nitrogen and sulphur, but the variation was too high to draw any conclusions. To facilitate the analysis, it could be useful to select a model API which is composed for a larger part out of characteristic atoms.

Despite the fact that XPS can possibly give an idea if any API is present in the upper layers of the surface, it will not give any more knowledge on the distribution of the API throughout the entire core-

shell particle. Another method that could be useful for the characterization of the composition is time of flight secondary ion mass spectrometry (ToF-SIMS)[239-241]. During ToF-SIMS, the sample is irradiated with an ion beam resulting in the desorption of *inter alia* ionised molecular fragments from the upper surface. The ionised fragments of same polarity will all be accelerated to the same kinetic energy and the velocity of the fragments will thus be related to their mass-to-charge ratio. Consequently, the fragments can be separated based on the time it takes to reach the detector and a mass spectrum for a specific region of the particle surface can be created. Furthermore, by sputtering the surface with C_{60}^+ ions, the first layers of the surface can be removed and the underlying layer can again be analysed to obtain a depth profile.

Besides the measurement of the API release during the dissolution test, it could also be interesting to follow the release of the polymers, e.g. PVP and P(MAA/MMA) during the acidic stage in order to further clarify the origin of the burst release. Measuring the PVP concentration can for instance be done via a photometric method via complexation with iodine[91]. Otherwise, the concentration of the released polymers can be quantified by HPLC-size exclusion chromatography[242,243].

7.4.3. Morphology

The control of the morphology is another challenge that should be considered for further research. Despite several actions, spherical core-shell particles with darunavir were never obtained. Intuitively it was thought that a spherical particle would be easier to coat homogenously, leading to more reproducible release results, while the wrinkles in the obtained particles would give rise to imperfections or cracks in the coating layer. As explained in the introduction, the transition of the droplets emitted by the cone-jet to a solid particle is governed by solvent evaporation and influenced by the electric field. A possible reason for the non-spherical and dimpled morphology can be found in the applied polymer concentration and the concept of the Peclet number (Pe). As reported before, when working at low polymer concentrations, insufficient chain entanglements can be formed to withstand the electric stress, which results in irregular morphologies[72,104,213]. Also, in a study on coaxial electrospraying with PLGA in the core and poly(D,L-lactic acid) in the shell, an improvement in sphericity was seen with increasing polymer concentration[156]. In this thesis, improving the morphology by increasing the polymer concentration was predominantly limited by clogging of the nozzle or fibre formation. On the other hand, solvents with a rather low boiling point were used, which most likely means that Pe is larger than 1, yielding collapsed particles as described in Fig 1.7 (Introduction). Using a solvent with lower volatility resulted in incomplete evaporation and hence particles that were not complete solidified when reaching the collector, a problem that was also encountered by Jafari-Nodoushan *et al.*[200] .

The anticipated need for sphericity however, was disproved because the best performing particles had a dimpled morphology and reproducibility of the drug release was confirmed. Notwithstanding, increasing the polymer concentration of the shell layer undoubtfully improved the enteric performance, most likely through an increase of the coating thickness and it would thus be beneficial from this point of view to be able to use higher concentrations without the current problem of clogging

or fibre formation. Since as good as all types of commercially available enteric polymers were tested and all encountered the problem, it would be interesting for further research to adapt the properties of the polymers in order to avoid clogging or fibre formation. Among others, the polymers should be soluble at high concentration in an organic solvent with low volatility, resulting in a solution with rather low viscosity.

Another concern which was not touched upon in the experimental parts is the particle size distribution of the created particles. In some cases, it can be seen on the SEM images that small off-spring particles were present. Despite the fact that they only count for a small percentage of the total volume, it is difficult to predict whether they are also coated particles or that they possibly are enriched with darunavir or a specific polymer, which could give rise to discrepancies in the drug release. The use of a corona neutralizer is reported in literature in order to narrow the particle size distribution and prevent the creation of small off-spring particles[122,196]. Therefore, a steel needle or ring which is connected to a second high voltage generator, is added to the setup. When the highly charged droplets pass, they become discharged and this will prevent uncontrolled Coulomb fission during the rest of the evaporation process.

7.5. UPSCALING

For the experimental work in this thesis, a setup with only one nozzle was used. Due to the extreme low feed flow rate applied, the production rate is a major drawback and it would be indisputably impossible to be used as such in the pharmaceutical industry. Despite the fact that throughout the years a lot of progress has been made regarding the upscaling of the single nozzle electrospraying process, as also indicated in the general introduction of this thesis, the research on high throughput coaxial systems is rather limited.

Organising a series of standalone coaxial nozzles into a parallel array would not be a convenient solution. The inner and outer channel of every nozzle should than each be connected to a syringe pump. It would be more efficient if one pump can supply all inner channels and another one all outer channels via a construction of divergent tubes. However, care must be taken that every channel is supplied evenly and a constant feed flow is guaranteed. Even more challenging is the fact that the electric field of each nozzle is influenced by the field of the neighbouring nozzles. Yan *et al.* studied the electrostatic repulsion between two jets emitted from two neighbouring coaxial nozzles as well as the influence on the deposition pattern of the particles and on the morphology of the produced core-shell particles[244]. If the distance between the nozzles was less than 18 mm, the particle morphology and core shell structure became irregular as visualised with confocal microscopy. This means that around 3 emitters per cm^2 would be the maximal packing density. Olvera-Trejo and Velásquez-García designed a miniaturised nozzle setup via 3D-printing containing 25 emitters per cm^2 [140]. Instead of connecting the high voltage generator to the nozzle, an extractor plate was used instead, which contained holes concentric to each emitter. This way, every emitter is shielded from the electric field shadowing caused by the neighbouring ones.

Still, the design of a high throughput coaxial nozzle is not the only concern towards the scale-up of the process. Collecting the particles should also be automated in such a way that continuous manufacturing becomes possible. Ideally, the particles are removed via an air stream, this would moreover prevent damage to the particles due to the impact on reaching the collector. Otherwise a rotating collector system could allow continuous collection.

All in all, coaxial electrospraying is a redoubtable option to obtain coated ASD particles, despite all the remaining challenges for further research.

Chapter 8 Summary/Samenvatting

This thesis revolves around electrospraying as manufacturing method for amorphous solid dispersions (ASDs). Moreover, the production of coated ASD particles that can serve as a powder for reconstitution was studied, with the overall aim of understanding the fundamental principles governing the process, in order the facilitate the prediction and tuning of the API release from the individually coated particles.

The first chapter gives an overall introduction to provide a theoretical background regarding the consecutive experimental projects that constitute this thesis. To start, the increasing amount of poorly water soluble drug compounds and the impact towards the formulation of oral drug delivery systems are discussed. One of the strategies to address this poor solubility is the use of amorphous solid dispersions which forms together with its manufacturing methods and downstream processing, the topic of the second part of the introduction. The analytical methods to assess the solid state of these formulations are given as well. Subsequently, as this thesis revolves around electrospraying for ASD manufacturing, this method is highlighted and discussed in more detail. Not only the fundamentals of the technique and the process of particle formation are mentioned, but also the influence of the different process and formulation parameters as well as the advantages and limitations are touched upon. The introduction is concluded with a section on coaxial electrospraying and how it can produce coated ASD particles.

In the second chapter, the objectives of the four following experimental projects are described. A step-by-step approach was applied, starting with electrospraying in the single nozzle configuration and gradually increasing the complexity to eventually study the manufacturing of coated ASD particles via coaxial electrospraying.

Single nozzle electrospraying of polymers that can be used to formulate ASDs, was investigated in the third chapter. It was evaluated how a variety of polymer solutions behave during the electrospraying process and by gradually changing the process parameters, the limits of the cone-jet or working window were determined. This way, the influence and the interplay between both process and formulation parameters on the possibility to obtain a cone-jet mode was assessed. The polymer concentration and solvent used to prepare the solution had an important impact, however it was not possible to correlate it to the solution properties, namely the viscosity and conductivity. Nonetheless, it was seen that an increasing viscosity limited the process via clogging of the nozzle and an increasing conductivity limited the feed flow rate. A classification of the tested solvents could be made with isopropanol standing at the top and water and dichloromethane being poor candidates. Besides, it was concluded that the cone-jet mode can be more easily obtained at lower feed flow rates and higher tip-to-collector distances. These observations enabled *inter alia* a more rational selection of the parameters in the following projects and reduce the struggle to find the right settings to obtain the cone-jet mode.

In the fourth chapter, amorphous solid dispersions of darunavir were prepared by electrospraying and this method was compared to the golden standard, spray drying. Hydroxypropyl methylcellulose (HPMC), hydroxypropyl methylcellulose acetate succinate (HPMC AS) and polyvinylpyrrolidone K-30 (PVP) were first tested regarding there capability of generating supersaturation of darunavir, but no conclusive differences were obtained and consequently, they were all used to manufacture the ASDs. With all three polymers and both techniques, amorphous systems were obtained with similar levels of residual solvent. Generally, the particles had a dimpled morphology, except for the electrosprayed particles with PVP, which were more spherical. The particle size distribution of the electrosprayed particles was smaller with a slightly lower mean value but it still resulted in similar dissolution profiles for both manufacturing techniques. Via a design of experiments, the influence of four parameters on the characteristics of the electrosprayed ASDs with PVP was evaluated, which led to the following conclusions: increasing the feed flow rate generated larger particles which were more tailed; increasing the drug loading decreased the homogeneity of the ASDs and the residual solvent level; increasing the total solids content increased the homogeneity and less tailed particles were produced. Lastly, the tip-to-collector distance did not show to have a significant influence within the range tested and all parameter combinations led to amorphous systems. Hence, it could be overall concluded that electrospraying was as successful as spray drying to prepare these particular ASD formulations and finally, the characteristics of the particles can be tuned by adapting the parameters.

In order to prepare enteric coated ASD particles of darunavir in one single step, coaxial electrospraying was studied in the fifth chapter. The core of the particles consisted of DRV with either PVP or HPMC and a variety of enteric polymers was tested for the shell. Nevertheless, only the particles coated with the copolymer poly(methacrylic acid-co-methyl methacrylate) in monomer ratio 1/2 (Eudragit® S100), complied with the guidelines of the European Pharmacopoeia regarding enteric formulations, stating that maximum 10 % of the API can be released after two hours in acidic medium. By adding dyes to the core and shell solution, the particles were analysed with confocal microscopy and this revealed their core-shell structured nature. This observation was supported with the results obtained by modulated differential scanning calorimetry, demonstrating that the core and shell polymers were not mixed. Still, no matter the type of coating polymer used, a burst release in acidic medium was observed, which means that the maximal concentration was measured at the first time point of dissolution and this concentration barely increased during the following two hours. Depending on the type of polymer and solvent used, the extent of the burst release was different. Similarly, it was seen that the monomer ratio of methacrylic acid to methyl methacrylate in the copolymer was a determining factor. Most likely, a certain amount of darunavir migrates during the evaporation process to the shell layer, becoming readily available for dissolution at the surface of the particle.

In the sixth chapter, a fixed dose combination of atenolol, lovastatin and acetylsalicylic acid for cardiovascular treatment, in the form of an easy-to-swallow powder consisting of individual coated particles, was manufactured via coaxial electrospraying. The core was made up of an ASD of Soluplus® and lovastatin, in order to overcome the poor solubility of the latter, and atenolol. To avoid lovastatin degradation by the acidic medium and CYP 3A4 enzymes in the proximal part of the small intestines,

Eudragit® S100 was chosen as coating polymer and acetylsalicylic acid was added to this shell layer. First, uncoated ASDs were prepared with single nozzle electrospraying. Dissolution experiments showed that a fast and complete release of both atenolol and lovastatin could be obtained. Consequently, coated particles were prepared via coaxial electrospraying. Regarding lovastatin, an adequate gastro-resistant profile was obtained, indicating that hardly any of the API was released in acidic conditions and high supersaturation levels were reached quickly after the switch to a neutral pH. In contrast, a significant amount of atenolol was already released in the acidic conditions. Similar behaviour was seen for particles with another poorly soluble API, fenofibrate, and paracetamol, another soluble API. Probably, the coating formed during the electrospraying process is not dense enough as compared to a coating made during film coating of a tablet, allowing the highly soluble atenolol to diffuse through the coating layer. These results point to the applicability of coaxial electrospraying in manufacturing powders for reconstitution including fixed dose combinations, however further research will be necessary to optimize the release behaviour of the different compounds.

In the final chapter, a general discussion combining the results and conclusions of the four experimental chapters is given. The connection between the consecutive projects is highlighted and a flowchart is presented that depicts the rationale behind the selection of the process and formulation parameters applied throughout the different projects. Finally, the challenges with respect to the burst release in coaxial electrospraying and upscaling of the process are discussed.

Samenvatting

Deze thesis staat in het teken van electrosprayen als productietechniek voor het maken van amorfe vaste dispersies (AVD). Meer bepaald werd het maken van gecoate AVD-partikels die kunnen dienen als poeders voor reconstitutie bestudeerd. Het overkoepelende doel bestond erin om de fundamentele principes die het proces bepalen te begrijpen opdat de vrijstelling van het geneesmiddel vanuit de individueel gecoate deeltjes beter voorspeld en geoptimaliseerd zou kunnen worden.

Het eerste hoofdstuk bestaat uit een algemene introductie en geeft een theoretische achtergrond aangaande de verschillende experimentele projecten waaruit deze thesis is opgebouwd. Om te beginnen wordt het stijgende aandeel van geneesmiddelen die slecht oplossen in water en de impact hiervan op de formulatie van orale toedieningsvormen beschreven. Een mogelijke optie om met de slechte oplosbaarheid om te gaan is het gebruik van AVDs. Samen met de mogelijke productietechnieken en verdere verwerkingsprocedures, vormen AVDs het onderwerp van het tweede deel van de introductie. De analytische methoden om de vaste toestand van deze formulaties te beoordelen, worden eveneens behandeld. Aangezien deze thesis draait rond electrosprayen, wordt deze methode vervolgens in meer detail besproken. Niet alleen worden de basisprincipes van electrosprayen en de het proces van partikelvorming vermeld, maar ook de voordelen, beperkingen en invloed van de verschillende proces en formulatie gerelateerde parameters worden aangehaald. Tenslotte wordt de introductie afgesloten met het beschrijven van coaxiaal electrosprayen en hoe er gecoate AVD-deeltjes mee kunnen gemaakt worden.

In het tweede hoofdstuk worden de objectieven van de vier experimentele projecten uiteengezet. Een stapsgewijze aanpak werd toegepast die startte met electrosprayen in een single nozzle setup en waarbij gradueel de complexiteit werd verhoogd om uiteindelijk het maken van gecoate AVD-partikels met coaxiaal electrosprayen te kunnen bestuderen.

Single nozzle electrosprayen van polymeren die gebruikt worden voor het maken van AVDs, werd in het derde hoofdstuk onderzocht. Er werd nagegaan hoe een breed gamma van polymeeroplossingen geëlectrosprayd kan worden en door gradueel de proces parameters te veranderen, werden de limieten voor het bekomen van een cone-jet mode bepaald. Op deze manier werd de invloed en wisselwerking tussen zowel de proces als formulatie gerelateerde parameters op de mogelijkheid om een cone-jet mode te bekomen, in kaart gebracht. De polymeerconcentratie en het gebruikte solvent hadden een belangrijke impact, maar het was niet mogelijk om dit te correleren aan de eigenschappen van de oplossingen zoals de viscositeit of conductiviteit. Desondanks was het wel duidelijk dat een stijgende viscositeit een limiterende factor was omdat het tot verstopping van de nozzle leidde en de conductiviteit limiteerde de stroomsnelheid. Een classificatie van de geteste solventen kon gemaakt worden waarbij isopropanol aan de top stond en water en dichloormethaan het slechtst presteerden. Daarnaast kon er geconcludeerd worden dat een cone-jet mode makkelijker kan bereikt worden via een lage stroomsnelheid en hogere afstand tussen de tip van de nozzle en de collector. Deze

observaties maakten het mogelijk om onder meer een rationele selectie van de parameters voor de volgende projecten te maken en werd het minder moeilijk om de optimale instellingen voor het bekomen van een cone-jet mode te vinden.

In het vierde hoofdstuk werden AVDs van darunavir gemaakt via electrosprayen en deze methode werd vergeleken met de gouden standaard, sproeidrogen. Er werd getest of met de polymeren hydroxypropyl methylcellulose (HPMC), hydroxypropyl methylcellulose acetaat succinaat (HPMC AS) of polyvinylpyrrolidone K-30 (PVP) supersaturatie van darunavir kon worden bekomen, maar omdat er geen duidelijk verschil was tussen de drie polymeren, werden ze allemaal gebruikt om AVDs te maken. Met de drie polymeren en beide technieken werden amorfe systemen bekomen die een gelijkaardige hoeveelheid residueel solvent bevatten. Over het algemeen vertoonden de deeltjes een ingedeukte morfologie, met uitzondering van de geëlectrosprayde PVP-deeltjes die meer sferisch waren. De deeltjesgrootteverdeling bij electrosprayen was nauwer met een lichtjes kleinere gemiddelde diameter maar dit resulteerde desondanks in gelijkaardige dissolutieprofielen voor beide productietechnieken. Via een *design of experiments* werd de invloed van vier parameters op de eigenschappen van de geëlectrosprayde AVDs met PVP nagegaan en dit leidde tot de volgende conclusies: een stijgende stroomsnelheid genereerde grotere deeltjes die meer staartvorming vertoonden; een stijgende geneesmiddelbelading deed de homogeniteit en de hoeveelheid aan residueel solvent afnemen; een stijging van de totale concentratie aan vaste stoffen in de oplossing kwam de homogeniteit dan weer ten goede en deed staartvorming verminderen. Tot slot bleek de afstand tussen de nozzle en collector geen invloed te hebben binnen de geteste limieten en alle parametercombinaties leidden tot amorfe systemen. Het kon dus besloten worden dat electrosprayen even succesvol was als sproeidrogen voor het produceren van deze specifieke AVD formulaties en dat de eigenschappen van de partikels kunnen bepaald worden via aanpassing van de parameters.

Om enterisch gecoate AVDs deeltjes met darunavir te maken in één stap, werd coaxiaal electrosprayen bestudeerd in het vijfde hoofdstuk. De kern van de deeltjes bestond uit darunavir met PVP of HPMC en een variëteit aan enterische polymeren werd getest voor de buitenste laag. Enkel de deeltjes omhuld met het copolymeer poly(methacrylic zuur-co-methyl methacrylaat) in een monomeer ratio 1/2 (Eudragit® S100) voldeden aan de eisen van de Europese Farmacopee omtrent gastro-resistente formulaties, die voorschrijft dat maximum 10 % van het geneesmiddel mag vrijkomen na twee uur in zuur milieu. Na toevoeging van fluorescente merkers aan de kern en coating oplossing werd de *core-shell* structuur van partikels gevisualiseerd met confocale microscopie. Deze bevindingen werden ondersteund door de resultaten bekomen met gemoduleerde differentiële scanning calorimetrie die aantoonden dat de kern en coating polymeren niet gemengd waren. Niettemin werd bij het gebruik van alle coating polymeren een *burst release* in zuur milieu waargenomen. De maximale concentratie werd al gemeten bij het eerste tijdspunt van de dissolutietest en deze concentratie veranderde amper gedurende de rest van de twee uur. Afhankelijk van het gebruikte coatingpolymeer en solvent was de hoeveelheid van deze *burst release* wel anders. Zo werd er onder meer waargenomen dat de monomeerratio van methacrylzuur tot methyl methacrylaat in het copolymeer een bepalende factor was. Hoogstwaarschijnlijk migreert er een

bepaald deel van de darunavir moleculen tijdens het evaporatie proces naar de coating en op deze manier is het op het oppervlak van de deeltjes rechtstreeks beschikbaar voor dissolutie.

In het zesde deel werd via coaxiaal electrosprayen een vaste dosis combinatie gemaakt met atenolol, lovastatine en acetylsalicyl zuur voor de behandeling van cardiovasculaire aandoeningen en dit onder vorm van een poeder voor reconstitutie bestaande uit individueel gecoate deeltjes. De kern bestond uit een AVD van Soluplus® en lovastatine om de oplosbaarheid van dit laatste geneesmiddel te verbeteren, te samen met atenolol. Om afbraak van lovastatine in zuur midden en door CYP 3A4 in het proximale deel van de dunne darm tegen te gaan, werd Eudragit® S100 als coatingpolymeer gebruikt en acetylsalicyl zuur werd ook aan deze coatinglaag toegevoegd. Om te beginnen werden AVDs gemaakt via single nozzle electrosprayen. Dissolutie experimenten toonden aan dat een snelle en volledige vrijstelling werd bekomen voor zowel atenolol als lovastatine. Vervolgens werden gecoate deeltjes gemaakt via coaxiaal electrosprayen. Voor lovastatine werd een adequaat gastro-resistent profiel bekomen met nagenoeg geen vrijstelling van het geneesmiddel in zuur milieu en een hoge graad van supersaturatie bij de verandering naar een neutrale pH. In tegenstelling werd er wel een significante hoeveel atenolol vrijgesteld in het zure milieu. Gelijkaardige bevindingen waren gemaakt voor een ander slecht oplosbaar geneesmiddel, fenofibraat en een ander oplosbaar product, paracetamol. Waarschijnlijk is de coating die gevormd wordt met electrosprayen niet compact genoeg in vergelijking met een coating bij het film coaten van tabletten en dit zou als gevolg kunnen hebben dat de goed oplosbare atenolol moleculen door de coating kunnen diffunderen. De resultaten tonen de mogelijkheid aan om coaxiaal electrosprayen te gebruiken om vaste dosis combinaties te maken in de vorm van een poeder voor reconstitutie, maar meer onderzoek zal nodig zijn om de vrijstelling van de verschillende componenten te kunnen controleren.

Het laatste hoofdstuk omvat een algemene discussie waarin de resultaten en conclusies van de vier experimentele hoofdstukken worden gecombineerd. De samenhang tussen de opeenvolgende projecten wordt aangetoond en er wordt een stroomschema gegeven dat de rationele selectie van de proces- en formulatieparameters zoals toegepast in de verschillende onderdelen, verklaart. Tot slot worden de uitdagingen aangaande de *burst release* bij coaxiaal electrosprayen en de opschaling van het proces besproken.

References

1. DiMasi JA, Grabowski HG, Hansen RW. Innovation in the pharmaceutical industry: New estimates of R&D costs. J Health Econ. 2016;47:20-33.
2. Stewart KD, Johnston JA, Matza LS, et al. Preference for pharmaceutical formulation and treatment process attributes. Patient Prefer Adherence. 2016;10:1385-1399.
3. Boyd BJ, Bergström CAS, Vinarov Z, et al. Successful oral delivery of poorly water-soluble drugs both depends on the intraluminal behavior of drugs and of appropriate advanced drug delivery systems. Eur J Pharm Sci. 2019;137:104967.
4. Khojasteh S, Wong H, Hop C. Oral absorption. Drug Metabolism and Pharmacokinetics Quick Guide. New York: Springer; 2011.
5. Khojasteh S, Wong H, Hop C. Transporters. Drug Metabolism and Pharmacokinetics Quick Guide. New York: Springer; 2011.
6. Lipinski CA, Lombardo F, Dominy BW, Feeney PJ. Experimental and computational approaches to estimate solubility and permeability in drug discovery and development settings. Adv Drug Deliv Rev. 2001;46(1-3):3-26.
7. Lipinski CA. Lead- and drug-like compounds: the rule-of-five revolution. Drug Discov Today Technol. 2004;1(4):337-341.
8. Bergström CAS, Charman WN, Porter CJH. Computational prediction of formulation strategies for beyond-rule-of-5 compounds. Adv Drug Deliv Rev. 2016;101:6-21.
9. Walters WP, Green J, Weiss JR, Murcko MA. What do medicinal chemists actually make? A 50-year retrospective. J Med Chem. 2011;54(19):6405-6416.
10. Amidon GL, Lennernäs H, Shah VP, Crison JR. A theoretical basis for a biopharmaceutic drug classification: the correlation of in vitro drug product dissolution and in vivo bioavailability. Pharm Res. 1995;12(3):413-420.
11. Multisource (Generic) Pharmaceutical Products: Guidelines on Registration Requirements to Establish Interchangeability. WHO Technical Report Series, No. 1003, 2017, Annex 6. Available from http://apps.who.int/medicinedocs/en/m/abstract/Js23245en/.
12. Takagi T, Ramachandran C, Bermejo M, Yamashita S, Yu LX, Amidon GL. A provisional biopharmaceutical classification of the top 200 oral drug products in the United States, Great Britain, Spain, and Japan. Mol Pharm. 2006;3(6):631-643.
13. Taylor LS, Zhang GGZ. Physical chemistry of supersaturated solutions and implications for oral absorption. Adv Drug Deliv Rev. 2016;101:122-142.
14. Williams HD, Trevaskis NL, Charman SA, et al. Strategies to address low drug solubility in discovery and development. Pharmacol Rev. 2013;65(1):315-499.
15. Butler JM, Dressman JB. The developability classification system: application of biopharmaceutics concepts to formulation development. J Pharm Sci. 2010;99(12):4940-4954.
16. Dokoumetzidis A, Macheras P. A century of dissolution research: from Noyes and Whitney to the biopharmaceutics classification system. Int J Pharm. 2006;321(1-2):1-11.
17. Rosenberger J, Butler J, Muenster U, Dressman J. Application of a Refined Developability Classification System. J Pharm Sci. 2019;108(3):1090-1100.
18. Van den Mooter G. The use of amorphous solid dispersions: A formulation strategy to overcome poor solubility and dissolution rate. Drug Discov Today Technol. 2012;9(2):e71-e174.
19. Singh A, Van den Mooter G. Spray drying formulation of amorphous solid dispersions. Adv Drug Deliv Rev. 2016;100:27-50.

20. Lin X, Hu Y, Liu L, et al. Physical Stability of Amorphous Solid Dispersions: a Physicochemical Perspective with Thermodynamic, Kinetic and Environmental Aspects. Pharm Res. 2018;35(6):125.

21. Vasconcelos T, Marques S, das Neves J, Sarmento B. Amorphous solid dispersions: Rational selection of a manufacturing process. Adv Drug Deliv Rev. 2016;100:85-101.

22. Van Duong T, Van den Mooter G. The role of the carrier in the formulation of pharmaceutical solid dispersions. Part II: amorphous carriers. Expert Opin Drug Deliv. 2016;13(12):1681-1694.

23. Janssens S, Van den Mooter G. Review: physical chemistry of solid dispersions. J Pharm Pharmacol. 2009;61(12):1571-1586.

24. Hancock BC, Shamblin SL, Zografi G. Molecular mobility of amorphous pharmaceutical solids below their glass transition temperatures. Pharm Res. 1995;12(6):799-806.

25. Kissi EO, Grohganz H, Löbmann K, Ruggiero MT, Zeitler JA, Rades T. Glass-Transition Temperature of the β-Relaxation as the Major Predictive Parameter for Recrystallization of Neat Amorphous Drugs. J Phys Chem B. 2018;122(10):2803-2808.

26. Mehta M, Ragoonanan V, McKenna GB, Suryanarayanan R. Correlation between Molecular Mobility and Physical Stability in Pharmaceutical Glasses. Mol Pharm. 2016;13(4):1267-1277.

27. Vaka SRK, Bommana MM, Desai Di, Djordjevic J, Phuapradit W, Shah N. Excipients for Amorphous Solid Dispersions. In: Shah N, Sandhu H, Choi DS, Chokshi H, Malick AW. Amorphous Solid Dispersions: Theory and Practice: Springer; 2014.

28. Huang S, Williams RO. Effects of the Preparation Process on the Properties of Amorphous Solid Dispersions. AAPS PharmSciTech. 2017.

29. Dedroog S, Huygens C, Van den Mooter G. Chemically identical but physically different: A comparison of spray drying, hot melt extrusion and cryo-milling for the formulation of high drug loaded amorphous solid dispersions of naproxen. Eur J Pharm Biopharm. 2019;135:1-12.

30. Tian Y, Caron V, Jones DS, Healy AM, Andrews GP. Using Flory-Huggins phase diagrams as a pre-formulation tool for the production of amorphous solid dispersions: a comparison between hot-melt extrusion and spray drying. J Pharm Pharmacol. 2014;66(2):256-274.

31. Paudel A, Meeus J, Van den Mooter G. Structural Characterization of Amorphous Solid Dispersions. In: Shah N, Sandhu H, Choi DS, Chokshi H, Malick AW. Amorphous Solid Dispersions: Theory and Practice: Springer; 2014.

32. Liu X, Feng X, Williams R, Zhang F. Characterization of amorphous solid dispersions. Journal of Pharmaceutical Investigation. 2017;48(1):19-41.

33. Vogt F. solid-state characterization of amorphous solid dispersions. In: Newman A. pharmaceutical amorphous solid dispersions: Wiley; 2015.

34. Baird JA, Taylor LS. Evaluation of amorphous solid dispersion properties using thermal analysis techniques. Adv Drug Deliv Rev. 2012;64(5):396-421.

35. Reading M, Craig D, Murphy J, Kett V. Modulated temperature differential scanning calorimetry. In: Craig C, Reading M. Thermal analysis of pharmaceuticals: CRC press; 2007.

36. Sandhu H, Shah N, Chokshi H, Malick A. Overview of Amorphous Solid Dispersion Technologies In: Shah N, Sandhu H, Choi DS, Chokshi H, Malick AW. Amorphous Solid Dispersions: Theory and Practice: Springer; 2014.

37. Haser A, Zhang F. New Strategies for Improving the Development and Performance of Amorphous Solid Dispersions. AAPS PharmSciTech. 2018;19(3):978-990.

38. Paudel A, Worku ZA, Meeus J, Guns S, Van den Mooter G. Manufacturing of solid dispersions of poorly water soluble drugs by spray drying: formulation and process considerations. Int J Pharm. 2013;453(1):253-284.

39. Sosnik A, Seremeta KP. Advantages and challenges of the spray-drying technology for the production of pure drug particles and drug-loaded polymeric carriers. Adv Colloid Interface Sci. 2015;223:40-54.

40. Dereymaker A, Van Den Mooter G. The peculiar behavior of the glass transition temperature of amorphous drug-polymer films coated on inert sugar spheres. J Pharm Sci. 2015;104(5):1759-1766.
41. Pas T, Vergauwen B, Van den Mooter G. Exploring the feasibility of the use of biopolymers as a carrier in the formulation of amorphous solid dispersions - Part I: Gelatin. Int J Pharm. 2018;535(1-2):47-58.
42. https://www.particlesciences.com/news/technical-briefs/2011/hot-melt-extrusion.html. Accessed at 19/09/2019.
43. Patil H, Tiwari RV, Repka MA. Hot-Melt Extrusion: from Theory to Application in Pharmaceutical Formulation. AAPS PharmSciTech. 2016;17(1):20-42.
44. Bertoni S, Albertini B, Ferraro L, Beggiato S, Dalpiaz A, Passerini N. Exploring the use of spray congealing to produce solid dispersions with enhanced indomethacin bioavailability: In vitro characterization and in vivo study. Eur J Pharm Biopharm. 2019;139:132-141.
45. Kang N, Lee J, Choi JN, Mao C, Lee EH. Cryomilling-induced solid dispersion of poor glass forming/poorly water-soluble mefenamic acid with polyvinylpyrrolidone K12. Drug Dev Ind Pharm. 2015;41(6):978-988.
46. Boldyrev VV, Shakhtshneider TP, Burleva LP, Severtsev VA. Preparation of the Disperse Systems of Sulfathiazole-Polyvinylpyhrolidone by Mechanical Activation. Drug Development and Industrial Pharmacy. 2008;20(6):1103-1114.
47. Zhang J, Han R, Chen W, et al. Analysis of the Literature and Patents on Solid Dispersions from 1980 to 2015. Molecules. 2018;23(7).
48. Démuth B, Nagy ZK, Balogh A, et al. Downstream processing of polymer-based amorphous solid dispersions to generate tablet formulations. Int J Pharm. 2015;486(1-2):268-286.
49. Page S, Maurer R. Downstream processing considerations. In: Shah N, Sandhu H, Choi DS, Chokshi H, Malick AW. Amorphous Solid Dispersions: Theory and Practice: Springer; 2014.
50. Felton LA, Porter SC. An update on pharmaceutical film coating for drug delivery. Expert Opin Drug Deliv. 2013;10(4):421-435.
51. Sauer D, Cerea M, DiNunzio J, McGinity J. Dry powder coating of pharmaceuticals: a review. Int J Pharm. 2013;457(2):488-502.
52. Thakral S, Thakral NK, Majumdar DK. Eudragit: a technology evaluation. Expert Opin Drug Deliv. 2013;10(1):131-149.
53. Brögmann B, Beckert T. Enteric Targeting Through Enteric Coating. In: Schreier H. Drug Targeting Technology: Physical Chemical Biological Methods. 1 ed: CRC Press; 2001.
54. Maderuelo C, Lanao JM, Zarzuelo A. Enteric coating of oral solid dosage forms as a tool to improve drug bioavailability. Eur J Pharm Sci. 2019;138:105019.
55. Miller D, McGinity J. Aqueous Polymeric Film Coating. In: Augsburger L, Hoag S. Pharmaceutical Dosage Forms - Tablets: Unit Operations and Mechanical Properties: CRC press; 2008.
56. Lau ETL, Steadman KJ, Cichero JAY, Nissen LM. Dosage form modification and oral drug delivery in older people. Advanced Drug Delivery Reviews. 2018;135:75-84.
57. Paparella S. Identified safety risks with splitting and crushing oral medications. J Emerg Nurs. 2010;36(2):156-158.
58. Zhang L, Huang J, Si T, Xu RX. Coaxial electrospray of microparticles and nanoparticles for biomedical applications. Expert Rev Med Devices. 2012;9(6):595-612.
59. Xie J, Jiang J, Davoodi P, Srinivasan M, Wang C. Electrohydrodynamic atomization: A two-decade effort to produce and process micro-/nanoparticulate materials. Chemical Engineering Science. 2015;125:32-57.
60. Taylor G. Disintegration of water drops in an electric field. proceedings of the royal society A. 1964;280(1382):383-397.
61. Taylor G. The force exerted by an electric field on a long cylindrical conductor. Proceedings of the royal society A. 1966;291(1425):145-158.

62. Qi S, Craig D. Recent developments in micro-and nanofabrication techniques for the preparation of amorphous pharmaceutical dosage forms. Advanced Drug Delivery Reviews. 2016;100:67-84.
63. Yurteri C, Hartman R, Marijnissen J. Producing Pharmaceutical Particles via Electrospraying with an Emphasis on Nano and Nano Structured Particles - A Review. Kona Powder and Particle Journal. 2010(28):91-115.
64. Nguyen DN, Clasen C, Van den Mooter G. Pharmaceutical Applications of Electrospraying. J Pharm Sci. 2016.
65. Smeets A, Clasen C, Van den Mooter G. Electrospraying of polymer solutions: Study of formulation and process parameters. Eur J Pharm Biopharm. 2017;119:114-124.
66. Bodnár E, Grifolla J, Rosell-Llomparta J. Polymer solution electrospraying: A tool for engineering particles and films with controlled morphology. Journal of Aerosol Science. 2018;125:93-118.
67. Gupta P, Elkins C, Long T, Wilkes G. Electrospinning of linear homopolymers of poly(methyl methacrylate): exploring relationships between fiber formation, viscosity, molecular weight and concentration in a good solvent. Polymer. 2005;46(13):4799-4810.
68. Shenoy S, Bates W, Frisch H, Wnek G. Role of chain entanglements on fiber formation during electrospinning of polymer solutions: good solvent, non-specific polymer-polymer interaction limit. Polymer. 2005;46(10):3372-3384.
69. Verreck G, Chun I, Peeters J, Rosenblatt J, Brewster ME. Preparation and characterization of nanofibers containing amorphous drug dispersions generated by electrostatic spinning. Pharm Res. 2003;20(5):810-817.
70. Vehring R. Pharmaceutical particle engineering via spray drying. Pharm Res. 2008;25(5):999-1022.
71. Bohr A, Boetker JP, Rades T, Rantanen J, Yang M. Application of spray-drying and electrospraying/electospinning for poorly water-soluble drugs: a particle engineering approach. Curr Pharm Des. 2014;20(3):325-348.
72. Almería B, Deng W, Fahmy TM, Gomez A. Controlling the morphology of electrospray-generated PLGA microparticles for drug delivery. J Colloid Interface Sci. 2010;343(1):125-133.
73. Bock N, Dargaville T, Woodruff M. Electrospraying of polymers with therapeutic molecules: State of the art. Progress in Polymer Science. 2012;37(11):1510-1551.
74. Alehosseini A, Ghorani B, Sarabi-Jamab M, Tucker N. Principles of electrospraying: A new approach in protection of bioactive compounds in foods. Crit Rev Food Sci Nutr. 2018;58(14):2346-2363.
75. Sosnik A. Production of drug-loaded polymeric nanoparticles by electrospraying technology. J Biomed Nanotechnol. 2014;10(9):2200-2217.
76. Chakraborty S, Liao IC, Adler A, Leong KW. Electrohydrodynamics: A facile technique to fabricate drug delivery systems. Adv Drug Deliv Rev. 2009;61(12):1043-1054.
77. Tsai S, Ting Y. Synthesize of alginate/chitosan bilayer nanocarrier by CCD-RSM guided co-axial electrospray: A novel and versatile approach. Food Res Int. 2019;116:1163-1172.
78. Nguyen DN, Palangetic L, Clasen C, Van den Mooter G. One-step production of darunavir solid dispersion nanoparticles coated with enteric polymers using electrospraying. J Pharm Pharmacol. 2016;68(5):625-633.
79. Grafahrend D, Jungbecker D, Seide G, et al. Development and optimization of an electrospraying device for the continuous collection of nano- and microparticles. The Open Chemical and Biomedical Methods Journal. 2010;3:1-9.
80. Bocanegra R, Galána D, Márquez M, Loscertales IG, Barrero A. Multiple electrosprays emitted from an array of holes. journal of aerosol science. 2005.
81. https://nanocopoeia.com/ consulted at 30/07/2019.
82. http://nanocopoeia.com/wp-content/uploads/2017/01/CRS-2016_07_07-ENS-Poster-Final-crs.pdf consulted at 30/07/2019.

83. Pawar A, Thakkar S, Misra M. A bird's eye view of nanoparticles prepared by electrospraying: advancements in drug delivery field. J Control Release. 2018;286:179-200.
84. Shams T, Illangakoon UE, Parhizkar M, et al. Electrosprayed microparticles for intestinal delivery of prednisolone. J R Soc Interface. 2018;15(145).
85. Felton LA. Mechanisms of polymeric film formation. Int J Pharm. 2013;457(2):423-427.
86. Lin H, Dong Y, Markl D, et al. Measurement of the Intertablet Coating Uniformity of a Pharmaceutical Pan Coating Process With Combined Terahertz and Optical Coherence Tomography In-Line Sensing. J Pharm Sci. 2017;106(4):1075-1084.
87. Korasa K, Vrečer F. Overview of PAT process analysers applicable in monitoring of film coating unit operations for manufacturing of solid oral dosage forms. Eur J Pharm Sci. 2018;111:278-292.
88. Aslam M, Vaezi MF. Dysphagia in the elderly. Gastroenterol Hepatol (N Y). 2013;9(12):784-795.
89. Cilurzo F, Musazzi UM, Franzé S, Selmin F, Minghetti P. Orodispersible dosage forms: biopharmaceutical improvements and regulatory requirements. Drug Discov Today. 2018;23(2):251-259.
90. Augustijns P, Brewster ME. Supersaturating drug delivery systems: fast is not necessarily good enough. J Pharm Sci. 2012;101(1):7-9.
91. Everaerts M, Van den Mooter G. Complex amorphous solid dispersions based on poly(2-hydroxyethyl methacrylate): Study of drug release from a hydrophilic insoluble polymeric carrier in the presence and absence of a porosity increasing agent. Int J Pharm. 2019;566:77-88.
92. Amidon S, Brown JE, Dave VS. Colon-targeted oral drug delivery systems: design trends and approaches. AAPS PharmSciTech. 2015;16(4):731-741.
93. Nguyen DN, Van den Mooter G. The fate of ritonavir in the presence of darunavir. Int J Pharm. 2014;475(1-2):214-226.
94. Müller RH, Keck CM. Twenty years of drug nanocrystals: where are we, and where do we go? Eur J Pharm Biopharm. 2012;80(1):1-3.
95. Kawabata Y, Wada K, Nakatani M, Yamada S, Onoue S. Formulation design for poorly water-soluble drugs based on biopharmaceutics classification system: basic approaches and practical applications. Int J Pharm. 2011;420(1):1-10.
96. Patterson JE, James MB, Forster AH, Lancaster RW, Butler JM, Rades T. The influence of thermal and mechanical preparative techniques on the amorphous state of four poorly soluble compounds. J Pharm Sci. 2005;94(9):1998-2012.
97. Willart JF, Descamps M. Solid state amorphization of pharmaceuticals. Mol Pharm. 2008;5(6):905-920.
98. Yun Wu AD, L. James Lee and Barbara E. Wyslouzi. Electrospray Production of Nanoparticles for Drug/Nucleic Acid Delivery, The Delivery of Nanoparticles, Dr. Abbass A. Hashim (Ed.): InTech; 2012.
99. Fenn JB, Mann M, Meng CK, Wong SF, Whitehouse CM. Electrospray ionization for mass spectrometry of large biomolecules. Science. 1989;246(4926):64-71.
100. Malik SA, Ng WH, Bowen J, et al. Electrospray synthesis and properties of hierarchically structured PLGA TIPS microspheres for use as controlled release technologies. J Colloid Interface Sci. 2016;467:220-229.
101. Zarrabi A, Vossoughi M. electrospray: a novel fabrication method for biodegradable polymeric nanoparticles for further applications in drug delivery systems. Nanocon 2009, Conference Proceedings. 2009:324-331.
102. Jaworek A, Sobczyk A. Electrospraying route to nanotechnology: An overview. Journal of Electrostatics. 2008;66(3-4):197-219.
103. Tang K, Gomez A. Monodisperse electrosprays of low electric conductivity liquids in the cone-jet mode. Journal of Colloid and Interface Science. 1996;184(2):500-511.

104. Xie J, Wang C. Encapsulation of proteins in biodegradable polymeric microparticles using electrospray in the Taylor Cone-Jet mode. Biotechnology and Bioengineering. 2007;97(5):1278-1290.
105. Deng W, Klemic J, Li X, Reed M, Gomez A. Increase of electrospray throughput using multiplexed microfabricated sources for the scalable generation of monodisperse droplets. Journal of Aerosol Science. 2006;37(6):696-714.
106. Liu ZP, Cui L, Yu DG, Zhao ZX, Chen L. Electrosprayed core-shell solid dispersions of acyclovir fabricated using an epoxy-coated concentric spray head. Int J Nanomedicine. 2014;9:1967-1977.
107. Bohr A, Kristensen J, Stride E, Dyas M, Edirisinghe M. Preparation of microspheres containing low solubility drug compound by electrohydrodynamic spraying. Int J Pharm. 2011;412(1-2):59-67.
108. Bohr A, Kristensen J, Dyas M, Edirisinghe M, Stride E. Release profile and characteristics of electrosprayed particles for oral delivery of a practically insoluble drug. J R Soc Interface. 2012;9(75):2437-2449.
109. Yousaf AM, Mustapha O, Kim DW, et al. Novel electrosprayed nanospherules for enhanced aqueous solubility and oral bioavailability of poorly water-soluble fenofibrate. Int J Nanomedicine. 2016;11:213-221.
110. Roine J, Kaasalainen M, Peurla M, et al. Controlled Dissolution of Griseofulvin Solid Dispersions from Electrosprayed Enteric Polymer Micromatrix Particles: Physicochemical Characterization and in Vitro Evaluation. Mol Pharm. 2015;12(7):2254-2264.
111. Jain AK, Sood V, Bora M, Vasita R, Katti DS. Electrosprayed inulin microparticles for microbiota triggered targeting of colon. Carbohydr Polym. 2014;112:225-234.
112. Yu D, Williams, G. , Wang, X. , Yang, J. , Li, X. , Qian, W. and Li, Y. Polymer-based nanoparticulate solid dispersions prepared by a modified electrospraying process. *Journal of Biomedical Science and Engineering*. 2011;4, 741-749.
113. Li C, Yu DG, Williams GR, Wang ZH. Fast-dissolving core-shell composite microparticles of quercetin fabricated using a coaxial electrospray process. PLoS One. 2014;9(3):e92106.
114. Lee SY, Lee JJ, Park JH, et al. Electrosprayed nanocomposites based on hyaluronic acid derivative and Soluplus for tumor-targeted drug delivery. Colloids Surf B Biointerfaces. 2016;145:267-274.
115. Sakuma S, Matsumoto S, Ishizuka N, et al. Enhanced Boosting of Oral Absorption of Lopinavir Through Electrospray Coencapsulation with Ritonavir. J Pharm Sci. 2015;104(9):2977-2985.
116. Nath SD, Son S, Sadiasa A, Min YK, Lee BT. Preparation and characterization of PLGA microspheres by the electrospraying method for delivering simvastatin for bone regeneration. Int J Pharm. 2013;443(1-2):87-94.
117. Kawakami K. Miscibility analysis of particulate solid dispersions prepared by electrospray deposition. Int J Pharm. 2012;433(1-2):71-78.
118. Mohammadi G, Hemati V, Nikbakht M, et al. In vitro and in vivo evaluation of clarithromycin-urea solid dispersions prepared by solvent evaporation, electrospraying and freeze drying methods. Powder Technology. 2014;257:168-174.
119. Fung WY, Liong MT, Yuen KH. Preparation, in-vitro and in-vivo characterisation of CoQ10 microparticles: electrospraying-enhanced bioavailability. J Pharm Pharmacol. 2016;68(2):159-169.
120. Kawakami K, Zhang S, Chauhan RS, et al. Preparation of fenofibrate solid dispersion using electrospray deposition and improvement in oral absorption by instantaneous post-heating of the formulation. Int J Pharm. 2013;450(1-2):123-128.
121. Zhang S, Kawakami K, Yamamoto M, et al. Coaxial electrospray formulations for improving oral absorption of a poorly water-soluble drug. Mol Pharm. 2011;8(3):807-813.

122. Nystrom M, Murtomaa M, Salonen J. Fabrication and characterization of drug particles produced by electrospraying into reduced pressure. Journal of Electrostatics. 2010;68(1):42-48.
123. Nystrom M, Murtomaa M, Salonen J. Fabrication of amorphous pharmaceutical materials by electrospraying into reduced pressure. Journal of Electrostatics. 2011;69(4):351-356.
124. Jaworek A, Krupa A. Jet and drops formation in electrohydrodynamic spraying of liquids. A systematic approach. Experiments in Fluids. 1999;27(1):43-52.
125. Cloupeau M. Recipes for use of EHD spraying in cone-jet mode and notes on corona discharge effects. Journal of Aerosol Science. 1994;25(6):1143-1157.
126. Delamora J, Loscertales I. The current emitted by highly conducting Taylor cones. Journal of Fluid Mechanics. 1994;260:155-184.
127. Ganan-Calvo A, Davila J, Barrero A. Current and droplet size in the electrospraying of liquids. Scaling laws. Journal of Aerosol Science. 1997;28(2):249-275.
128. Hartman R, Brunner D, Camelot D, Marijnissen J, Scarlett B. Jet break-up in electrohydrodynamic atomization in the cone-jet mode. Journal of Aerosol Science. 2000;31(1):65-95.
129. Ciach T. Application of electro-hydro-dynamic atomization in drug delivery. Journal of Drug Delivery Science and Technology. 2007;17(6):367-375.
130. Marginean I, Kelly R, Page J, Tang K, Smith R. Electrospray characteristic curves: In pursuit of improved performance in the nanoflow regime. Analytical Chemistry. 2007;79(21):8030-8036.
131. Palangetic L, Reddy N, Srinivasan S, Cohen R, McKinley G, Clasen C. Dispersity and spinnability: Why highly polydisperse polymer solutions are desirable for electrospinning. Polymer. 2014;55(19):4920-4931.
132. Smith D. The electrohydrodynamic atomization of liquids. IEEE Trans. Ind. Appl. 1986;IA-22(3):527.
133. Cloupeau M, Prunetfoch B. Electrostatic spraying of liquids in cone-jet mode. Journal of Electrostatics. 1989;22(2):135-159.
134. Jaworek A. Micro- and nanoparticle production by electrospraying. Powder Technology. 2007;176(1):18-35.
135. Enayati M, Ahmad Z, Stride E, Edirisinghe M. Size mapping of electric field-assisted production of polycaprolactone particles. J R Soc Interface. 2010;7 Suppl 4:S393-402.
136. Rietveld IB, Kobayashi K, Yamada H, Matsushige K. Morphology control of poly(vinylidene fluoride) thin film made with electrospray. J Colloid Interface Sci. 2006;298(2):639-651.
137. Deitzel JM, Kleinmeyer JD, Hirvonen JK, Tan NCB. Controlled deposition of electrospun poly(ethylene oxide) fibers. Polymer. 2001;42(19):8163-8170.
138. Sahay R, Thavasi V, Ramakrishna S. Design Modifications in Electrospinning Setup for Advanced Applications. Journal of Nanomaterials. 2011.
139. Rutledge GC, Fridrikh SV. Formation of fibers by electrospinning. Advanced Drug Delivery Reviews. 2007;59(14):1384-1391.
140. Olvera-Trejo D, Velásquez-García LF. Additively manufactured MEMS multiplexed coaxial electrospray sources for high-throughput, uniform generation of core-shell microparticles. Lab Chip. 2016;16(21):4121-4132.
141. Paudel A, Van den Mooter G. Influence of solvent composition on the miscibility and physical stability of naproxen/PVP K 25 solid dispersions prepared by cosolvent spray-drying. Pharm Res. 2012;29(1):251-270.
142. Riekes MK, Engelen A, Appeltans B, Rombaut P, Stulzer HK, Van den Mooter G. New Perspectives for Fixed Dose Combinations of Poorly Water-Soluble Compounds: a Case Study with Ezetimibe and Lovastatin. Pharm Res. 2016;33(5):1259-1275.
143. Bohr A, Wan F, Kristensen J, et al. Pharmaceutical microparticle engineering with electrospraying: the role of mixed solvent systems in particle formation and characteristics. J Mater Sci Mater Med. 2015;26(2):61.

144. Craig DQ. The mechanisms of drug release from solid dispersions in water-soluble polymers. Int J Pharm. 2002;231(2):131-144.
145. Jansook P, Ogawa N, Loftsson T. Cyclodextrins: structure, physicochemical properties and pharmaceutical applications. Int J Pharm. 2018;535(1-2):272-284.
146. Friščić T, Jones W. Benefits of cocrystallisation in pharmaceutical materials science: an update. J Pharm Pharmacol. 2010;62(11):1547-1559.
147. Feeney OM, Crum MF, McEvoy CL, et al. 50years of oral lipid-based formulations: Provenance, progress and future perspectives. Adv Drug Deliv Rev. 2016;101:167-194.
148. Bukara K, Schueller L, Rosier J, et al. Ordered mesoporous silica to enhance the bioavailability of poorly water-soluble drugs: Proof of concept in man. Eur J Pharm Biopharm. 2016;108:220-225.
149. Junghanns JU, Müller RH. Nanocrystal technology, drug delivery and clinical applications. Int J Nanomedicine. 2008;3(3):295-309.
150. Van den Mooter G. Colon drug delivery. Expert Opin Drug Deliv. 2006;3(1):111-125.
151. Strickley RG, Iwata Q, Wu S, Dahl TC. Pediatric drugs--a review of commercially available oral formulations. J Pharm Sci. 2008;97(5):1731-1774.
152. Hao S, Wang B, Wang Y, Xu Y. Enteric-coated sustained-release nanoparticles by coaxial electrospray: preparation, characterization, and in vitro evaluation. Journal of Nanoparticle Research. 2014;16(1).
153. Ho HN, Laidmäe I, Kogermann K, et al. Development of electrosprayed artesunate-loaded core-shell nanoparticles. Drug Dev Ind Pharm. 2017;43(7):1134-1142.
154. European. Pharmacopoeia Edition 9.0. Volume I: 2.9.3 dissolution test for solid dosage forms.
155. Qianbiao Li YB, Hu Wang, Fanfan Du, Qing Li, Bangkun Jin and Ruke Bai. A facile and highly efficient strategy for esterification of poly(meth)acrylic acid with halogenated compounds at room temperature promoted by 1,1,3,3-tetramethylguanidine. Polymer Chemistry. 2013;4(9):2891-2897.
156. Xu Q, Qin H, Yin Z, Hua J, Pack DW, Wang CH. Coaxial electrohydrodynamic atomization process for production of polymeric composite microspheres. Chem Eng Sci. 2013;104.
157. Smallwood I. Handbook of organic solvent properties. London: Arnold, a member of the Hodder Headline Group; 1996.
158. Zamani M, Prabhakaran M, Thian E, Ramakrishna S. Protein encapsulated core-shell structured particles prepared by coaxial electrospraying: Investigation on material and processing variables. International Journal of Pharmaceutics. 2014;473(1-2):134-143.
159. Bekturov EA, Bimendina LA. Interpolymer complexes. Advances in polymer Science, speciality polymers. Vol 41. Springer, Berlin, Heidelberg 1981.
160. Iliopoulus I, Halary J, Audebert R. Polymer complexes stabilized through hydrogen bonds. Influence of 'structure defects' on complex formation: viscometry and fluorescence polarization measurements. European Polymer Journal. 1988;24(2):171-175.
161. Xie J, Lim K, Phua Y, Hua J, Wang C. Electrohydrodynamic atomization for biodegradable polymeric particle production. Journal of Colloid and Interface Science. 2006;302(103-112).
162. Park C, Lee J. Electrosprayed Polymer Particles: Effect of the Solvent Properties Journal of Applied Polymer Science. 2009;114:430-437.
163. Bock N, Woodruff M, Hutmacher D, Dargaville T. Electrospraying, a reproducible method for production of polymeric microspheres for biomedical applications. polymers. 2010;3:131-149.
164. Hwang Y, Jeong U, Cho E. Production of uniform-sized polymer core-shell microcapsules by coaxial electrospraying. Langmuir. 2008;24:2446-2451.
165. Skrdla P, Floyd P, Dell'Orco P. The amorphous state: first-principles derivation of the Gordon-Taylor equation for direct prediction of the glass transition temperature of mixtures; estimation of the crossover temperature of fragile glass formers; physical basis of the "Rule of 2/3". Physical Chemistry Chemical Physics. 2017;19(31):20523-20532.

166. Smeets A, Koekoekx R, Clasen C, Van den Mooter G. Amorphous solid dispersions of darunavir: Comparison between spray drying and electrospraying. Eur J Pharm Biopharm. 2018;130:96-107.
167. Cilurzo F, Minghetti P, Casiraghi A, Montanari L. Evaluation of Compatibility of Methacrylic Copolymers by Capillary Viscometry. Journal of Applied Polymer Science. 1999;76:1662–1668 (2000).
168. Hansen C. Hansen solubility parameters: a user's handbook: CRC Press; 2007, 2th edition.
169. Mark JE. Physical properties of polymers handbook: Springer; 2007, 2nd edition.
170. World Health Organization (WHO), 2017. www.who.int/en/news-room/fact-sheets/detail/cardiovascular-diseases-(cvds). Accessed 23 May 2019.
171. World Health Organization (WHO), 2007. Prevention of cardiovascular disease (CVDs). Available from www.who.int/cardiovascular_diseases/guidelines/Pocket_GL_information/en. Accessed 23 May 2019.
172. Naderi SH, Bestwick JP, Wald DS. Adherence to drugs that prevent cardiovascular disease: meta-analysis on 376,162 patients. Am J Med. 2012;125(9):882-887.e881.
173. Banerjee A, Khandelwal S, Nambiar L, et al. Health system barriers and facilitators to medication adherence for the secondary prevention of cardiovascular disease: a systematic review. Open Heart. 2016;3:e000438.
174. Thom S, Poulter N, Field J, et al. Effects of a fixed-dose combination strategy on adherence and risk factors in patients with or at high risk of CVD: the UMPIRE randomized clinical trial. JAMA. 2013;310(9):918-929.
175. Desai D, Wang J, Wen H, Li X, Timmins P. Formulation design, challenges, and development considerations for fixed dose combination (FDC) of oral solid dosage forms. Pharm Dev Technol. 2013;18(6):1265-1276.
176. Frantz S. The trouble with making combination drugs. Nat Rev Drug Discov. 2006;5(11):881-882.
177. Andrews GP, Li S, Almajaan A, et al. Fixed Dose Combination Formulations: Multilayered Platforms Designed for the Management of Cardiovascular Disease. Mol Pharm. 2019;16(5):1827-1838.
178. Khaled SA, Burley JC, Alexander MR, Yang J, Roberts CJ. 3D printing of five-in-one dose combination polypill with defined immediate and sustained release profiles. J Control Release. 2015;217:308-314.
179. Igel M, Sudhop T, von Bergmann K. Metabolism and drug interactions of 3-hydroxy-3-methylglutaryl coenzyme A-reductase inhibitors (statins). Eur J Clin Pharmacol. 2001;57(5):357-364.
180. Riekes MK, Dereymaker A, Berben P, Augustijns P, Stulzer HK, Van den Mooter G. Development of enteric-coated fixed dose combinations of amorphous solid dispersions of ezetimibe and lovastatin: Investigation of formulation and process parameters. Int J Pharm. 2017;520(1-2):49-58.
181. Tubic-Grozdanis M, Hilfinger JM, Amidon GL, et al. Pharmacokinetics of the CYP 3A substrate simvastatin following administration of delayed versus immediate release oral dosage forms. Pharm Res. 2008;25(7):1591-1600.
182. Shin-Etsu AQCOAT (hypromellose Acetate Succinate) product brochure of supplier Shin-Etsu Chemical Co. (Ohtemachi, Japan).
183. Henwood JM, Heel RC. Lovastatin. A preliminary review of its pharmacodynamic properties and therapeutic use in hyperlipidaemia. Drugs. 1988;36(4):429-454.
184. Yeh HW, Chen DR. In vitro release profiles of PLGA core-shell composite particles loaded with theophylline and budesonide. Int J Pharm. 2017;528(1-2):637-645.
185. Baird JA, Van Eerdenbrugh B, Taylor LS. A classification system to assess the crystallization tendency of organic molecules from undercooled melts. J Pharm Sci. 2010;99(9):3787-3806.

186. Martínez V, Maguregui MI, Jiménez RM, Alonso RM. Determination of the pKa values of beta-blockers by automated potentiometric titrations. J Pharm Biomed Anal. 2000;23(2-3):459-468.
187. Clasen C, Kulicke W. Determination of viscoelastic and rheo-optical material functions of water-soluble cellulose derivatives. progress in polymer science. 2001;26(9):1839-1919.
188. Pas T, Struyf A, Vergauwen B, Van den Mooter G. Ability of gelatin and BSA to stabilize the supersaturated state of poorly soluble drugs. Eur J Pharm Biopharm. 2018;131:211-223.
189. Alhnan MA, Cosi D, Murdan S, Basit AW. Inhibiting the gastric burst release of drugs from enteric microparticles: the influence of drug molecular mass and solubility. J Pharm Sci. 2010;99(11):4576-4583.
190. Jayasinghe SN, Edirisinghe MJ. Effect of viscosity on the size of relics produced by electrostatic atomization. Aerosol science. 2002;33:1379-1388.
191. Zhang S, Kawakami K. One-step preparation of chitosan solid nanoparticles by electrospray deposition. Int J Pharm. 2010;397(1-2):211-217.
192. Pareta R, Brindley A, Edirisinghe MJ, Jayasinghe SN, Luklinska ZB. Electrohydrodynamic atomization of protein (bovine serum albumin). J Mater Sci Mater Med. 2005;16(10):919-925.
193. Rasekh M, Ahmad Z, Cross R, Hernández-Gil J, Wilton-Ely JDET, Miller PW. Facile Preparation of Drug-Loaded Tristearin Encapsulated Superparamagnetic Iron Oxide Nanoparticles Using Coaxial Electrospray Processing. Mol Pharm. 2017;14(6):2010-2023.
194. Browne E, Charifou R, Worku ZA, Babu RP, Healy AM. Amorphous solid dispersions of ketoprofen and poly-vinyl polymers prepared via electrospraying and spray drying: A comparison of particle characteristics and performance. Int J Pharm. 2019;566:173-184.
195. Bohr A, Yang M, Baldursdottir S, et al. particle formation and characteristics of celecoxib-loaded poly(lactic-co-glycolic acid) microparticles prepared in different solvents using electrospraying. polymer. 2012;53:3220-3229.
196. Xie J, Marijnissen JC, Wang CH. Microparticles developed by electrohydrodynamic atomization for the local delivery of anticancer drug to treat C6 glioma in vitro. Biomaterials. 2006;27(17):3321-3332.
197. Hong Y, Li Y, Yin Y, Li D, Zou G. Electrohydrodynamic atomization of quasi-monodisperse drug-loaded spherical/wrinkled microparticles. journal of aerosol science. 2008;39:525-536.
198. Zhou FL, Hubbard Cristinacce PL, Eichhorn SJ, Parker GJ. Preparation and characterization of polycaprolactone microspheres by electrospraying. Aerosol Sci Technol. 2016;50(11):1201-1215.
199. Arya N, Chakraborty S, Dube N, Katti DS. Electrospraying: a facile technique for synthesis of chitosan-based micro/nanospheres for drug delivery applications. J Biomed Mater Res B Appl Biomater. 2009;88(1):17-31.
200. Jafari-Nodoushan M, Barzin J, Mobedi H. Size and morphology controlling of PLGA microparticles produced by electro hydrodynamic atomization. polymers advanced technology. 2015;26:502-513.
201. Xu Y, Skotak M, Hanna M. Electrospray encapsulation of water-soluble protein with polylactide. I. Effects of formulations and process on morphology and particle size. J Microencapsul. 2006;23(1):69-78.
202. López-Rubio A, Lagaron J. Whey protein capsules obtained through electrospraying for the encapsulation of bioactives. Innovative Food Science & Emerging Technologies. 2012;13:200-206.
203. Lee B, Tajima A, Kim J, Yamagata Y, Nagamune T. Fabrication of protein microarrays using the electrospray deposition (ESD) method: Application of microfluidic chips in immunoassay. Biotechnology and Bioprocess Engineering. 2010;15.
204. Guo X, Xia T, Wang H, et al. Electrosprayed microparticles with loaded pDNA-calcium phosphate nanoparticles to promote the regeneration of mature blood vessels. Pharm Res. 2014;31(4):874-886.

205. Wu Y, Fei Z, Lee LJ, Wyslouzil BE. Coaxial electrohydrodynamic spraying of plasmid DNA/polyethylenimine (PEI) polyplexes for enhanced nonviral gene delivery. Biotechnol Bioeng. 2010;105(4):834-841.
206. Davies L, Hannavy K, Davies N, et al. Electrohydrodynamic Comminution: A Novel Technique for the Aerosolisation of Plasmid DNA. Pharmaceutical Research. 2005;22(8):1294-1304.
207. Braghirolli DI, Zamboni F, Chagastelles PC, et al. Bio-electrospraying of human mesenchymal stem cells: An alternative for tissue engineering. Biomicrofluidics. 2013;7(4):44130.
208. Ye C, He Z, Lin Y, et al. Bio-electrospraying is a safe technology for delivering human adipose-derived stem cells. Biotechnol Lett. 2015;37(2):449-456.
209. Gasperini L, Maniglio D, Migliaresi C. Microencapsulation of cells in alginate through an electrohydrodynamic process. journal of bioactive and compatible polymers. 2013;28(5):413-425.
210. Clarke JD, Jayasinghe SN. Bio-electrosprayed multicellular zebrafish embryos are viable and develop normally. Biomed Mater. 2008;3(1):011001.
211. Ding L, Lee T, Wang CH. Fabrication of monodispersed Taxol-loaded particles using electrohydrodynamic atomization. J Control Release. 2005;102(2):395-413.
212. Moghadam H, Samimi M, Samimi A, Khorram M. Electro-spray of high viscous liquids for producing mono-sized spherical alginate beads. Particuology. 2008;6(4):271-275.
213. Almería B, Gomez A. Electrospray synthesis of monodisperse polymer particles in a broad (60 nm-2 µm) diameter range: guiding principles and formulation recipes. J Colloid Interface Sci. 2014;417:121-130.
214. Davoodi P, Feng F, Xu Q, et al. Coaxial electrohydrodynamic atomization: microparticles for drug delivery applications. J Control Release. 2015;205:70-82.
215. Naghibi Beidokhti HR, Ghaffarzadegan R, Mirzakhanlouei S, Ghazizadeh L, Dorkoosh FA. Preparation, Characterization, and Optimization of Folic Acid-Chitosan-Methotrexate Core-Shell Nanoparticles by Box-Behnken Design for Tumor-Targeted Drug Delivery. AAPS PharmSciTech. 2017;18(1):115-129.
216. Xie J, Ng WJ, Lee LY, Wang CH. Encapsulation of protein drugs in biodegradable microparticles by co-axial electrospray. J Colloid Interface Sci. 2008;317(2):469-476.
217. Voltaren 25 mg maagsapresistente tabletten, samenvattingen van de kenmerken van het product (skp) available from http://bijsluiters.fagg-afmps.be/?localeValue=nl. Accessed at 17/09/2019.
218. Naproxen EC Mylan 250 mg, maagsapresistente tabletten, samenvattingen van de kenmerken van het product (skp) available from http://bijsluiters.fagg-afmps.be/?localeValue=nl. Accessed at 17/09/2019.
219. Losec-Mups 10 mg, maagsapresistente tabletten samenvattingen van de kenmerken van het product (skp) available from http://bijsluiters.fagg-afmps.be/?localeValue=nl. Accessed at 17/09/2019.
220. Sakai T, Hirai D, Kimura SI, Iwao Y, Itai S. Effects of tablet formulation and subsequent film coating on the supersaturated dissolution behavior of amorphous solid dispersions. Int J Pharm. 2018;540(1-2):171-177.
221. Luo D, Kim JH, Park C, et al. Design of fixed dose combination and physicochemical characterization of enteric-coated bilayer tablet with circadian rhythmic variations containing telmisartan and pravastatin sodium. Int J Pharm. 2017;523(1):343-356.
222. Xie Y, Xie P, Song X, Tang X, Song H. Preparation of esomeprazole zinc solid dispersion and study on its pharmacokinetics. Int J Pharm. 2008;360(1-2):53-57.
223. Thenapakiam S, Saravanan M, Pushpamalar J, Hong C. Spray dried solid dispersions of piroxicam in carboxymethyl sago cellulose using aqueous solvents: A simple, novel and green approach to produce enteric microparticles with enhanced dissolution drying technology. 2019;37(10):1191-1200.

224. Dai J, Nagai T, Wang X, Zhang T, Meng M, Zhang Q. pH-sensitive nanoparticles for improving the oral bioavailability of cyclosporine A. Int J Pharm. 2004;280(1-2):229-240.
225. Ariyasu A, Hattori Y, Otsuka M. Non-destructive prediction of enteric coating layer thickness and drug dissolution rate by near-infrared spectroscopy and X-ray computed tomography. Int J Pharm. 2017;525(1):282-290.
226. Bikiaris D, Koutri I, Alexiadis D, Damtsios A, Karagiannis G. Real time and non-destructive analysis of tablet coating thickness using acoustic microscopy and infrared diffuse reflectance spectroscopy. Int J Pharm. 2012;438(1-2):33-44.
227. Koller DM, Hannesschläger G, Leitner M, Khinast JG. Non-destructive analysis of tablet coatings with optical coherence tomography. Eur J Pharm Sci. 2011;44(1-2):142-148.
228. Hao S, Wang B, Wang Y. Porous hydrophilic core/hydrophobic shell nanoparticles for particle size and drug release control. Mater Sci Eng C Mater Biol Appl. 2015;49:51-57.
229. Lee YH, Mei F, Bai MY, Zhao S, Chen DR. Release profile characteristics of biodegradable-polymer-coated drug particles fabricated by dual-capillary electrospray. J Control Release. 2010;145(1):58-65.
230. Mangrio FA, Dwivedi P, Han S, et al. Characteristics of Artemether-Loaded Poly(lactic-co-glycolic) Acid Microparticles Fabricated by Coaxial Electrospray: Validation of Enhanced Encapsulation Efficiency and Bioavailability. Mol Pharm. 2017;14(12):4725-4733.
231. Cao Y, Wang B, Wang Y, Lou D. Dual drug release from core-shell nanoparticles with distinct release profiles. J Pharm Sci. 2014;103(10):3205-3216.
232. Zeng H, Pang X, Wang S, et al. The preparation of core/shell structured microsphere of multi first-line anti-tuberculosis drugs and evaluation of biological safety. Int J Clin Exp Med. 2015;8(6):8398-8414.
233. Roine J, Murtomaa M, Myllys M, J S. Dual-capillary electroencapsulation of mesoporous silicon drug carrier particles for controlled oral drug delivery. Journal of Electrostatics. 2012;70(5):428-437.
234. Kampschulte M, Langheinirch AC, Sender J, et al. Nano-Computed Tomography: Technique and Applications. Rofo. 2016;188(2):146-154.
235. Application document ZEISS Xradia 810 Ultra Nanoscale X-ray Imaging: Explore at the Speed of Science. Version 2.0. https://applications.zeiss.com/C125792900358A3F/0/D60B411D09D221FDC125835B003B6D57/$FILE/EN_42_011_080_xradia-810-ultra_rel2-0.pdf consulted at 19/08/2019.
236. Withers P. X-ray nanotomography. materialstoday. 2007;10(12):26-34.
237. Stewart PL. Cryo-electron microscopy and cryo-electron tomography of nanoparticles. Wiley Interdiscip Rev Nanomed Nanobiotechnol. 2017;9(2).
238. Reardon PJ, Parhizkar M, Harker AH, et al. Electrohydrodynamic fabrication of core-shell PLGA nanoparticles with controlled release of cisplatin for enhanced cancer treatment. Int J Nanomedicine. 2017;12:3913-3926.
239. Barnes TJ, Kempson IM, Prestidge CA. Surface analysis for compositional, chemical and structural imaging in pharmaceutics with mass spectrometry: a ToF-SIMS perspective. Int J Pharm. 2011;417(1-2):61-69.
240. Meeus J, Chen X, Scurr DJ, et al. Nanoscale surface characterization and miscibility study of a spray-dried injectable polymeric matrix consisting of poly(lactic-co-glycolic acid) and polyvinylpyrrolidone. J Pharm Sci. 2012;101(9):3473-3485.
241. Dereymaker A, Scurr DJ, Steer ED, Roberts CJ, Van den Mooter G. Controlling the Release of Indomethacin from Glass Solutions Layered with a Rate Controlling Membrane Using Fluid-Bed Processing. Part 1: Surface and Cross-Sectional Chemical Analysis. Mol Pharm. 2017;14(4):959-973.
242. Saboo S, Mugheirbi NA, Zemlyanov DY, Kestur US, Taylor LS. Congruent release of drug and polymer: A "sweet spot" in the dissolution of amorphous solid dispersions. J Control Release. 2019;298:68-82.

243. Patel SG, Bummer PM. Development of a Robust Method for Simultaneous Quantification of Polymer (HPMC) and Surfactant (Dodecyl β-D-Maltoside) in Nanosuspensions. AAPS PharmSciTech. 2016;17(5):1182-1191.

244. Yan W, Tong Y, Wang C. Coaxial Electrohydrodynamic Atomization Toward Large Scale Production of Core-Shell Structured Microparticles. AIChE Journal. 2017;63(12):5303-5319.

Annex

Annex 1: structures of polymers with their corresponding names/abbreviations used in the thesis.

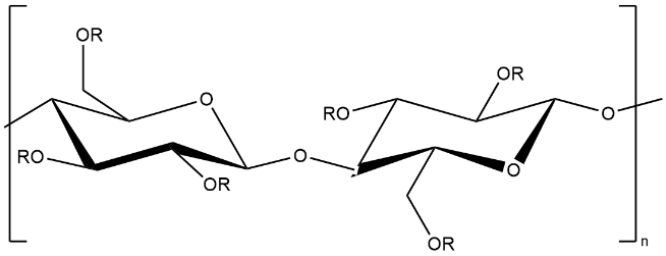

Ethyl cellulose (EC)

R= H or CH_2CH_3

Hydroxypropyl cellulose (HPMC)

R= H or $CH_2CH(OH)CH_3$

Hydroxypropyl methylcellulose (HPMC)

R= H or CH_3 or $CH_2CH(OH)CH_3$

Hydroxypropyl methylcellulose acetate succinate (HPMC AS)

R= H or CH_3 or $CH_2CH(OH)CH_3$ or

R= $COCH_2CH_2COOH$ or $CH_2CH(CH_3)OCOCH_3$ or

R= $COCH_3$ or $CH_2CH(CH_3)OCOCH_3CH_2CH_2COOH$

Hydroxypropyl methylcellulose phthalate (HPMC P)

R= H or CH_3 or $CH_2CH(OH)CH_3$ or

R= 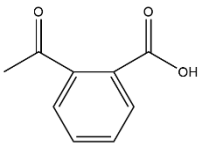 or 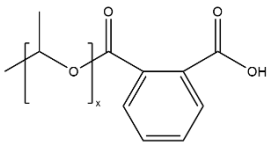

Cellulose acetate phthalate (CAP)

R= H or $COCH_3$ or 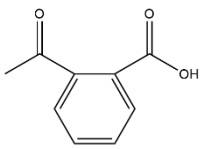

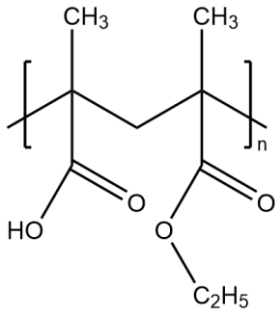

Copolymer poly(methacrylic acid-co-ethyl acrylate)
P(MAA/EA) = Eudragit® L100-55

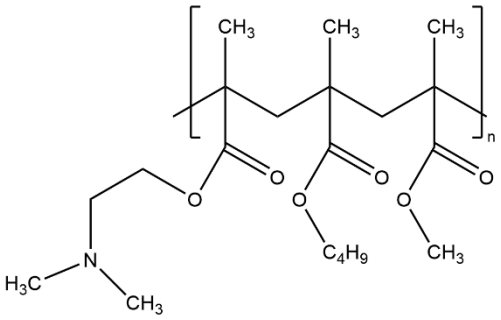

Basic methacrylate copolymer
Eudragit®E100

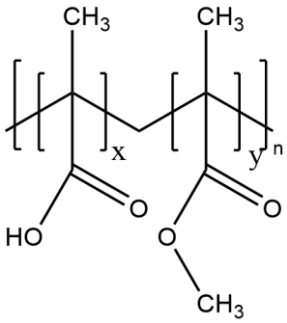

Copolymer poly(methacrylic acid-co-methyl methacrylate)
P(MAA/MMA) 1/1 = Eudragit® L100
1/2 = Eudragit® S100

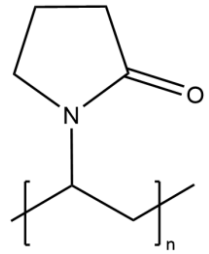

Polyvinylpyrrolidone
PVP

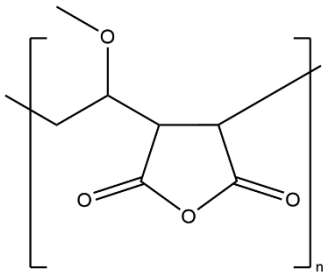

Poly(methyl vinyl ether-alt-maleic anhydride)
P(MV/MA)

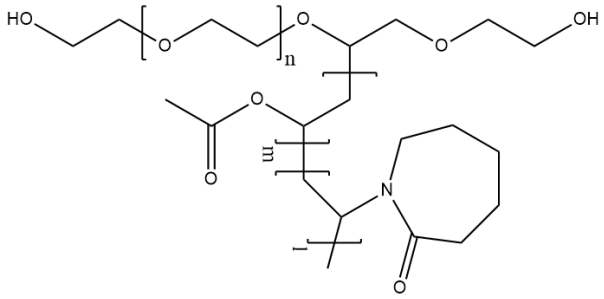

Vinyl caprolactam-polyvinyl acetate-polyethylene glycol graft copolymer = Soluplus®

Annex 2: Validation of the HPLC methods

*** R^2 = determination coefficient of linear regression**

****LOQ = limit of quantification**

Compound	Range (µg/mL)	R^2*	LOQ** (µg/mL)
Darunavir	0.2-60	> 0.999	0.15
Lovastatin	0.05-30	> 0.999	0.05
β-hydroxy acid metabolite of lovastatin	0.05-30	> 0.999	0.05
Atenolol	1-30	> 0.999	0.25
Acetylsalicylic acid	1-30	> 0.999	0.25
Salicylic acid	1-30	> 0.999	0.5
Fenofibrate	0.05-30	> 0.999	0.05
Paracetamol	0.05-30	> 0.999	0.05

Contributions

Scientific acknowledgements

Annelies Smeets acknowledges the Soft Matter, Rheology and Technology (SMaRT) division, the department of Materials Engineering (MTM) and the Polymer Chemistry and Materials division for the use of their facilities. Bernard Appeltans, Nico Coenen and Anja Vananroye are acknowledged for the technical support in the lab.

Personal contributions

Annelies Smeets planned and performed the experiments, analysed the data and wrote the text, with following exceptions:

For chapter 3, Annouschka Laenen gave advice and performed the statistical analysis of the data. Thao Pauwels helped to perform the dynamic light scattering experiments.

For chapter 4, SEM was performed by Nico Coenen and TGA by Danny Winant. Annouschka Laenen gave advise on how to perform the statistical analysis.

Chapter 5 is a joint first authorship paper with Robin Koekoekx. Robin Koekoekx prepared the samples for SEM in Fig 5.4 and 5.5. He performed the Ubbelohde measurements for Fig 5.6, confocal microscopy for Fig 5.7, and intrinsic viscosity measurements and calculations regarding the solubility factors for Table 5.4 and 5.5. He also wrote the text concerning these results. Mario Smet and Wouter Ruelens helped to design the synthesis of P(MAA/MMA) with monomers ratios 1/1.5 and 1.9. Additionally, Wouter Ruelens helped with the performance of the synthesis. SEM was performed by Nico Coenen.

For chapter 6, SEM was performed by Nico Coenen.

Guy Van den Mooter and Christian Clasen were the supervisors of the project. They helped to develop the research strategy, design the experiments and they reviewed the text.

Conflict of interest statement

The authors acknowledge het Fonds voor Wetenschappelijk Onderzoek-Vlaanderen (FWO, project G0A3916N) for the financial support. Annelies Smeets also thanks the FWO and the Thermische Analyse Werkgroep Nederland (TAWN) for the travel grant.

The authors declare no conflict of interest.

Curriculum Vitae

Education

2016-2019: Doctoral Training in Pharmaceutical Sciences, KU Leuven, Belgium

2013-2015: MSc in Drug Development, specialisation pharmacy, KU Leuven, Belgium

2010-2013: BSc in Pharmaceutical Sciences, KU Leuven, Belgium

Scientific publications

- Electrospraying of polymer solutions: study of formulation and process parameters. Annelies Smeets, Christian Clasen, Guy Van den Mooter. European Journal of Pharmaceutics and Biopharmaceutics 2017. vol:119 pages:114-124
- Amorphous solid dispersions of darunavir: Comparison between spray drying and electrospraying. Annelies Smeets, Robin Koekoekx, Christian Clasen, Guy Van den Mooter. European Journal of Pharmaceutics and Biopharmaceutics 2018. Vol.130; pp. 96-10
- Comparative study of the potential of poly(2-ethyl-2-oxazoline) as carrier in the formulation of amorphous solid dispersions of poorly soluble drugs. Eline Boel and Annelies Smeets, Maarten Vergaelen, Victor R. De la Rosa, Richard Hoogenboom, Guy Van den Mooter. European Journal of Pharmaceutics and Biopharmaceutics 2019. Vol. 114; pp 79-90
- Gastro-resistant encapsulation of amorphous solid dispersions containing darunavir by coaxial electrospraying. Annelies Smeets and Robin Koekoekx, Wouter Ruelens, Mario Smet, Christian Clasen and Guy Van den Mooter. Accepted by the International Journal of Pharmaceutics.

Oral presentations at International Meetings

- Influence of formulation and process parameters on the formation of coated solid dispersion nano- and microparticles by single step coaxial electrospraying. PSSRC Annual Symposium edition 10. Copenhagen, Denmark: 6-8 July 2016
- Electrospraying versus spray drying for the preparation of amorphous solid dispersions. PSSRC Annual Symposium edition 11. Graz, Austria: 28-30 June 2017
- Single step coaxial electrospraying to produce coated amorphous solid dispersion particles of darunavir. PSSRC Annual Symposium edition 12. Leuven, Belgium: 12-14 September 2018
- Peculiar coating permeability of fixed dose combinations produced by coaxial electrospraying. PSSRC Annual Symposium edition 13. Düsseldorf, Germany. 12-14 September 2019

Poster presentations at International Meetings

- Electrospraying versus spray drying for the preparation of amorphous solid dispersions. ULLA Summer School edition 13. Leuven, Belgium: 8-15 July 2017
- Comparison between electrospraying and spray drying for the preparation of amorphous solid dispersions of darunavir. PBP world meeting edition 11. Granada, Spain. 19-22 March 2018

Oral presentations at National Meetings

- Influence of formulation and process parameters on the formation of coated solid dispersion nano- and microparticles by single step coaxial electrospraying. Society of Pharmaceutical Sciences - 19th forum. Brussels, Belgium: 17-18 October 2016
- Comparison between electrospraying and spray drying for the preparation of amorphous solid dispersions of darunavir. Meeting of the Belgian-Dutch Biopharmaceutical Society. Brussels, Belgium: 8 December 2017
- Single step coaxial electrospraying to produce coated amorphous solid dispersion particles of darunavir. Annual meeting TAWN (Thermische Analyse Werkgroep Nederland). Utrecht, The Netherlands: 30 November 2018
- Gastro-resistant encapsulation of amorphous solid dispersions of amorphous solid dispersions by coaxial electrospraying. Meeting of the Belgian-Dutch Biopharmaceutical Society. Brussels, Belgium: 20 May 2019